Durham E-Theses

The experimental investigation of a pipe robot

Chunlian Han

How to cite:

Han, Chunlian (1999) The experimental investigation of a pipe robot. Masters thesis, Durham University.

Use policy

The Experimental Investigation of a Pipe Robot

Chunlian Han

School of Engineering, University of Durham

A dissertation submitted for the degree of
Master of Science

October 1999

2 3 MAY 2000

Dedicate to my mother

Abstract

A novel mobile robot, using steel bristles for traction, was designed, built and tested during this research study. This kind of pipe robot can swiftly move forward in both straight and bent pipes and has been used for carrying out the inspection of the pipe.

A theory for the bristle traction mechanism has been proposed based upon using the Euler analysis for the critical buckling load of a bristle. Relationships between various bristle properties and performance have been proposed and investigated.

Experiments have been carried out on a steel bristled robot and a plastic bristled robot, using load cells to measure the forces at various points along its structure, during motion. Additional static tests have been carried out on bristles to investigate performance of the traction mechanism under transverse load.

Ideas for further enhancement of the robot are also discussed. These ideas include:

- Improving the robot control system
- Improving the robot structure alignment system
- Improvement for payload carrying capability

Acknowledgements

Contents

Nomenclature

Roman symbol

D	Diameter
d	Diameter
EI	Stiffness
F	Traction
F_{for}	Resistance in forward motion
F_{back}	Resistance in backward motion
h	Path between pipe's wall and bristle's core
L	Length of bristle
M	Moment
P	Force
P_{Euler}	Buckling force
R_{for}	Resultant force in forward motion
R_{back}	Resultant force in backward motion
s	A part length of bristle
v	Distance
z	Distance

Greek symbol

α	Angle
γ	Angle
θ	Angle
ϕ	Angle
δ	Deflation of bristle to the tangential co-ordinate
μ	Friction coefficient
ρ	Radius of curvature

1. Introduction

This research study is an extension of earlier work on developing a robot based upon traction bristles (Ref1). It was recognised that when a curved bristle is dragged across a surface, the bristles offer less resistance to sliding motion in one direction compared to the other direction. This kind of robot is capable of swiftly moving forward in both straight and bent pipe for carrying out the inspection of the pipes. During the course of this research the following contributions have been made:

- a theory for the actual bristle mechanism has been proposed

- a powerful robot with steel bristles was designed, built and tested

- experiments were carried out using a plastic bristled robot

- experimental results were examined to determine the mechanical behaviour of the robot under a different conditions

- ideas for further enhancement of the robot were discussed and conclusions were drawn

1.1 Previous work

'The capacity for self-directed motion is perhaps the most fundamental characteristic that separates a robot from other types of machinery.' (John M. Holland, 1983). Thring suggested in 1968 (Ref5.) that the most basic of robots have to meet the following criteria:

1

- have a form of hand and arm

- be capable of self-propelling and self-steering

- possess power and control systems to achieve these two purposes

- have means of detecting specific conditions

- incorporate some computer technology to achieve the foregoing, with memory capacity for instructions, facilitating decision making, senses of touch, roughness, hardness, position, weight, thermal conductivity, temperature, proximity, shape, size, sight, colour, distance, smell, position of limbs and hearing.

A more modern definition of a robot would, in some aspects, be somewhat wider. Both autonomous and directed devices used for exploration and telechirics used in hostile environments are given the title of 'robot'. The use of such a robot for inspection and servicing is now well established. It is possible to divide such devices into two functions: the inspection or processing function and the tractor device for achieving mobility.

The majority of inspection robots currently on the market are wheel-driven. From earlier study, no robots were found to be using bristles as a form of propulsion and suspension but a similar mechanism to this kind of propulsion can be found in a German patent, developed in 1974 by Dr. Joachim Schnell (Ref2). However, in this case the device was intended for propulsion through water or snow and the force of propulsion was generated by the viscous resistance of flow around the bristles and not by the contact of the tip of the bristle as in the mechanism in this work.

In one format, Dr. Schnell's patent uses flaps (with an 'angled saw-teeth' profile), in oscillatory motion to propel a device over a surface such as shallow water, mud, bog, grass, sand or snow. (Figure 1.1)

Forward Direction
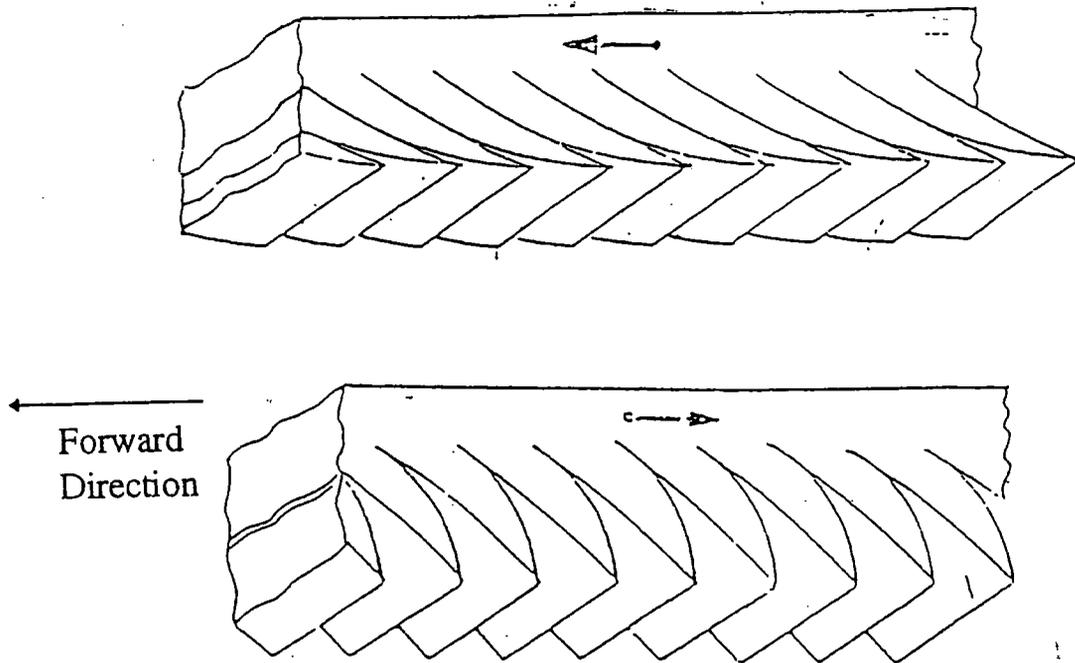
When the block oscillates back and forth, the profile offers less resistance the direction of travel than in the opposite direction.

Figure1.1

This sliding movement is achieved by the principle that the resistance, between the contact face and the surface to be traversed, is less in the direction of travel than if travel is in the opposite direction.

Although outwardly similar, in the case of the traction mechanism used in this work, the traction force is generated in quite a different manner to that in the German Patent. In this case the traction force is the summation of forces generated at the tip of a large number of bristles that are formed into a brush. The individual bristles have structural characteristics based upon their length, diameter, material, properties etc.

The relationship between these factors can be expressed in a geometric force diagram (Figure 1.2). Figure 1.2 shows a force vector diagram that illustrated why a single bristle will slide forward but not slide backward, that is $\mu Fback \geq \mu Ffor$. Where $\mu Ffor$ is the resistance to forward motion, $\mu Fback$ is the resistance to backward motion, γ is an angle of the bristle to the surface.
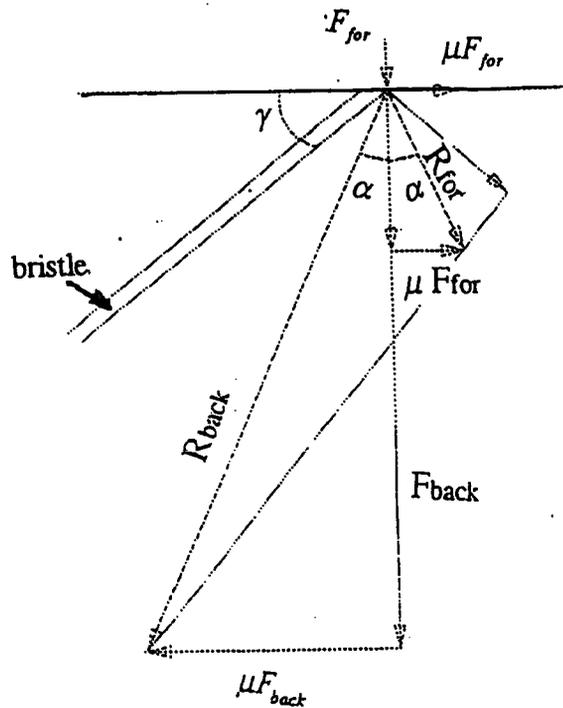
Figure 1.2   After suggestion of Prof. Appleton E (Ref.)

The Pipe Crawler

Another robot that is similar in principle to the proposed bristled pipe robot in Durham University's patent was registered under 'Patent Specification No. 2167829A', by John Luxmoore in 1984, and named 'Pipe Crawler'(Ref9). This Pipe Crawler used two members on axially displaceable component parts of the assembly, acting to alternately anchor and release the respective component parts (Figure 1.3a).
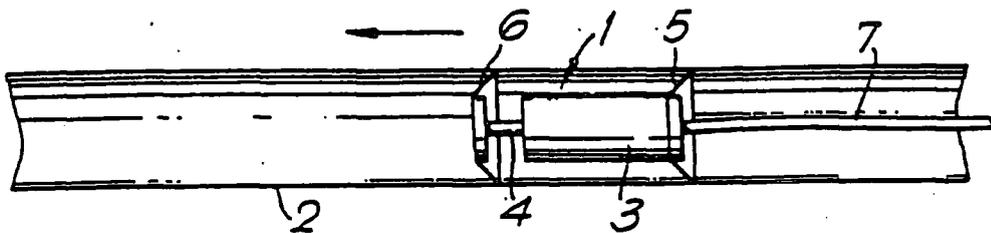
Figure 1.3a
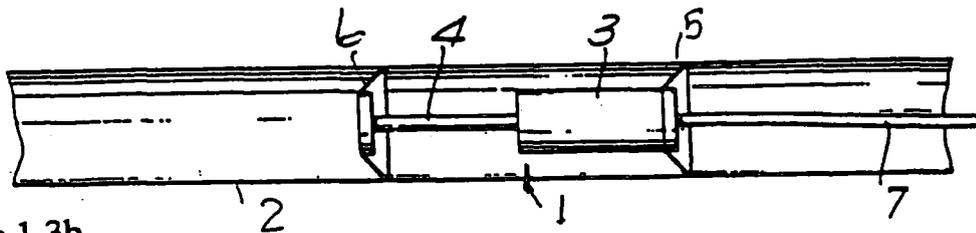
Figure 1.3b
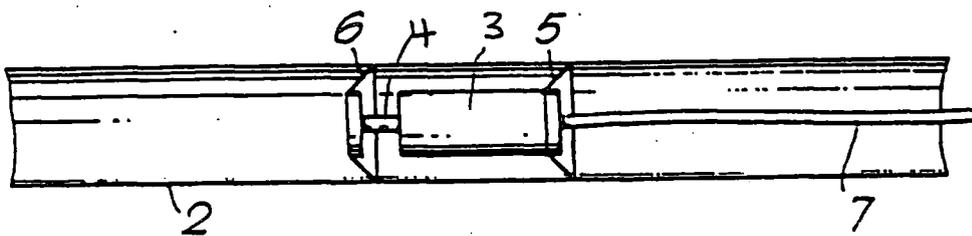
Figure 1.3c

Key
1 Piston & Cylinder Assembly
2 Pipe Wall
3 Cylinder

4 Piston
5 Member
6 Member
7 Connection

The piston and cylinder components (4&3) respectively are attached to members (6&5) respectively, which are biased into engagement with the pipe wall (2). Components 5 and 6 are flexed discs or spiders which more forward easily but offer a high resistance to pulling back. Fluid pressure acting through connection (7) can move the piston rod in or out of the cylinder.

To move the crawler along, the piston (4) is extended (Figure 1.3b). The member (5) resists the backward movement of the cylinder, so that as the piston extends, the member (6) moves forward. The supply to the cylinder is reversed and the cylinder moved forward and at the same time, since the member (6) resists movement of the piston rod (4), the member (5) moves forward. In this way, the crawler is able to move step-by-step along the bore of the pipe.

As already mentioned, in this type of pipe crawler, the members (5&6) can be annular plates or diaphragms secured to the cylinder (3) and the free end of the piston rod (4). Prior to the insertion of the pipe crawler into the bore of the pipe, the annular plate has an outside diameter or effective lateral dimension greater than the bore of the pipes.

Reversal of the direction of travel of the crawler can be achieved by braking the forward motion and flipping the discs as illustrated in figures 1.4a,b&c.
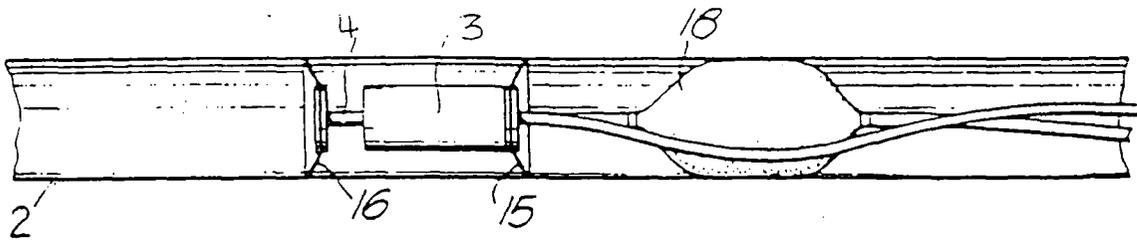
Figure 1.4a
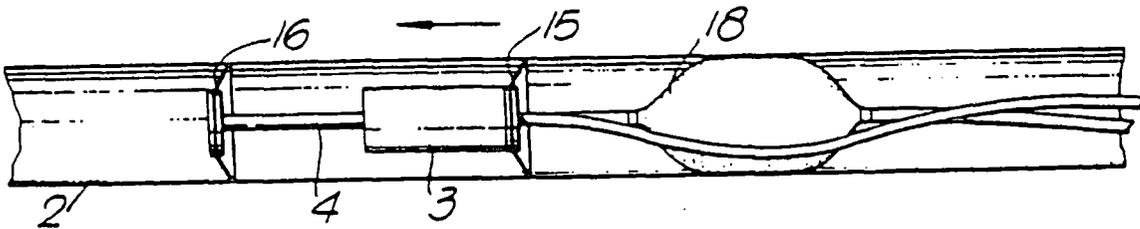
Figure 1.4b
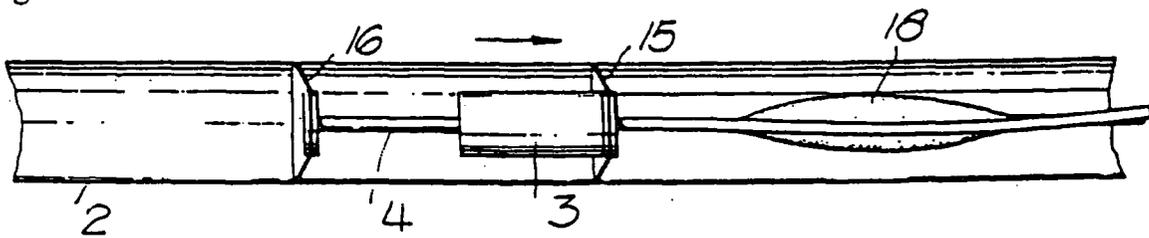
Figure 1.4c

The cylinder may trail a bladder (18) which can be inflated, holding the cylinder in place whilst the sequence is operated. The members (15 & 16) being made of a flexible material, are reversible, and when reversed, allow the crawler to be withdrawn by a reversed version of the step-by-step method, as outlined previously.

The Bristled Robot

The traction principle governing the pipe crawler is similar to that affecting the bristled pipe robot. However, despite this similarity, using bristles as the anchor and propulsion part of the robot carries advantages that surpass those of the crawler, the immediately apparent one being that bristles are easily deflected, and therefore can

7

overcome minor obstructions, moving effectively through a relatively large range of pipe diameters and conditions.

At the School of Engineering, University of Durham, in 1996, a plastic bristled robot was built and registered as Patent Specification GB 2305407A (Ref1). Vehicles of this type comprise of two or more bodies, each being supported upon a multiplicity of resilient bristles. Such a surface traversing vehicle proved to be very appropriate for use inside pipes and also to an extent, on the curved outer surfaces of chimneys, posts, cables and between parallel plates.

For a robot employing such a bristle mechanism, a single bristle can be considered to be a built in 'elastic column', having a very large deflection and an ability to deflect further to negotiate all sorts of pipe profiles and defects. Unlike the discs in the pipe crawler, the bristles allow gas or liquid to easily pass through the pipe without causing undue impedance.

1.2 Application

The research was to design a steel bristle robot for the purposes of carrying out inspection through a pipe containing 1½D bends, and investigate the mechanical behaviour of this kind of robot.

Through this study, it was found that this kind of bristled robot could be used by numerous utilities services, notably water and sewage companies. For instance, if

there were problems in a particular stretch of pipeline. The bristled pipe robot could use a CCTV camera as its eyes and carry the repair instrument along the pipe, allowing the repair to be carried out without disruption, and eliminating the need for any digging or other intrusion into the pipeline infrastructure.

2.Theory

The moving of the robot is achieved by the utilisation of curved brush as the means of propulsion and support, as illustrated in Figure 2.1. These brushes are pushed by a pneumatic cylinder. When the cylinder opens, the leading brush, offering lower resistance because of their curvature, move forward easily; the trailing brush, because of their higher resistance to backward forces, remain stationary. However, when the reverse happens, i.e. the cylinder closes, the leading brush (higher resistance to backward forces, this time) remain stationary, whereas the trailing brush, now offering the lower resistance, are pulled forward.
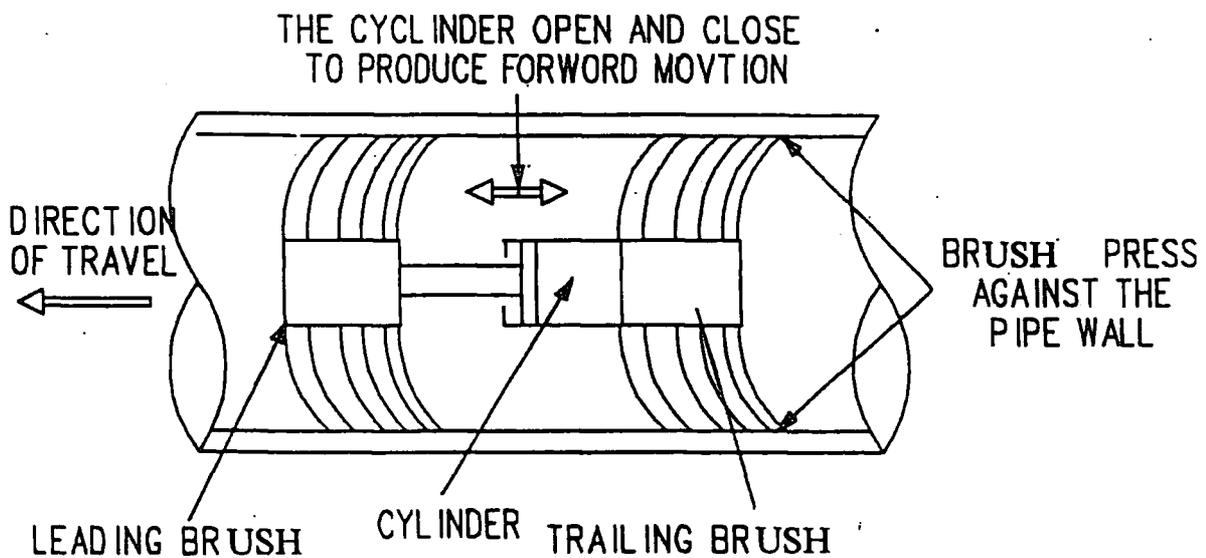
Figure 2.1 Motion principle

Based on this theory, the resultant traction depends entirely on the bristle mechanism setup, and can be illustrated in the following way, isolating a single bristle for the purpose of simplicity. When a bristle is put into a pipe, and because of its effective lateral dimension, is bent by the pipe wall, there will be a perpendicular force P acting

at the tip of the bristle from the wall of the pipe, as shown in Figure 2.2. When moving the core of bristles, traction F should be equal to μ P.
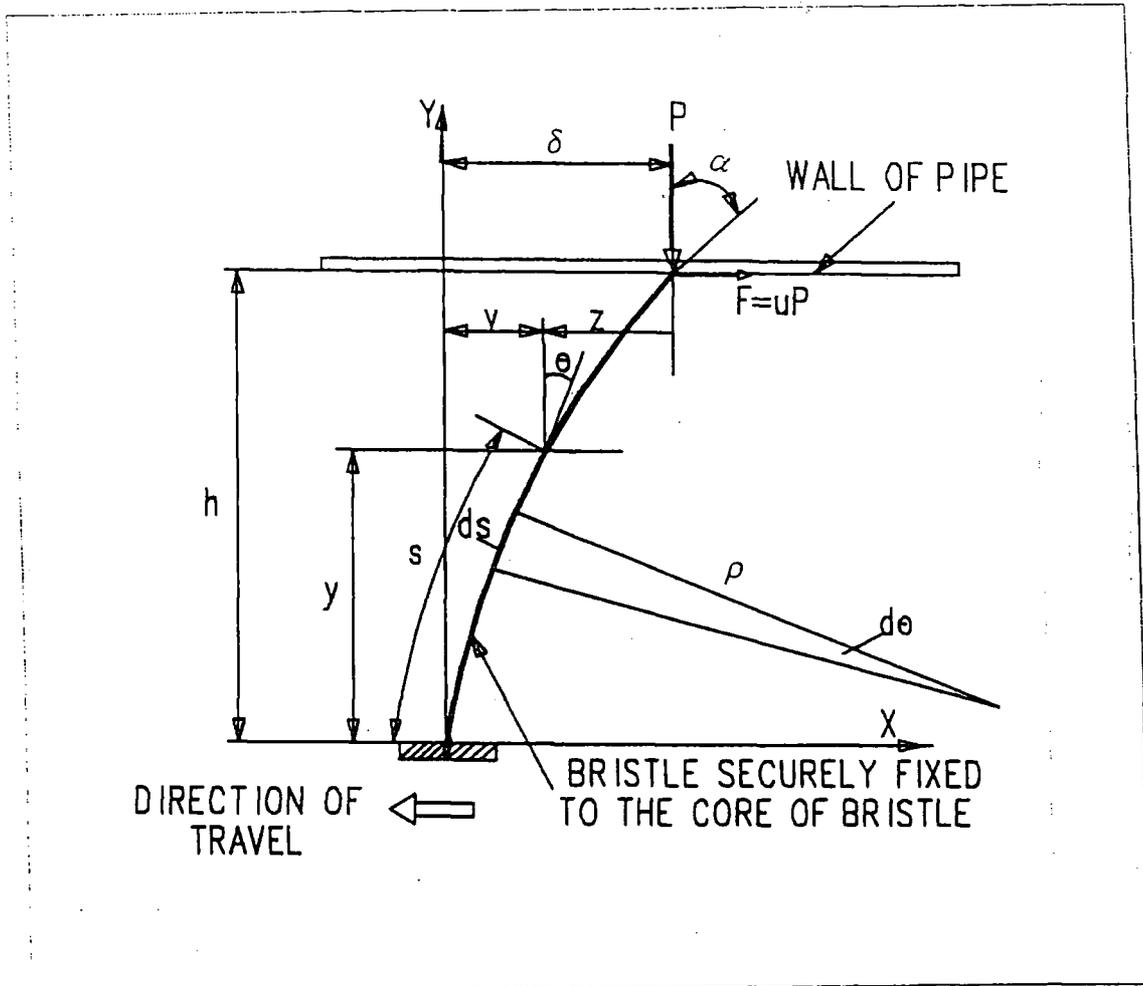
Fig. 2.2

For this sort of relatively straight bristle it might be reasonable to assume that the bristle behaves like a strut built in at one end which could be treated as a cantilever and therefore to a first approximate the Euler equation could be applied. Using the curvature form of the Bernoulli-Euler equation to solve the bristle of Fig. 2.2, then

$$\frac{1}{\rho} = \frac{d\theta}{ds} = \frac{M(y)}{EI} \qquad (2.1)$$

In Eq.2.1, ρ is the radius of curvature of the neutral plane at the point where the moment is M(y) and the stiffness is EI. When the bristle remains stationary.(μ=0)

Then $\qquad\qquad EI \frac{d\theta}{ds} = P(\delta - v) \qquad\qquad (2.2)$

Calling $\qquad\qquad z = \delta - v \qquad\qquad (2.3)$

and $\qquad\qquad Q^2 = \frac{P}{EI} \qquad\qquad (2.4)$

gives $\qquad\qquad \frac{d\theta}{ds} = Q^2 z \qquad\qquad (2.5)$

Now using trigonometric identities and relation which hold for the structure.

$$\sin \theta = \frac{dv}{ds} = \frac{dv}{d\theta}\frac{d\theta}{ds} \qquad (2.6)$$

using Eq. 2.5, $\qquad \sin \theta = \frac{dv}{d\theta}Q^2 z \qquad\qquad (2.7)$

and since, from Eq. 2.3,

$$dz = -dv \qquad (2.8)$$

Eq.2.7 becomes

$$\sin \theta \ d\theta = -Q^2 z dz \qquad (2.9)$$

Integrate this, to obtain

$$\cos \theta = \frac{Q^2 z^2}{2} + C \qquad (2.10)$$

Noting the boundary conditions

$$\left. \begin{array}{l} v = \delta \\ z = 0 \end{array} \right\} \text{ when } \theta = \alpha \qquad (2.11)$$

this gives

$$\cos \theta = C \qquad (2.12)$$

or

$$2(\cos \theta - \cos \alpha) = Q^2 z^2 \qquad (2.13)$$

Since

$$\left.\begin{matrix} v = 0 \\ z = \delta \end{matrix}\right\} \text{ when } \theta = 0 \qquad (2.14)$$

this gives

$$1 - \cos \alpha = \frac{Q^2 z^2}{2} \qquad (2.15)$$

$$= 2 \sin^2 \frac{\alpha}{2} \qquad (2.16)$$

or

$$\delta = \frac{2}{Q} \sin \frac{\alpha}{2} \qquad (2.17)$$

and this gives a relation between δ and α.

From the following well-known trigonometric identities:

$$\cos \theta = 1 - 2 \sin^2 \frac{\theta}{2} \qquad (2.18)$$

Subtract the Eq.2.16 from the Eq.2.18 and get

$$\cos \theta - \cos \alpha = 2(\sin^2 \frac{\alpha}{2} - \sin^2 \frac{\theta}{2}) \qquad (2.19)$$

which is also

$$\cos\theta - \cos\alpha = 2\sin^2\frac{\alpha}{2}\left(1 - \frac{\sin^2(\theta/2)}{\sin^2(\alpha/2)}\right) \qquad (2.20)$$

Define a new angle ϕ, by the relation

$$\sin\phi = \frac{\sin\dfrac{\theta}{2}}{\sin\dfrac{\alpha}{2}} \qquad (2.21)$$

Then Eq.2.20 becomes

$$\cos\theta - \cos\alpha = 2\sin^2\frac{\alpha}{2}\cos^2\phi \qquad (2.22)$$

or

$$\sqrt{2(\cos\theta - \cos\alpha)} = 2\sin\frac{\alpha}{2}\cos\phi \qquad (2.23)$$

Differentiate Eq.2.21, noting that ϕ and θ are the variables,

$$\cos\phi \, d\phi = \frac{\cos(\theta/2)d\theta}{2\sin(\alpha/2)} \qquad (2.24)$$

Now, returning to Eq.2.5, we have

$$ds = \frac{1}{Q^2 z}d\theta \qquad (2.25)$$

and, from Eq.2.13,

$$\frac{1}{Q^2 z} = \frac{1}{Q\sqrt{2(\cos\theta - \cos\alpha)}} \qquad (2.26)$$

so

$$ds = \frac{1}{Q\sqrt{2(\cos\theta - \cos\alpha)}}d\theta \qquad (2.27)$$

and, from Eq.2.23, this is also equal to

14

$$ds = \frac{1}{2Q\sin(\alpha/2)\cos\phi}\,d\theta \qquad (2.28)$$

But, from Eq.2.24,

$$\frac{1}{2\sin(\alpha/2)\cos\phi}\,d\theta = \frac{1}{\cos(\theta/2)}\,d\phi \qquad (2.29)$$

or

$$\frac{1}{2\sin(\alpha/2)\cos\phi}\,d\theta = \frac{1}{\sqrt{1-\sin^2(\theta/2)}}\,d\phi \qquad (2.30)$$

which, since Eq.2.21,

$$\sin\frac{\theta}{2} = \sin\phi \ \sin\frac{\alpha}{2} \qquad (2.31)$$

is also given by

$$\frac{1}{2\sin(\alpha/2)\cos\phi}\,d\theta = \frac{d\phi}{\sqrt{1-\sin^2(\alpha/2)\sin^2\phi}} \qquad (2.32)$$

so that

$$ds = \frac{1}{Q}\frac{d\phi}{\sqrt{1-\sin^2(\alpha/2)\sin^2\phi}} \qquad (2.33)$$

Integrate this Eq.2.33 and get

$$Qs = \int_0^{\phi_1} \frac{d\phi}{\sqrt{1-\sin^2(\alpha/2)\sin^2\phi}} \qquad (2.34)$$

when s equal to l, then $\theta = \alpha$, and

$$\sin \phi_1 = \frac{\sin\dfrac{\theta}{2}}{\sin\dfrac{\alpha}{2}} = 1 \qquad (2.35)$$

or

15

$$\phi_1 = \frac{\pi}{2} \qquad (2.36)$$

Hence, the expression becomes

$$Ql = \int_0^{\frac{\pi}{2}} \frac{d\phi}{\sqrt{1 - \sin^2(\frac{\alpha}{2})\sin^2\phi}} \qquad (2.37)$$

From 'A Short Table of Integrals' by B. O. Peirce, revised by RONALD.FOSTER, published by Ginn and Company, p.72.

$$Ql = \frac{\pi}{2}\left[1 + (\frac{1}{2})^2 \sin^2(\alpha/2) + (\frac{1*3}{2*4})^2 \sin^4(\alpha/2) + (\frac{1*3*5}{2*4*6})^2 \sin^6(\frac{\alpha}{2}) + \dots\dots\dots\right]$$

$$(2.38)$$

Noting that, for this bristle

$$P_{Euler} = \frac{\pi^2 EI}{4l^2} \qquad (2.39)$$

and, from Eq.2.4, the above relation gives

$$\frac{P}{P_{Euler}} = \frac{4}{\pi^2}(Ql)^2 \qquad (2.40)$$

and this gives a relation between P and Peuler.

From Eq.2.17,

$$\frac{\delta}{l} = \frac{2}{Ql}\sin\frac{\alpha}{2} \qquad (2.41)$$

and this gives a relation between δ and l.

Similarly, from Eq.2.13,

$$\frac{z}{l} = \frac{\sqrt{2(\cos\theta - \cos\alpha)}}{Ql} \qquad (2.42)$$

16

and using Eq.2.23,

$$\frac{z}{l} = \frac{2}{Ql} \sin \frac{\alpha}{2} \cos \phi \qquad (2.43)$$

Also,

$$\frac{dy}{ds} = \cos \theta \qquad (2.44)$$

But, from Eq.2.33 and Eq.2.18,Eq.2.44 becomes

$$dy = \frac{1}{Q} \frac{(1 - 2\sin^2(\theta/2))d\phi}{\sqrt{1 - \sin^2 \frac{\alpha}{2} \sin^2 \phi}} \qquad (2.45)$$

Then, from Eq.2.31, above Eq.2.45 become

$$Kdy = \frac{(1 - 2\sin^2 \frac{\alpha}{2} \sin^2 \phi)d\phi}{\sqrt{1 - \sin^2 \frac{\alpha}{2} \sin^2 \phi}}$$

Integrate this equation and get

$$Qdy = \frac{1}{\sqrt{1 - \sin^2 \frac{\alpha}{2} \sin^2 \phi}} - 2\sin^2 \frac{\alpha}{2} \frac{\sin^2 \phi}{\sqrt{1 - \sin^2 \frac{\alpha}{2} \sin^2 \phi}} d\phi \qquad (2.46)$$

If h equal to y, s equal l, the Eq.2.46 becomes

$$Qh = \int_0^{\frac{\pi}{2}} \frac{d\phi}{\sqrt{1 - \sin^2(\frac{\alpha}{2})\sin^2 \phi}} - 2\sin^2 \alpha/2 \int_0^{\pi/2} \frac{\sin^2 \phi}{\sqrt{1 - \sin^2 \alpha/2 \sin^2 \phi}} d\phi \qquad (2.47)$$

From 'A Short Table of Integrals' by B. O. Peirce, revised by RONALD.FOSTER, published by Ginn and Company, p.72, and Eq. 2.37, above equation becomes

$$\frac{h}{l} = 2 \frac{\int_0^{\frac{\pi}{2}} \sqrt{1 - \sin^2 \alpha/2 \sin^2 \phi} \, d\phi}{Ql} - 1 \qquad (2.48)$$

In Peirce's notation, define $E(k, \phi)$

$$E(\alpha) = \int_0^{\frac{\pi}{2}} \sqrt{1 - \sin^2 \frac{\alpha}{2} \sin \phi} \, d\phi$$

$$= \frac{\pi}{2} \left[1 - (\frac{1}{2})^2 \sin^2 \frac{\alpha}{2} - (\frac{1*3}{2*4})^2 \frac{\sin^4 \frac{\alpha}{2}}{3} - (\frac{1*3*5}{2*4*6})^2 \frac{\sin^6 \frac{\alpha}{2}}{5} - \cdots \right]$$

$$(2.49)$$

Eq.2.48 becomes

$$\frac{h}{l} = 2 \frac{E(\alpha)}{Ql} - 1 \qquad (2.50)$$

and this gives relation between h and l.

As an indication of the results obtained by applying the above theory, Table 1 has been prepared.

TABLE 1			
α (degree)	P/P$_{Euler}$	$\frac{\delta}{l}$	$\frac{h}{l}$
10	1.004	0.1116	0.9923
20	1.016	0.2193	0.9698
30	1.035	0.2588	0.9324
40	1.062	0.4221	0.8787
60	1.152	0.5930	0.6973
90	1.392	0.7925	0.4189

Thus, for a maximum load P is 39.2% greater than P$_{Euler}$ when a bristle is put in a pipe. The maximum length of a bristle is 41.89% longer than path gap between pipe wall and core of bristle.

3. Design

3.1 Specification

The specifications were that a steel bristled propelled robot be built, capable of handling 1½D bends and of towing a form of sensor device. A provision for mounting an inspection camera and appropriate lighting equipment also required consideration.

3.2 Embodiment

The robot was designed with three brushes ('leading', 'middle' and 'trailing') and with two pneumatic cylinders ('first' and 'second'). In line with the principles already discussed, the brush were curved away from the direction of desired motion, which was achieved by making the overall diameter of the brush greater than the diameter of the pipe interior.

When the robot was put into a pipe, all the brushes should be bent in the same direction as each other. By means of the pneumatic cylinders, the sets of brush were moved relative to each other repeatedly and the forward motion of the robot was thus achieved. The repeated cycle involves these three stages:

1. *When the first cylinder opens, the leading brush moves forward; the middle and trailing brush, remaining stationary, resisting the forward traction force.*

2. *The second cylinder opens as the first is closing, causing the middle brush to move forward, whilst the leading and trailing ones remain stationary.*

3. *As the second cylinder closes, the trailing brush move forward, whilst the leading and middle brush remain stationary.*

3.3 Construction

Figure 3.1 shows the construction of the robot that incorporates:

- three equally sized steel brushes,

- two pneumatic cylinders,

- two valves,

- six bearing joints,

- eighteen rubber joints,

- forty eight wheels.

The motion of the brushes is controlled by the two cylinders. A compressed air supply to the cylinders is regulated by the two valves, which are connected to a common compressed air supply line and an electrical controller. The robot, for the purpose of this experimental study was tested in an '8 inch' pipe, so the brush was made 214mm in diameter, and the diameter of the wheels was 192mm, which was consistent with the dimension requirements discussed earlier.

TOW

VALVES

TRAILING BRUSH

SECOND CYLINDER

MIDDLE BRUSH

FIRST CYLINDER

WHEELS

LEADING BRUSH

JOINT

CAMERA HOUSING

Figure 3.1

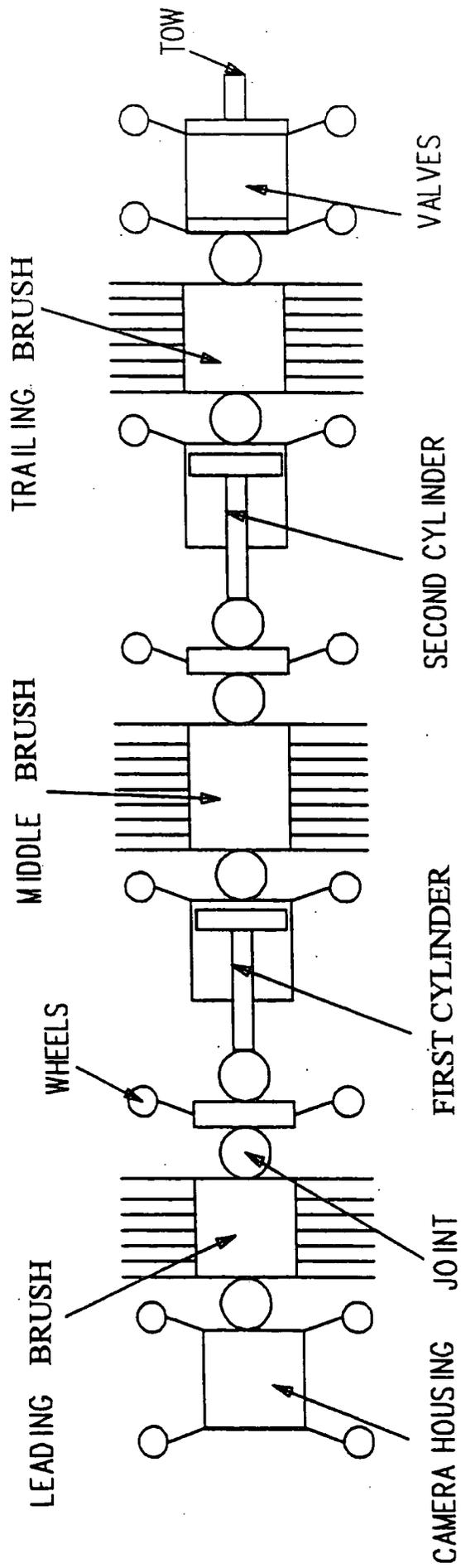Figure 3.2 illustrates the bearing joint assembly, each of which has a maximum angle
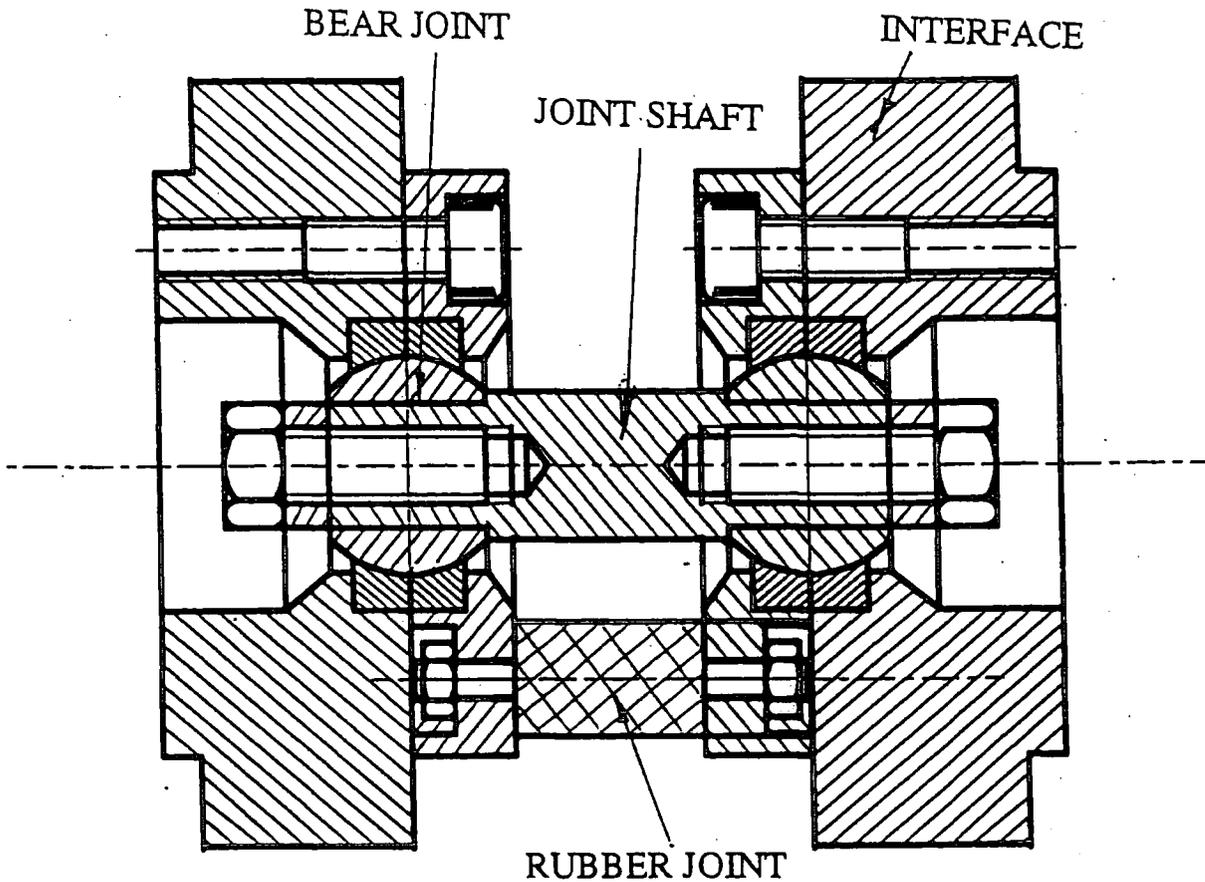
of displacement that was adjustable up to 15°.

Figure 3.2 Bearing joint assembly

Ahead of the leading brush, was a camera housing for mounting an inspection camera

and lighting. Behind the trailing brush there was a tow coupling, so that sensor

devices might be attached. The full set of drawings can be found in the Appendix A.

4. Experimental Study

4.1 Experimental Investigation on a Steel Bristled Robot

A steel bristled robot capable of handling 1½D bends and of towing a sensor device was designed, built and successfully tested.

The object of the following experiments was to investigate the mechanical behaviour of the robot during movement through the pipe, and also the effect of payload on the traction performance of the robot. The experiments were carried out using a load cell fitted at various points in the robot structure and a chart recorder logged the results.

4.1.1 Calibration

In order to convert the chart recorded readings into values of force; the load cell was calibrated.

The load cell was able to measure the force in both tension and compression. For calibration it was clamped into a tensometer, which indicated the load applied, while the chart recorder plotted a graph of the load cell measurement. The calibration graph is as shown in Figure 4.1.1

Figure4.1.1 LARGE LOAD CELL CALIBRATION
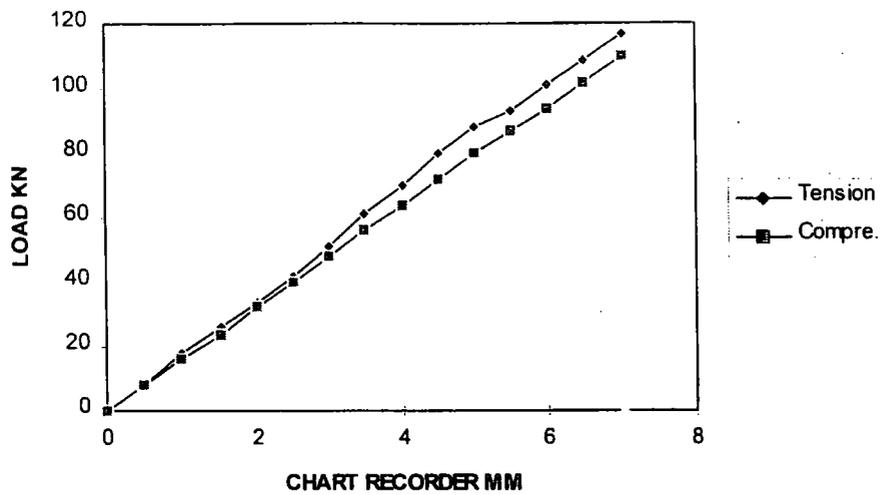
4.1.2 Experimental method and results

A load cell was used to measure the forces due to the robot moving. The load cell was put in two positions on the robot during experiments. Figure 4.1.2 shows the simplified structural model with the load cell in the first position; Figure 4.1.3 shows the simplified structural model with the load cell in the second position.
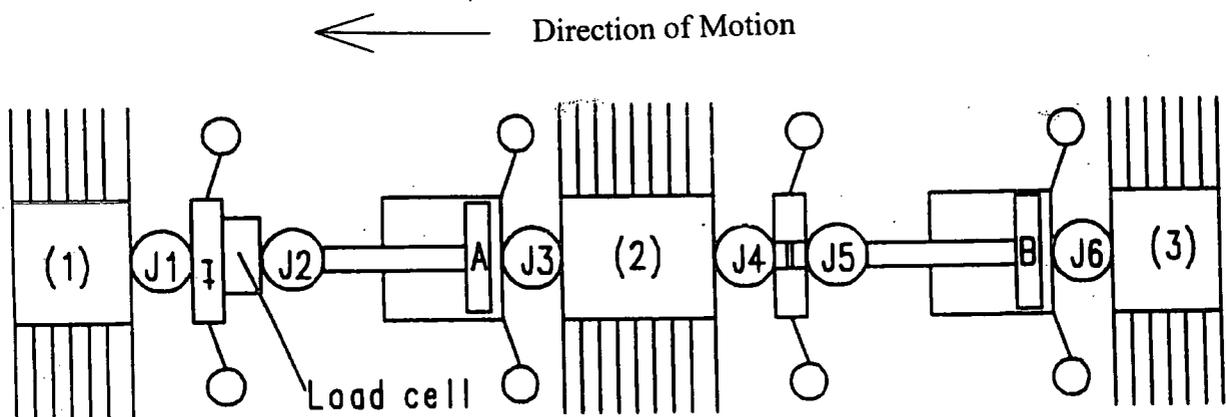
⟵——— Direction of Motion

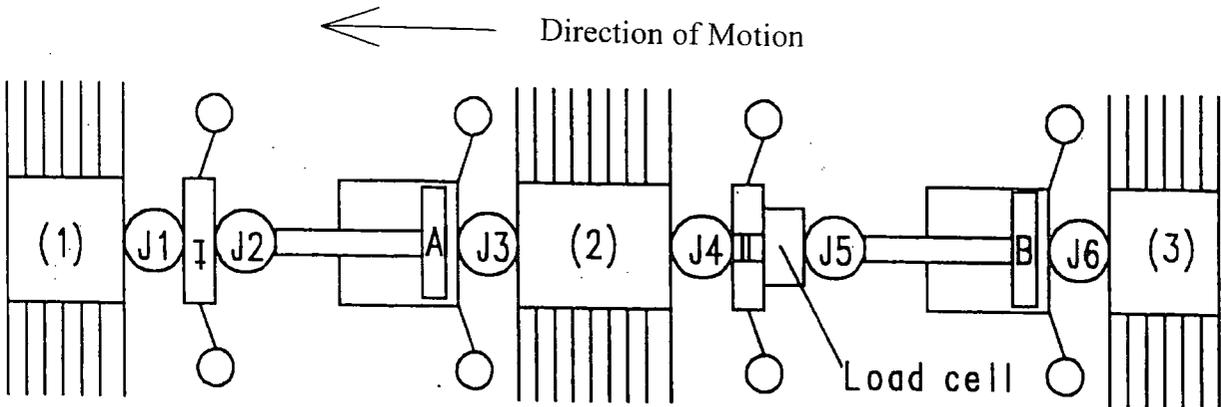Figure 4.1.2 Load cell on the first position

Figure 4.1.3 Load cell on the second position

Key:

(1)--- First brush; (2)--- Middle brush; (3)--- trailing brush;

J1, J2, J3, J4, J5, J6, --- Joint;

A--- First cylinder; B--- Second cylinder;

I--- First interface; II--- Second interface.

The moving of the robot was achieved by using the curved brush as the means of propulsion and suspension. The brushes were driven by the pneumatic cylinders. When the cylinder opens, the leading brush offers low resistance and will easily move, the trailing brush offers high resistance to backward motion and hence remains stationary. When the cylinder closes, the leading brush offers high resistance to movement and remains stationary whilst the trailing brush offers low resistance and is easily pulled forward. As mentioned previously, the movement of the robot was achieved by means of the three sets of steel brushes, which go through a specific cycle, consisting of three stages, repeatedly, to cause the robot to move. The following diagrams illustrate those stages in detail. Figures 4.1.4-6.
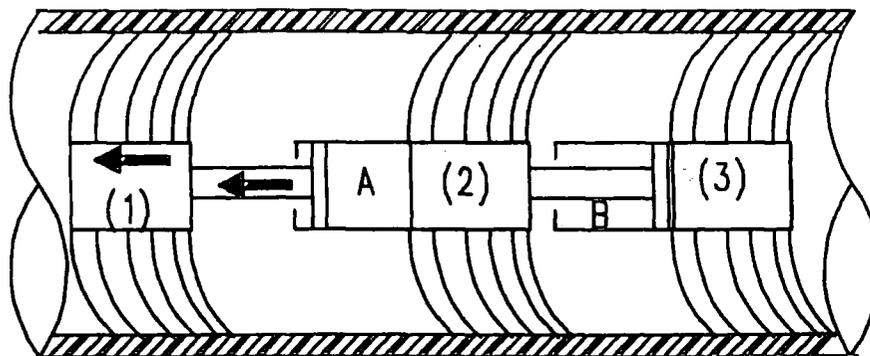
Figure 4.1.4 Stage1

Stage1: when cylinder A is opening, brush (1) moves, brush (2) and (3) remain stationary.
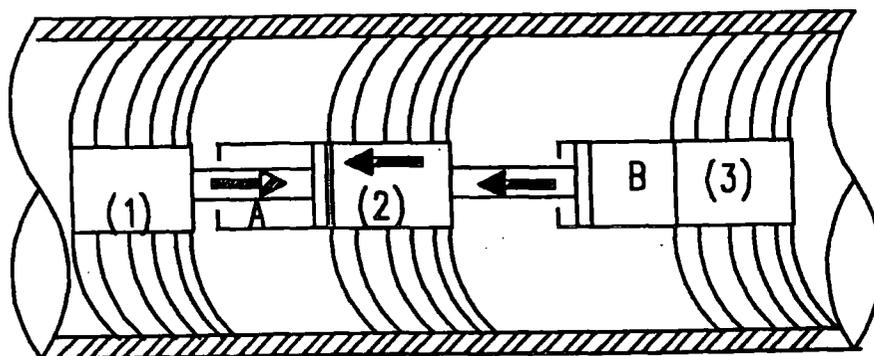
Figure 4.1.5 Stage2

Stage2: when cylinder B is opening and cylinder A is closing, brush (2) moves, brush (1) and (3) remain stationary.
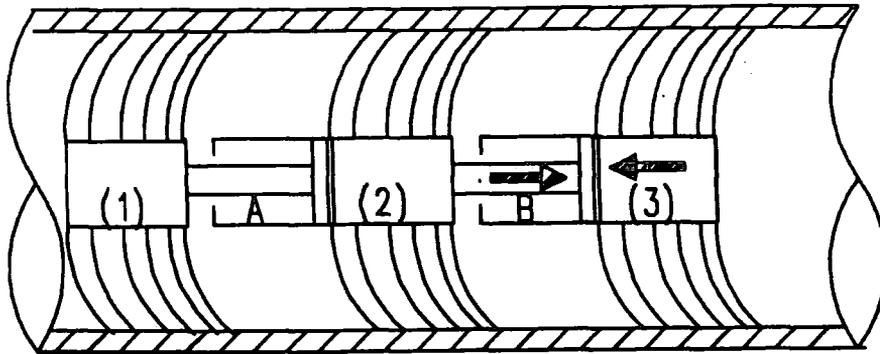
Figure 4.1.6 Stage3

Stage3: when cylinder B is closing, brush (3) moves, brush (1) and brush (2) remain stationary

The air supplied to the cylinder was controlled by two on-board solenoid valves, which are two - way, so the pneumatic cylinder could be driven under pressure in both directions. The actual speed of the opening and closing of the cylinders was regulated by a controller. An umbilical was used to connect the controller and air supply to the robot as fig.4.1.7 shows.

The Experimental Conditions:

The Fig.4.1.7 shows how the experimental conditions were set up. The system set up were as given below:

- Air pressure   16 bar

- Control speed of cylinder (straight pipe)   3.0

- Control speed of cylinder (bent pipe)   8.0

- Chart recorder feed rate   20mm/sec

- Chart sensitivity   40mV

- Load cell input   10mV
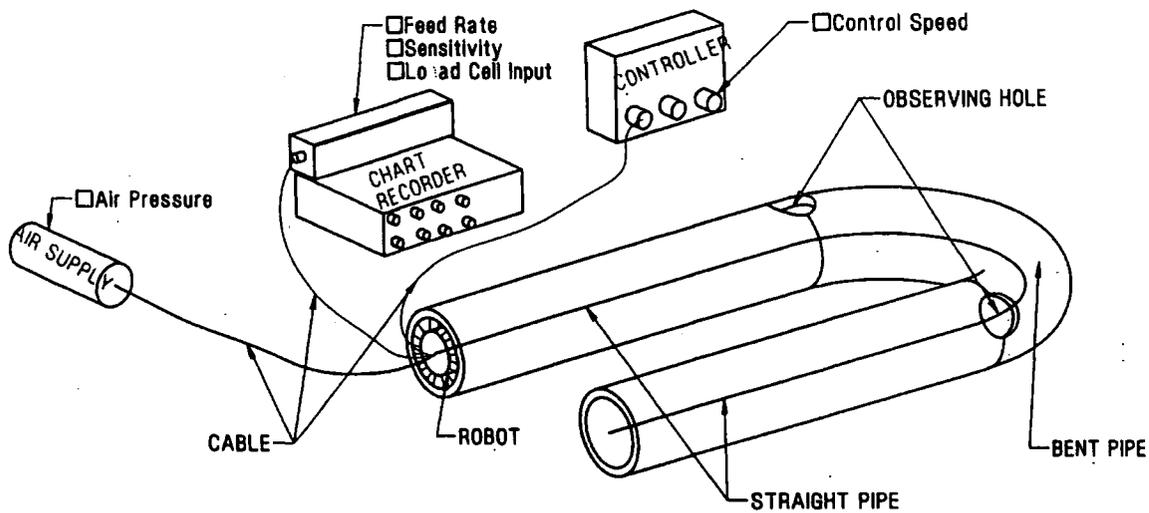
Figure 4.1.7 Schematic of the test rig.

The Experiments:

- *Test 1.* Load cell placed in first position

- *Test 2.* Load cell placed in first position with a wooden spacer in the trailing brush.

- *Test 3.* Load cell placed in the second position.

- *Test 4.* Load cell placed in the second position with a wooden spacer in the middle

brush.

- *Test 5.* Load cell placed in the second position with a steel spacer in the middle brush.

The Results

The force was created at the load cell when the brush was pulled forward or pushed back by the action of the cylinders. Figure 4.1.8 shows a cycle of the force plot logged by the chart recorder for load cell readings from the first position, Figure 4.1.9 shows the values for the readings taken from the second position.
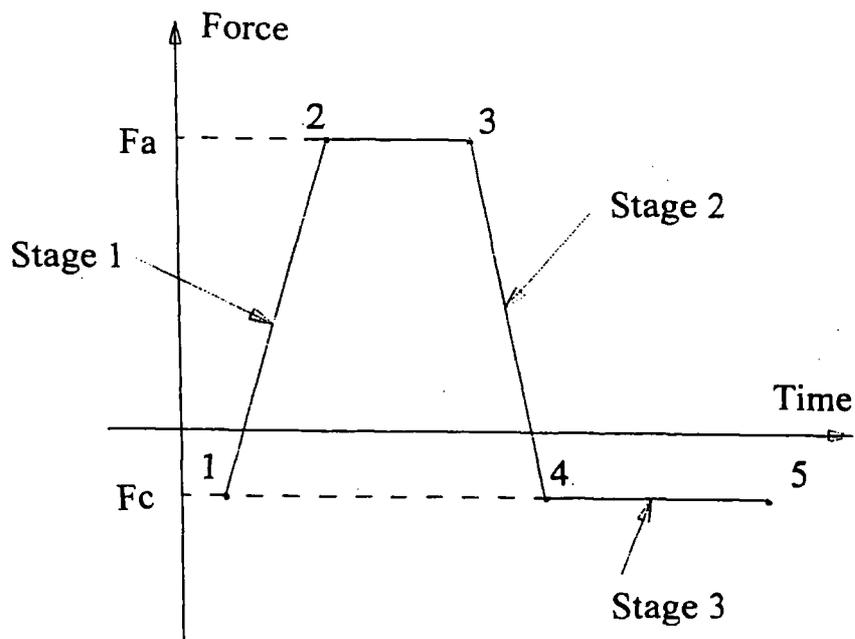
Figure 4.1.8 Force plot when the load cell on the first position
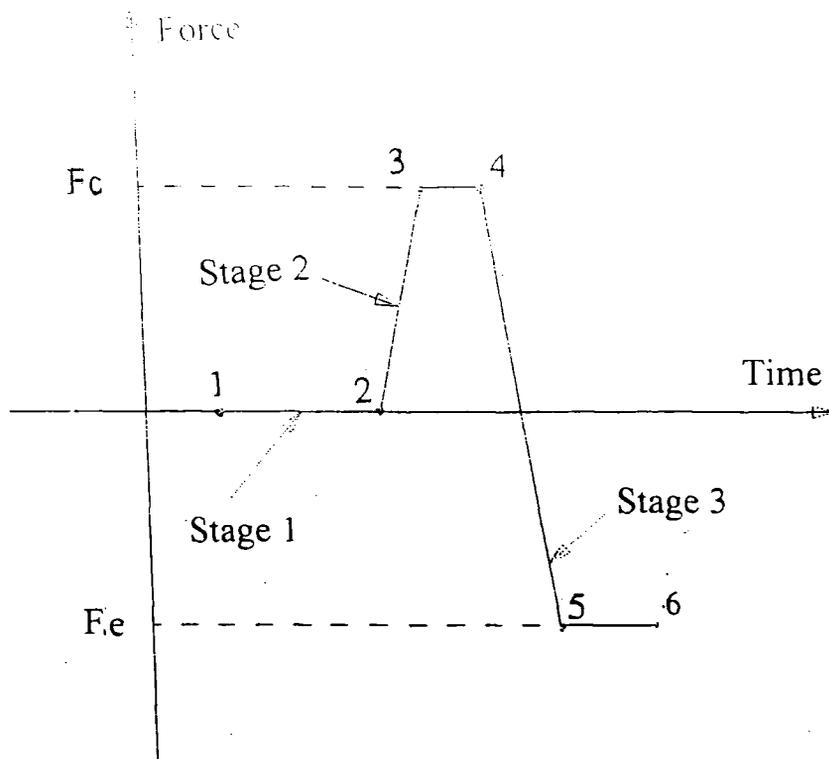
Figure 4.1.9 Force plot when the load cell on the second position

As the Figure 4.1.8 shows, the stage1 was from point 1 to point 3; the stage2 was from point 3 to point 4 and the stage3 was from point 4 to point 5. In the stage1, expand the first cylinder, force builds up from point 1 to point 2 until it overcomes friction then the leading brush moves forward. During the leading brush moving, the force was equal to the resistant force of the leading brush to point 3. In the stage2, contract the first cylinder, immediate reversal of load to a tensile load but friction could not be overcome so tension was locked at half level required to move the middle brush. In the stage3, hold the first cylinder as the second cylinder drags the trailing brush, it had no effect on force at load cell because middle brush was able to take all force. But friction and stiffness at the leading brush and the middle brush lock in tensile force, that was from point 4 to point 5 which was no force changed.

As the Figure 4.1.9 shows, the stage1 was from point 1 to point 2; the stage2 was from point 2 to point 4 and the stage3 was from point 4 to point 6. In the stage1, hold the second cylinder as the first cylinder push the leading brush, it had no effect on force at load cell because middle brush was able to take all force. In the stage2, contract the first cylinder and expand the second cylinder, increase in compressive force to overcome resilience then movement from point 2 to point 3, lock in force at end of movement from point 3 to point 4. In the stage3, hold the first cylinder as contract the second, tensile force was built up from point 4 to point 5 and the trailing brush moves tensile force locked in point 6.

As above description, the force 'Fa' was represented the resistance force of the leading brush; the force 'Fc' was represented the resistance force of the middle brush; the force 'Fe' was represented the resistance force of the trailing brush. Because the performance of the robot depends on the force in the brushes, the forces of 'Fa', 'Fc' and 'Fe' could be picked up from the full set plots of chart record. The results of the tests were able to be summed as the figure 4.1.2a, figure 4.1.2b and figure 4.1.2c.

Figure 4.1.2a shows the mechanical behaviour of the leading brush and the middle brush when the robot was run through a pipe. As the figure 4.1.2a shows, the robot was run through firstly a straight pipe and the resultant maximum forward force of them being 82 KN. Secondly the robot was run through a 1 1/2D bent pipe, which could be identified, by the observing hole (figure 4.1.7) and the maximum forward force was shown to be 197 KN.
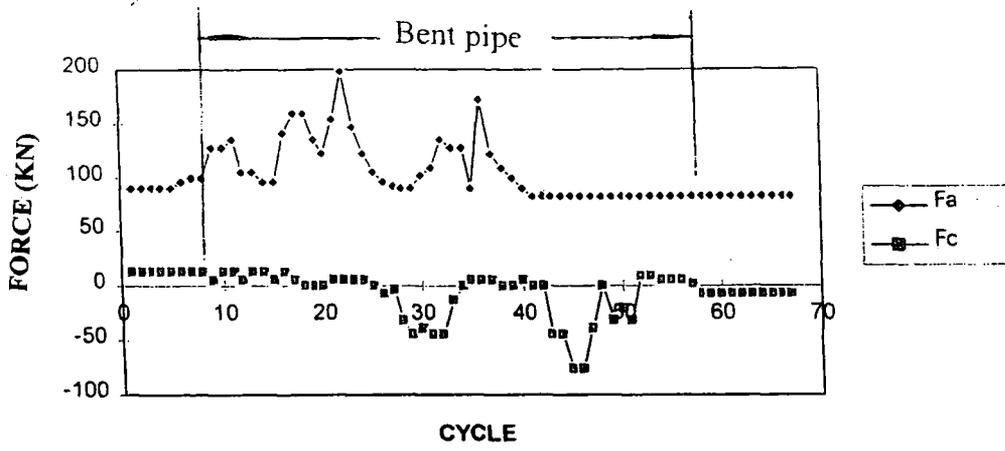
Figure 4.1.2a TEST1
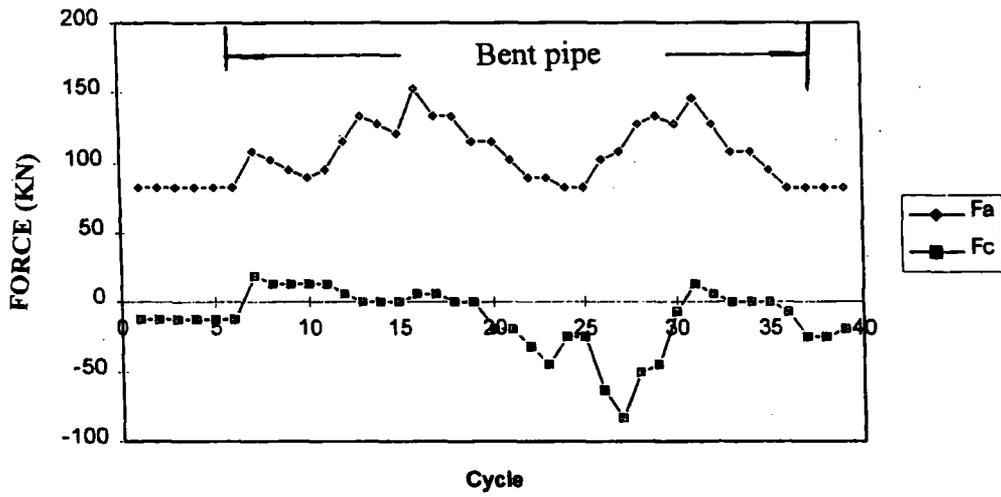
Figure 4.1.2b TEST2
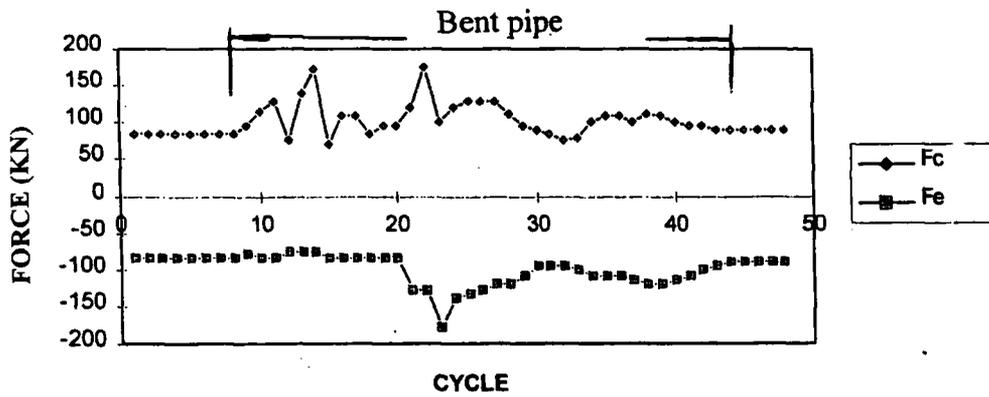
Figure 4.1.2c TEST3

33

In some particular requirment that the robot need to carry the inspection device in the brush. It means the length of the brush would be longer. So the investigation of the effect that the unit length of the brush had been carrying out. There were two sort of spacer had been put in the middle brush. One of them was a wood spacer and another was a 6.9kg steel spacer. The results were showed in figure 4.1.2d and figure 4.1.2e.
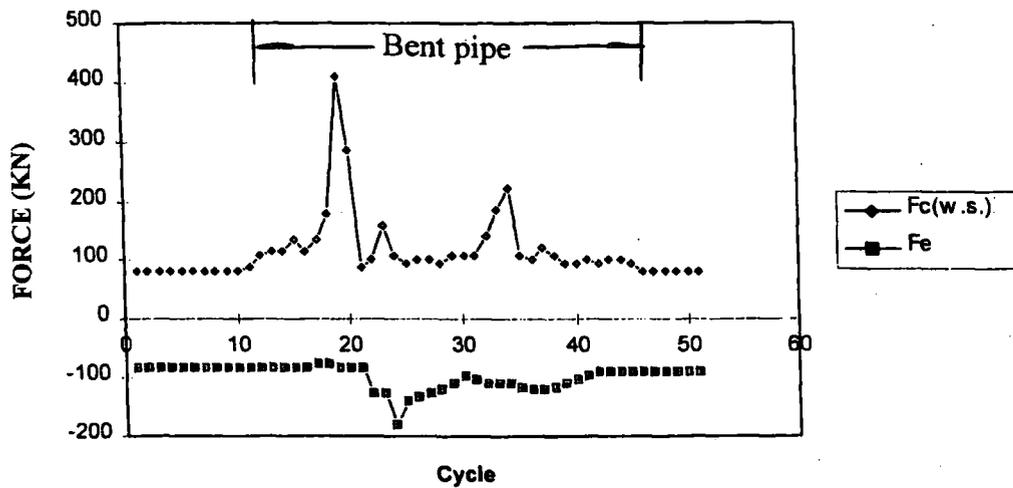
Figure 4.1.2d TEST4

Figure 4.1.2e TEST5

34
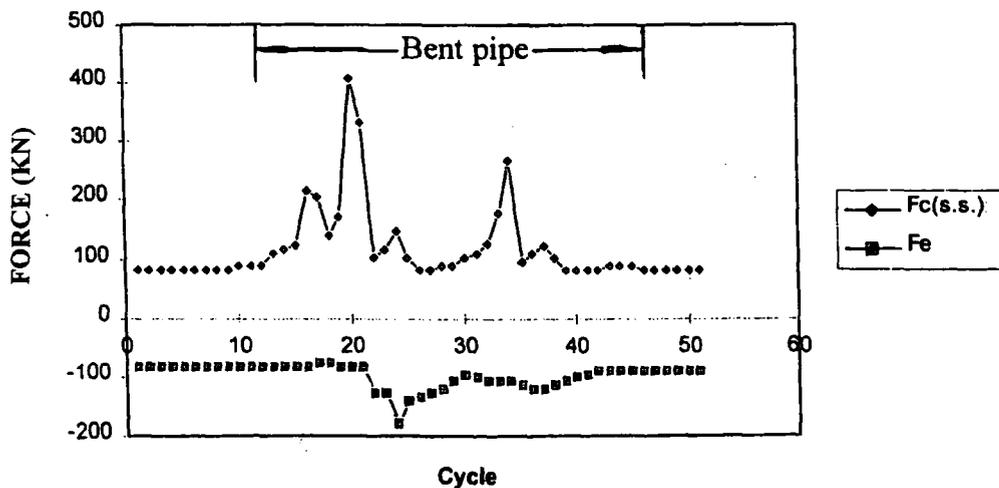
For comparison, sum figure 4.1.2c, figure 4.1.2d and figure 4.1.2e up as figure 4.1.10.
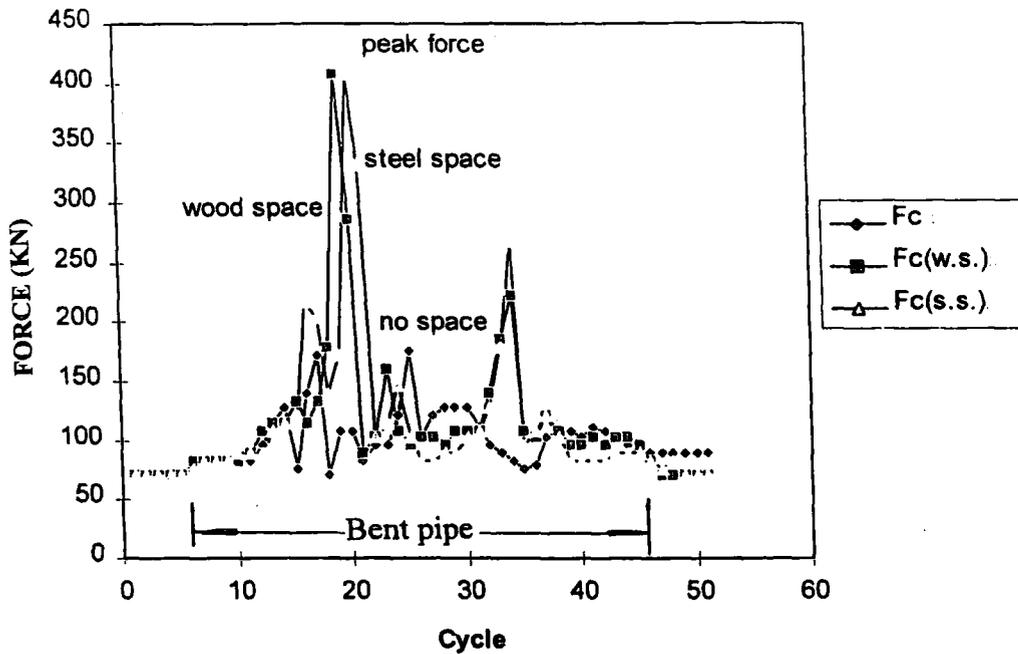
Figure 4.1.10 Mechanical behaviour of the middle brush through a pipe

(1) with no spacer; (2) with wood spacer; (3) with steel spacer.

Figure 4.1.10 shows the effect that the unit length of the brush had, on the robot's movement through a bent pipe. As can be seen, the weight of the spacer was not sufficient so as to be able to reverse the forward movement of the set of brush. In the straight pipe, the brush had the same amount of forward force with all three of the stipulated conditions, i.e. no spacer, with wooden spacer, with steel spacer. When the robot was sent through bent pipe, peak force was reached when there was a spacer in the brush. But when this point was reached, the robot stuck and the wheel was damaged before the robot could eventually pass. The full sets of records can be found in the Appendix D.

4.2   Experimental investigation of a plastic bristled robot

A plastic bristled robot has been developed at the School of Engineering University of Durham. This robot can swiftly move forward in the straight and bent pipe. The main feature of this robot was that it was easily controlled during experiments. The robot has a similar structure as the steel bristled robot.

This sort of robot was used to carry out inspection of the internal surfaces of pipe or other conduits. In the particular condition, the wheels would not be allowed to be used in the robot. The aim of this experimental study was to investigate the mechanical behaviour of the robot through a pipe without wheels compare with the robot with wheels.

The experiments were carried out using a load cell fitted at various points in the robot structure and a chart recorder recorded the results.

4.2.1   Calibration

In order to covert the chart recorder's readings into a value of force, the load cell was calibrated.

The load cell was put in a hanger. Weight block gives the load applied while the chart recorder records a graph. The load cell can measure the force by means of tension and compression. The calibration graph is shown on Figure 4.2.1a and Figure 4.2.1b.
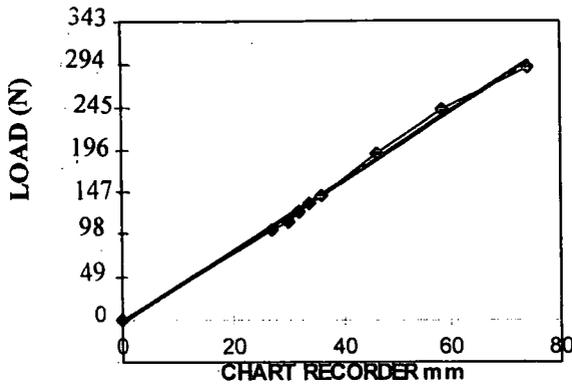
Figure 4.2.1a Small load cell calibration (compression)
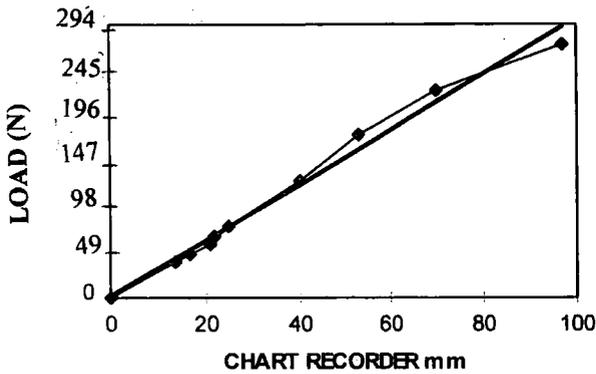
Figure 4.2.1b Small load cell calibration (tension)

4.2.2 Experimental method and results

A load cell was used to measure the forces due to the robot moving. The load cell was put in two positions on the robot during experiments. Figure 4.1.2 shows the simplified structural model with the load cell in the first position; Figure 4.1.3 shows the simplified structural model with the load cell in the second position.

Removed the wheels, Figure 4.2.2 shows the simplified structural model with the load cell in the first position; Figure 4.2.3 shows the simplified structural model with the load cell in the second position.
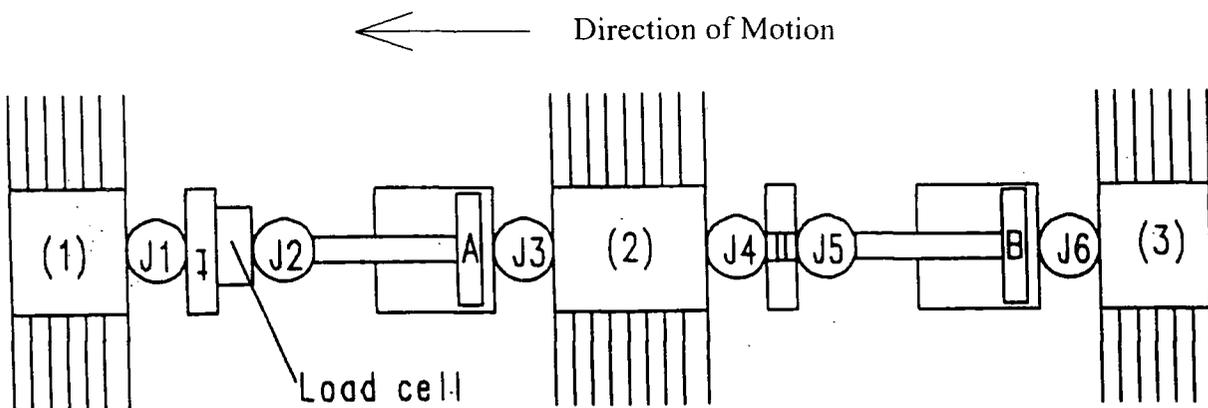
Figure 4.2.2 Load cell on the first position when the robot without wheels
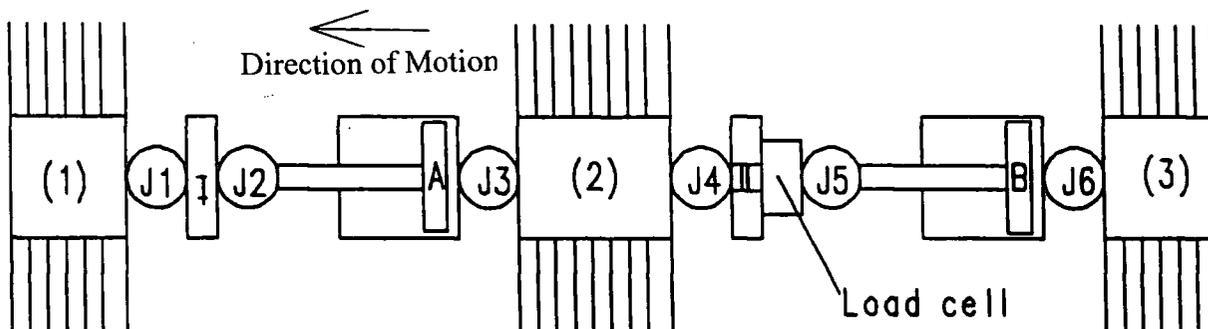
Figure 4.2.3 Load cell on the second position when the robot without wheels

(1)--- Leading brush; (2)--- Middle brush; (3)--- trailing brush;

J1, J2, J3, J4, J5, J6, --- Joint;

A--- First cylinder; B--- Second cylinder;

I--- First interface; II--- Second interface

The motion of the robot was achieved by the curved brush as the means of propulsion and suspension. The brush was driven by the pneumatic cylinders. When the cylinder opens, the leading brush offers low resistance and will easily move, the trailing brush offers high resistance to backward motion and hence remains stationary. When the cylinder closes, the leading brush offers high resistance to moment and remains stationary whilst the trailing brush offers low resistance and is easily pulled forward. As mentioned previously, the movement of the robot is achieved by means of the three sets of steel brushes, which go through a specific cycle, consisting of three

stages, repeatedly, to cause the robot to move. The cycle includes 3 stages as figures 4.1.4, figure4.1.5 and figure4.1.6 show.

Two on-board solenoid valves controlled the air supplied to the cylinder. These valves are two ways, so the pneumatic cylinder could be driven under pressure in both directions. The speed of the opening and closing of cylinders was regulated by a controller. An umbilical was used for connecting the controller and air supply to the robot as figure 4.1.7 shows.

The Experimental Conditions:

The figure 4.1.7 shows how the experimental conditions were set up. The system set up were as given below:

- Air pressure   8 bar

- Control speed of cylinder   3.0

- Chart recorder feed rate   20 mm/sec

- Chart sensitivity   10 mV

- Load cell input   25 mV

The Experiments:

- Test1. Load cell on the first position as Figure 4.1.2 shows.

- Test2. Load cell on the first position and removed off the wheels as Figure 4.2.2 shows.

- Test3. Load cell on the second position as Figure 4.1.3 shows.

- Test 4. Load cell on the second position and removed off the wheels as Figure 4.2.3 shows.

The Results:

The force was created at the load cell when the brush was pushed forward or pulled backward by the action of the cylinders. The figure 4.2.5 and figure 4.2.6 illustrated a cycle of the force plot logged by the chart recorder.

As the figure 4.2.5 shows, the stage1 was from point 1 to point 4; the stage2 was from point 4 to point 5 and the stage3 was from point 5 to point 6. In the stage1, expand the first cylinder, force builds up from point 1 to point 2 until it overcomes friction then the leading brush moves forward. When the leading brush was accomplished the forward motion, the spring joint released the compressor force that was from point 2 to point 3 and no force change to point 4 until the stage 2 occur. In the stage2, contract the first cylinder, immediate reversal of load to a tensile load to pull the middle brush and move it forward. In the stage3, hold the first cylinder as the second cylinder drags the trailing brush, it had no effect on force at load cell because middle brush was able to take all force. But friction and stiffness at the leading brush and the middle brush lock in tensile force, that was from point 5 to point 6 which was no force changed.

As the Figure 4.2.6 shows, the stage1 was from point 1 to point 2; the stage2 was from point 2 to point 5 and the stage3 was from point 5 to point 7. In the stage1, hold the second cylinder as the first cylinder push the leading brush, it had no effect on force at load cell because middle brush was able to take all force. In the stage2, contract the first cylinder and expand the second cylinder, increase in compressive
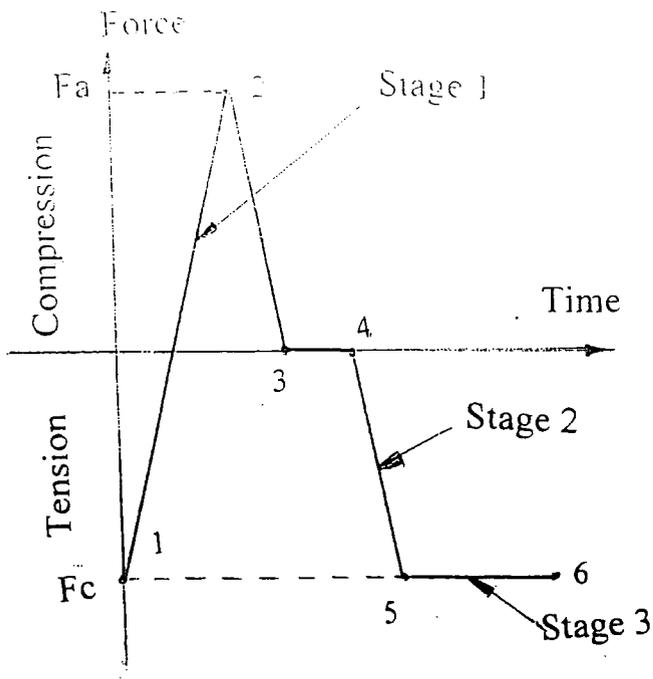
Figure 4.2.5 Force plot when the load cell on the first position
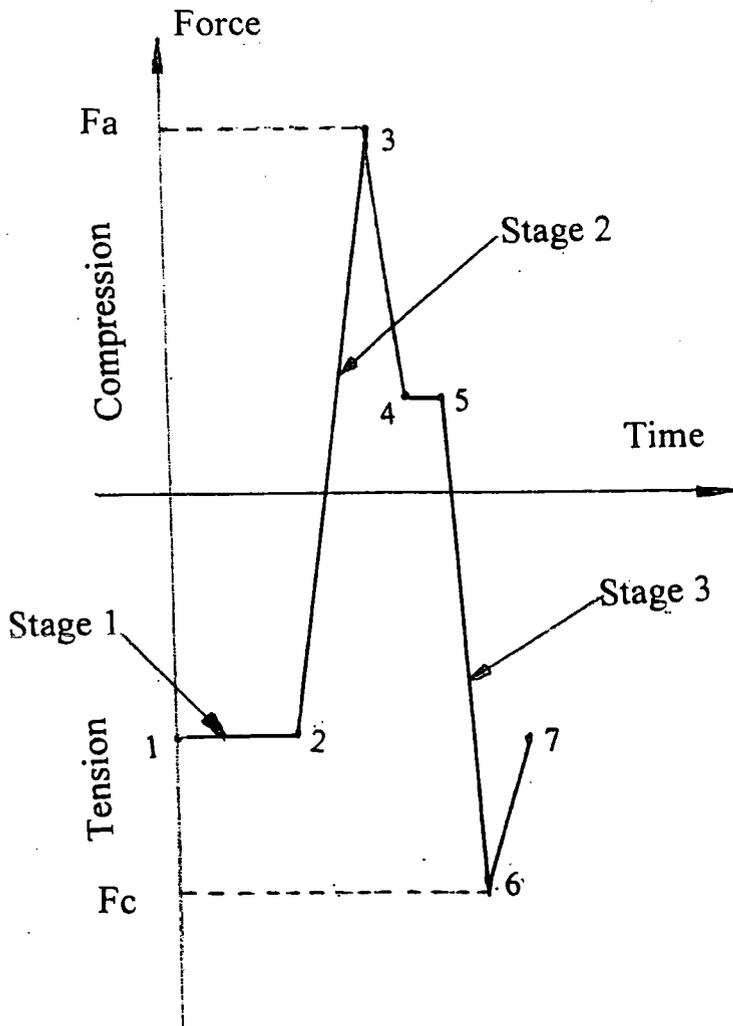
Figure 4.2.6 Force plot when the load cell on the second position

force to overcome the friction then movement from point 2 to point 3. The spring joint released the compressive force whilst the middle brush finished forward motion from point 3 to point 4 and locked this force to point 5 until the stage 3 occur. In the stage3, hold the first cylinder as contract the second, tensile force was built up from point 5 to point 6 and the trailing brush move, tensile force was released by the spring joint to point 7 when the trailing brush finished motion.

As above description, the force 'Fa' was represented the resistance force of the leading brush; the force 'Fc' was represented the resistance force of the middle brush; the force 'Fe' was represented the resistance force of the trailing brush.. Because the performance of the robot depends on the force in the brushes, the forces of 'Fa', 'Fc' and 'Fe' could be picked up from the full set plots of chart record. The results of the tests were able to be summed as the figure 4.2.7, figure 4.2.8, figure 4.2.9 and figure 4.2.10.
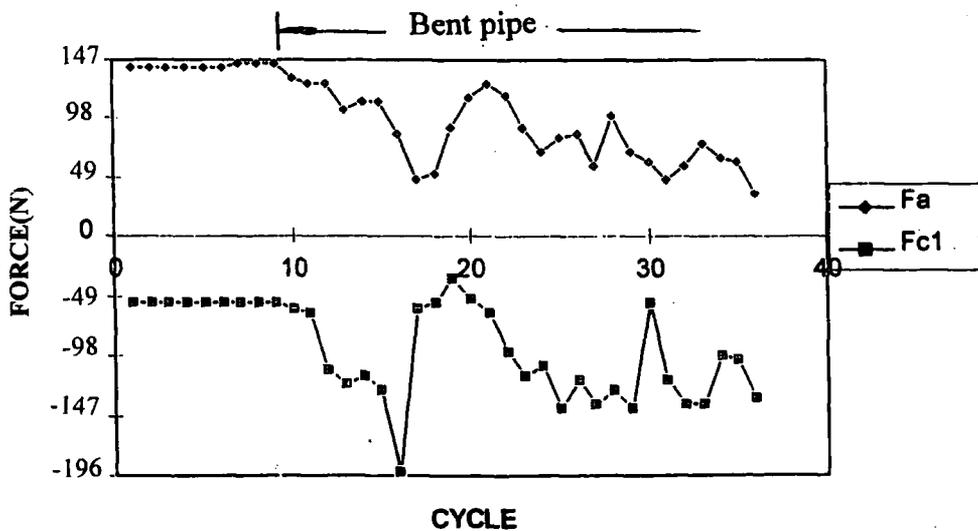
Figure 4.2.7 Test1
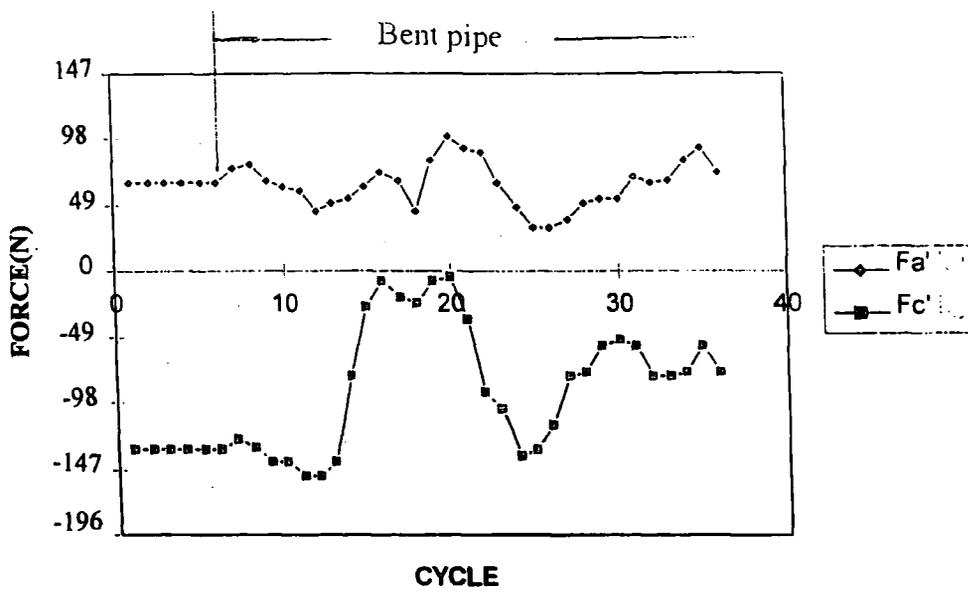
Figure 4.2.8 Test2

Figure 4.2.9 Test3
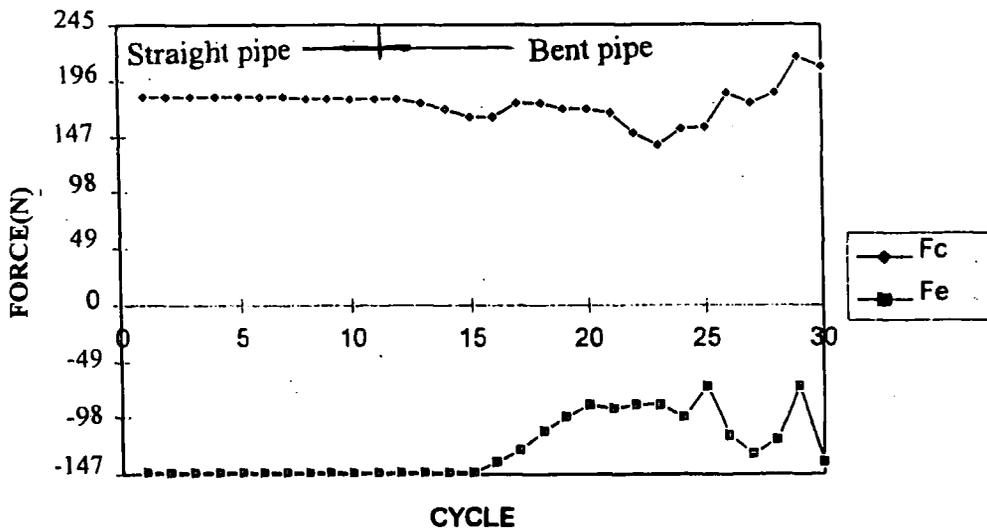
Figure 4.2.10 Test4

For investigating the effect of each brush whilst the robot had wheels and without wheels, sum figure 4.2.7 - 4.2.10 to figure 4.2.11 - 4.2.13:
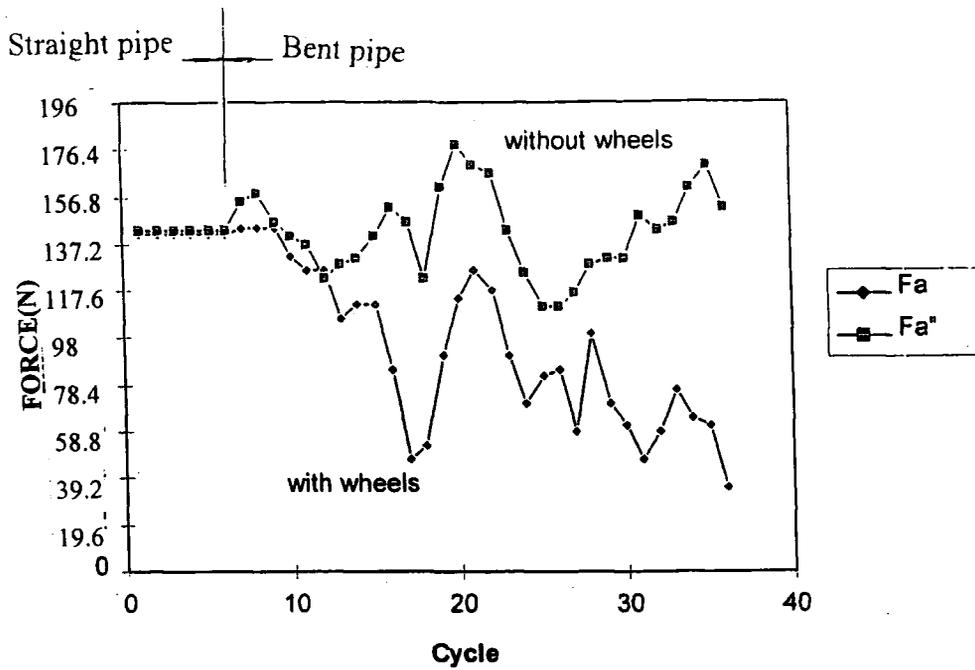
Figure 4.2.11 Mechanical behaviour of the leading brush whilst the robot with wheels and without wheels through a pipe.
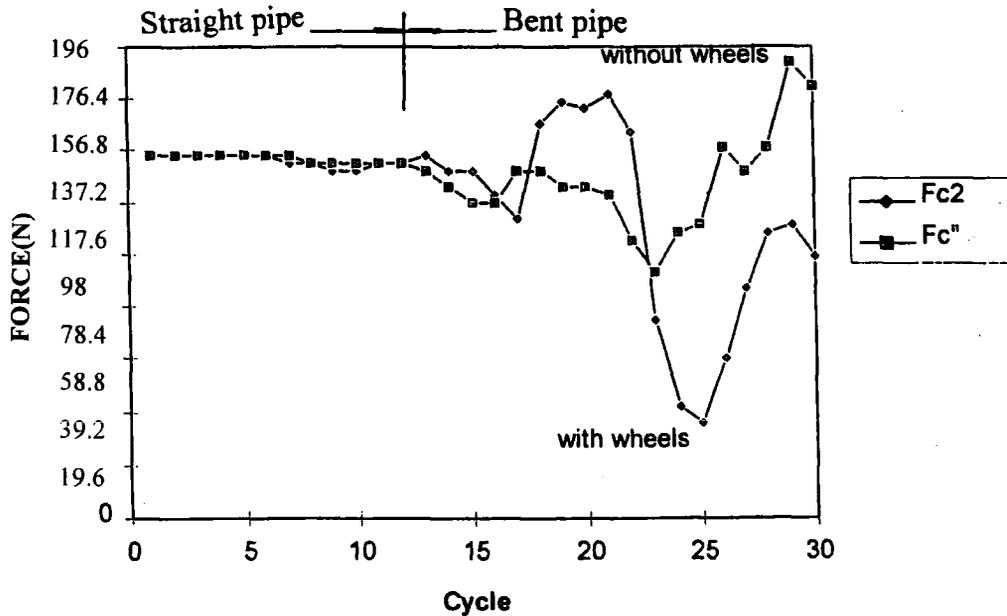
Figure 4.2.12 Mechanical behaviour of the middle brush whilst the robot with wheels and without wheels through a pipe.

Straight pipe | Bent pipe

FORCE(N)

0
-49
-98
-147
-196
-245

0   5   10   15   20   25   30

Cycle

wiith wheels

without wheels

Fe'
Fe

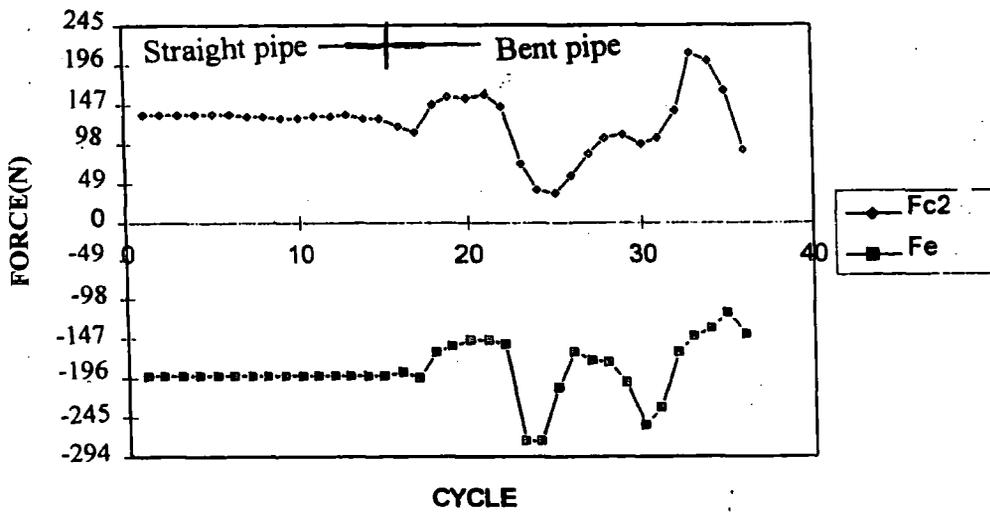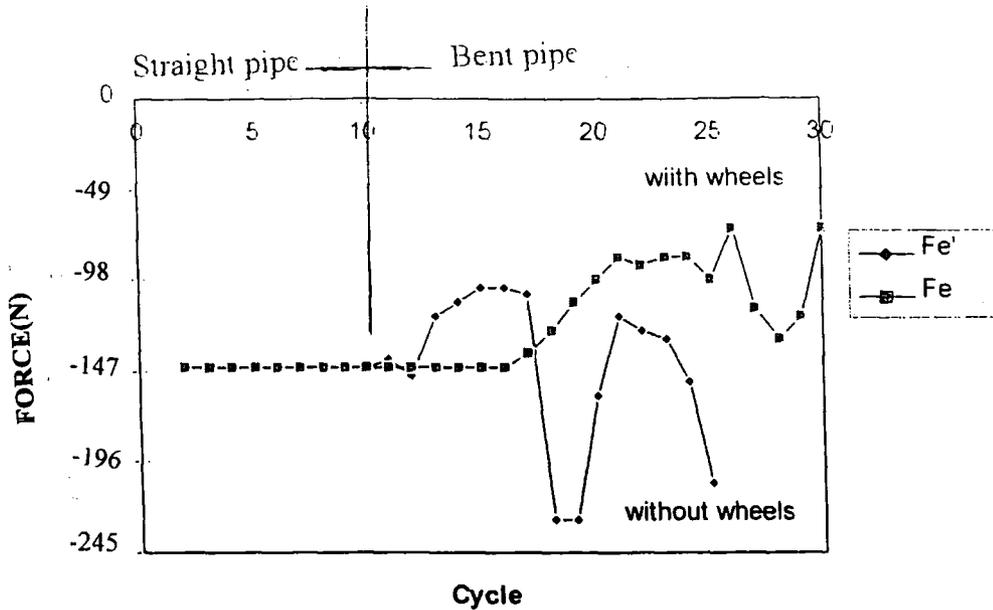Figure 4.2.13 Mechanical behaviour of the trailing brush whilst the robot with wheels and without wheels through a pipe.

Figure 4.2.11, figure 4.2.12 and figure 4.2.13 show the mechanical behaviour of the brushes due to the robot through a pipe, and the differences the addition of wheels making. In the straight pipe, the forward force of each brush was 15kg. The forward forces of pushed by cylinder when the robot with wheels was slightly lower than without wheels. It was because the wheels could restrict the twists of the joint to reduce the lost forces of the joint. So the forces of offering by the cylinder could be transferred effectively. In the bent pipe, the forward force of the brush when the robot without wheels was much higher than with wheels. One significant difference was that when the robot had no wheels, there was 'jack knifing' as it was sent through a bent pipe. The forward force in this type of robot was very depend on friction. While addition of wheels to the robot reduced this vital friction slightly, it did have the advantage of helping the robot to negotiate bends more safely through a bend smoothly. The forward force was major effect of sharp bend while the robot had wheels. The full readings can be found in appendix E.

The robot is used to carry the payload through a pipe. There are four types of payload could be used in the robot as follow:

1) No Payload:
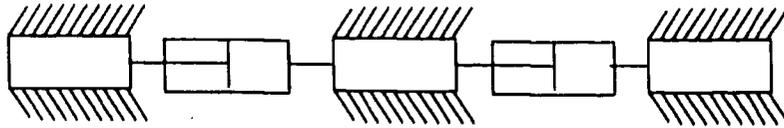
2) Tow load:
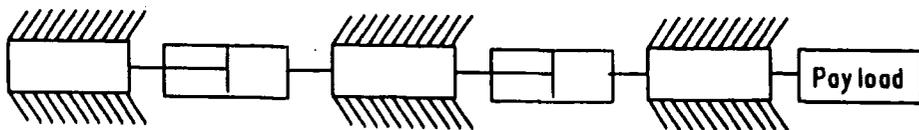
3) Transverse Load :
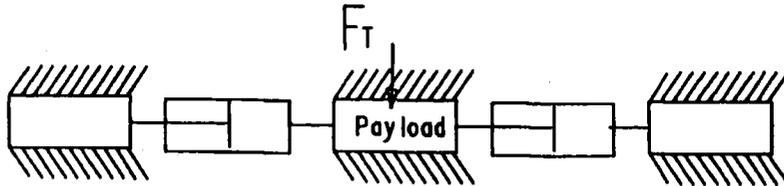
4) Torque Load:
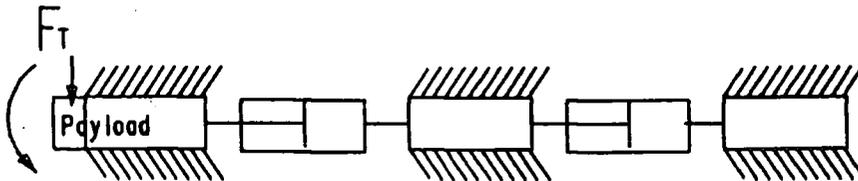
Since the performance of the robot depends so much on the brush. Static tests were carried out to investigate the effect of the transverse load and the torque load on the different brushes.

A test brush was put into a tube to simulate the action of the robot in a pipe. The tube was put onto a plate of a load machine. There was a fixture in the brush, which had contacted with a proving ring of the load machine and the machine applied the load to the brush. Three transducers were used to measure any displacements.
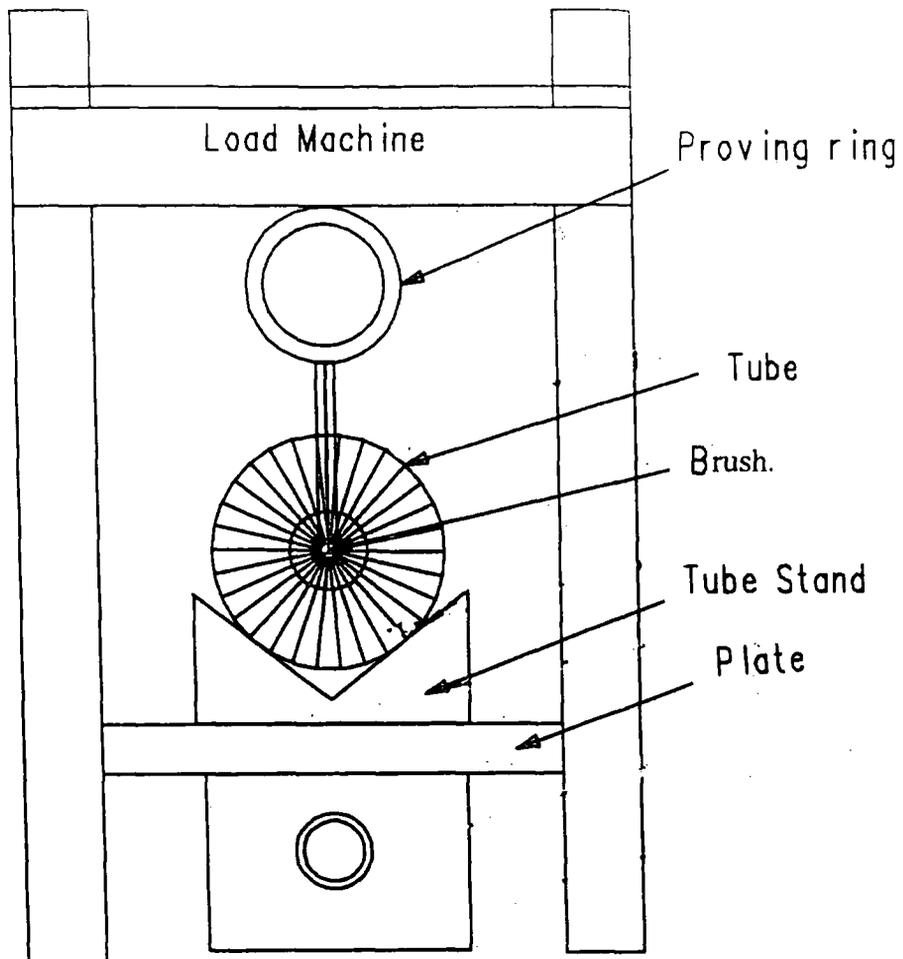
Figure 4.3.1 Test Assembly

As the Figure 4.3.1 shows, the plate of the load machine can move vertically by means of applying a load to it. A log was connected to the proving ring and the three transducers through different channels. The log can record automatically after a recording time was set up due to test.

4.3.1 Calibration

The log can record every channel signal by means of voltage. In order to convert the readings into a value of force and a value of displacement, proving ring and the three

transducers were calibrated. Calibrations were performed using a galvanometer and a specimen. The readings were shown on calibration graph.
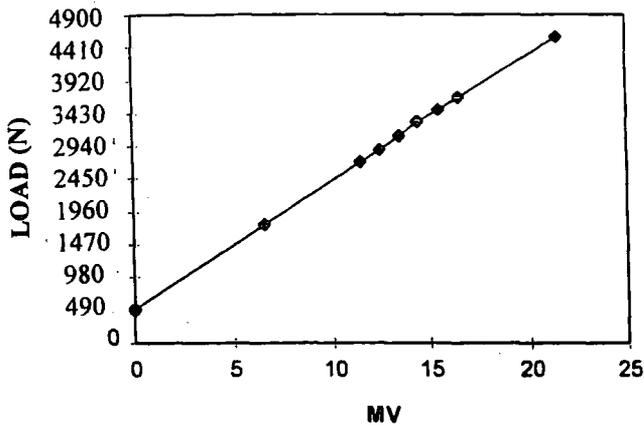
Figure 4.3.2 Proving ring calibration graph
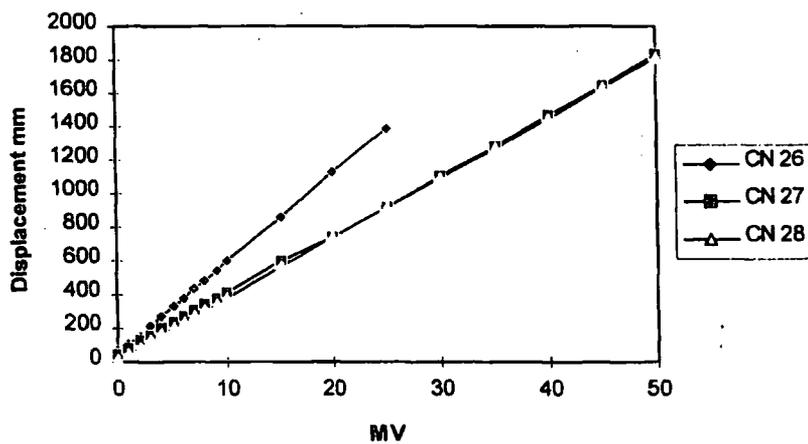
Figure 4.3.3 Three transducers calibration graph

4.3.2 Experimental Method and Results

4.3.2a Transverse load test

Three kinds of brush were used in this test:

(1) plastic brush: D = 182mm; d = 60mm; L = 100mm; a = $90°$

(2) steel brush: D = 182mm; d = 80mm; L = 70mm; a = $90°$

(3) 15 degree steel brush: D = 182mm; d = 80mm; L = 70mm; a = $75°$
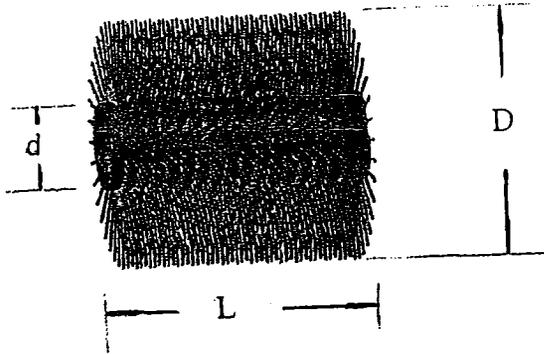
Figure 4.3.4 Test Brush

A 6 inches diameter tube of 200mm length was used. The log recorded channel 29
and channel 28 by means of load and displacement.
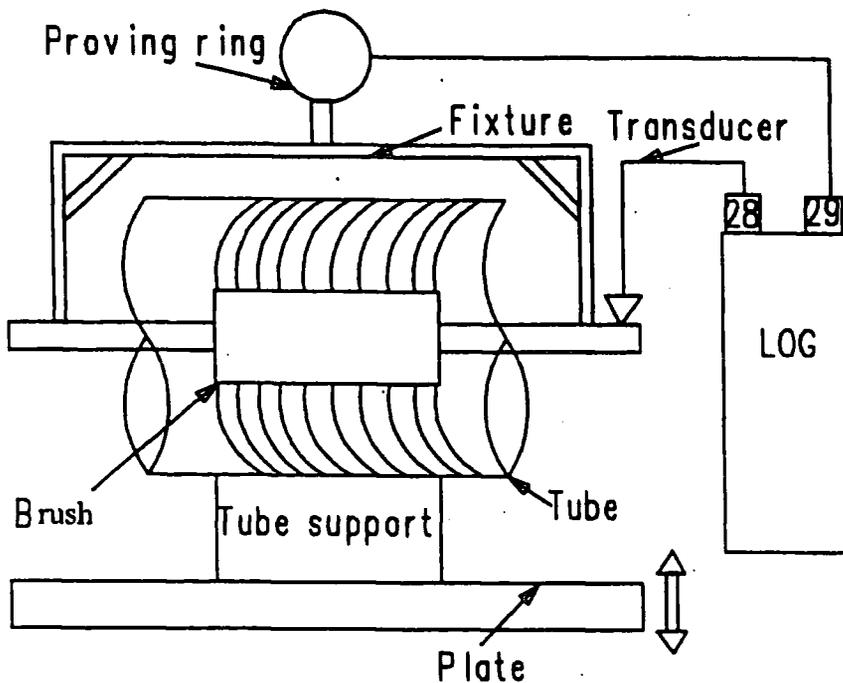
Figure 4.3.5 Schematic of transverse load test assembly

Figure 4.3.6 shows the results of the transverse load test. The maximum transverse load of the plastic brush was 392N. The maximum transverse load of the 15 degree steel brush was 1176N. The maximum transverse load of the steel brush was 1764N. The payload carrying capacity of steel brush was three times more than that of plastic brush when the load was applied on the brush.

4.3.2b Torque load test

Two brushes were used during this test: (1) plastic brush; (2) 15 degree steel brush. Log recorded channel 29, 28, 27, 26 by means of load and displacement. Figure 4.3.9 shows the results of torque load test for the two brushes.
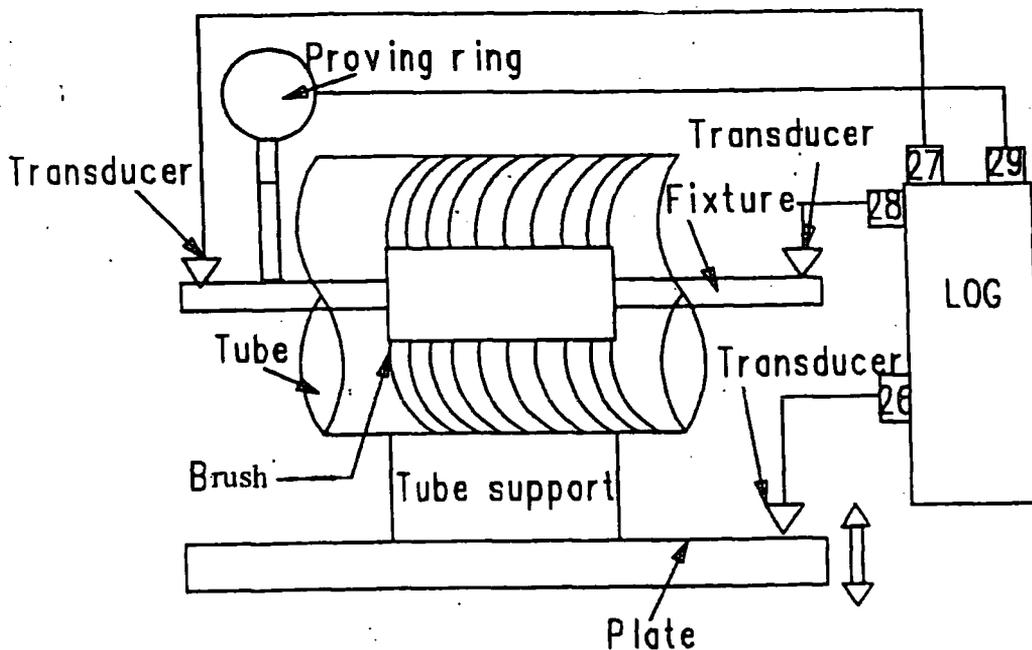
Figure 4.3.7 Schematic of torque load test assembly

TRANSVERSE LOAD TEST

Figure 4.3.6

51
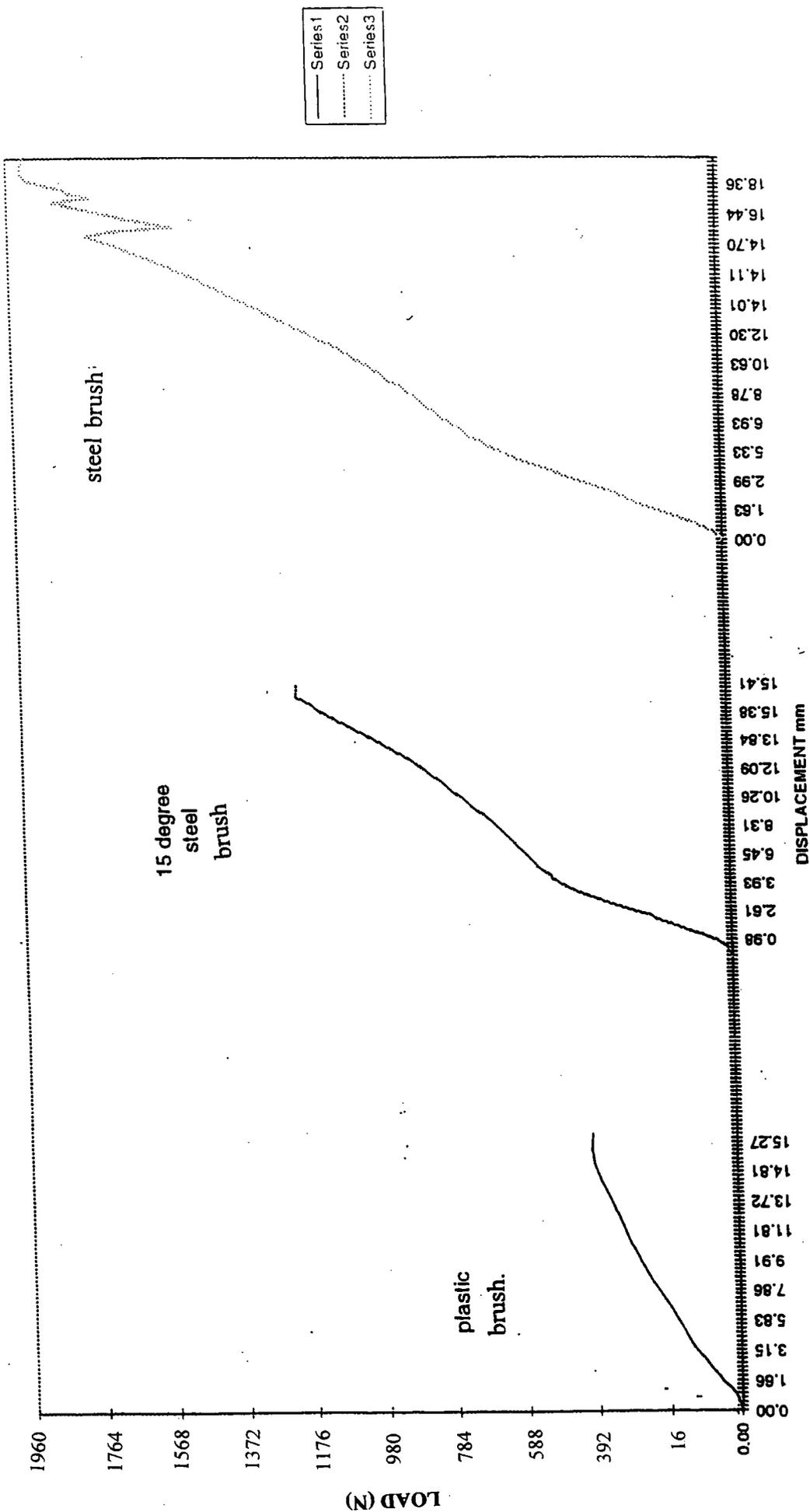
Angle was calculated from displacement of channel 28 (h1) and channel 27 (h2). As

Figure 4.3.8 shows: $\tan(a) = (h2) / h1 + L$.
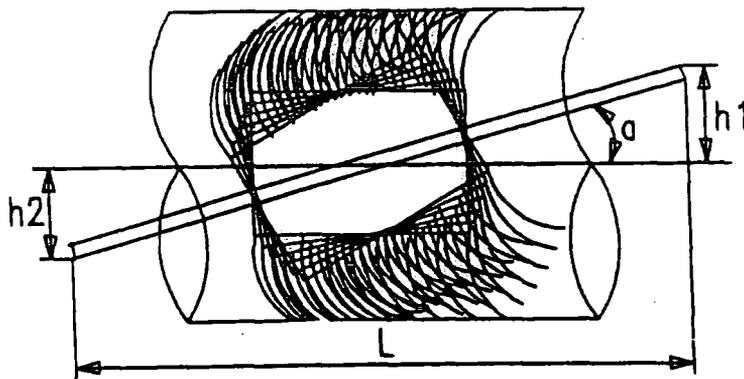
Figure 4.3.8 Angle calculate graph

Figure 4.3.9 shows the results of the torque load test. The maximum torque load of the plastic brush was 49N, whereas the maximum torque load of the 15 degree steel brush was 245N. The steel brush of head payload capacity was five times than plastic brush.

TORQUE LOAD TEST

steel brush

plastic brush

Series1
Series2

ANGLE DEGREE

LOAD (N)

Figure 4.3.9

53
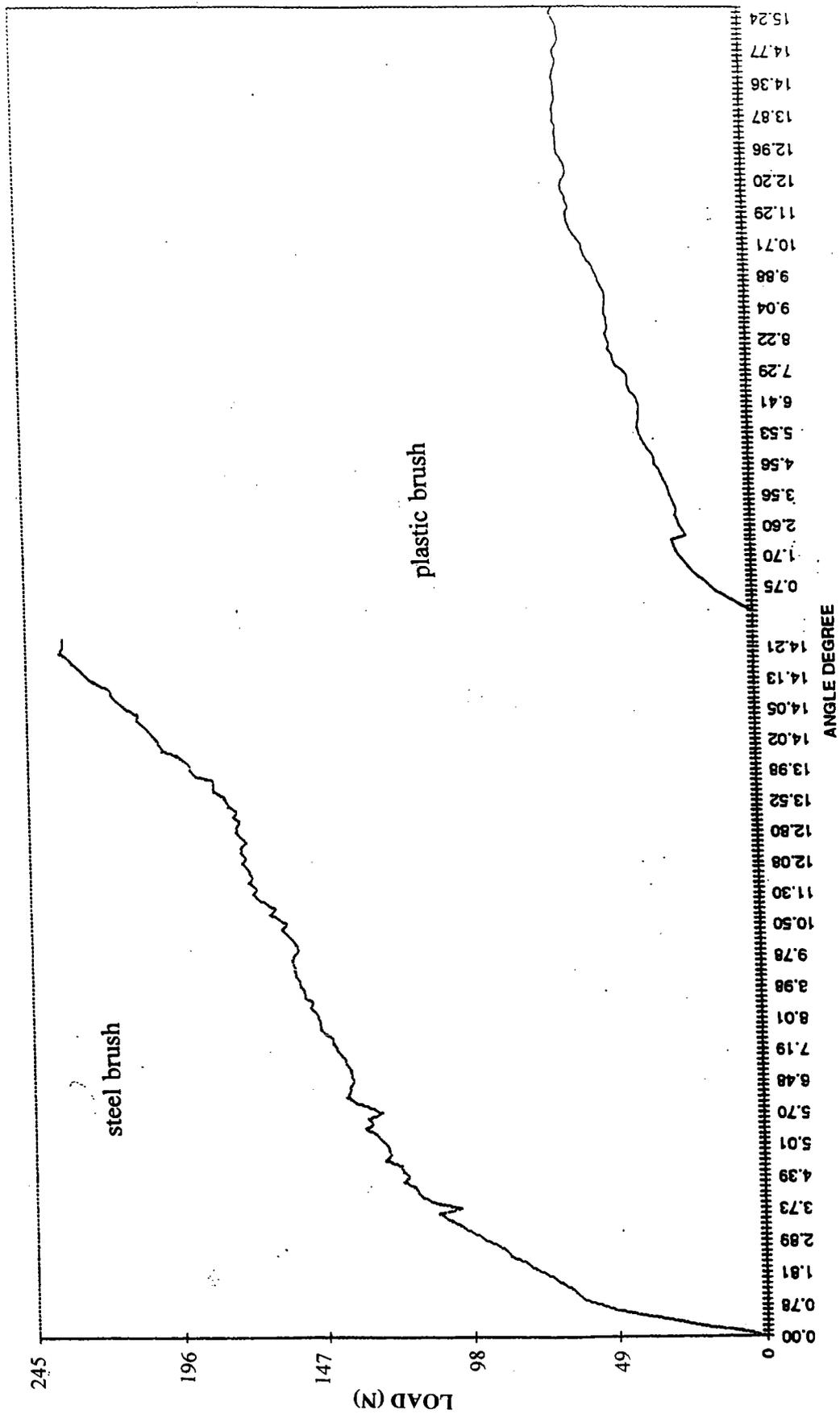
5 Discussion

5.1 Future Control Optimization

Compare Figure 4.1.8 with Figure 4.1.9, and then Figure 4.2.5 with Figure 4.2.6, which depict the force values recorded when the load cell was put in the two different positions.

Notice that the curves in Figures 4.1.9 and 4.1.8, show that there was no change in the force during stage 1 and stage 3 of the robot movement. This means that just one single stage could be used to replace the previous stages 1 and 3, thus optimising the motion of the robot to a two-stage cycle, which would work like this:

Stage 1: *When the first cylinder is opening and the second one is closing, the leading and the trailing brush move; the middle ones remaining stationary.*

Stage 2: *When the first cylinder is closing and the second one opening, the middle brush move; the leading and trailing brush remaining stationary.*

This control optimisation can be achieved by using a new valve instead of the previous two valves as Figures 5.1 and 5.2 show.
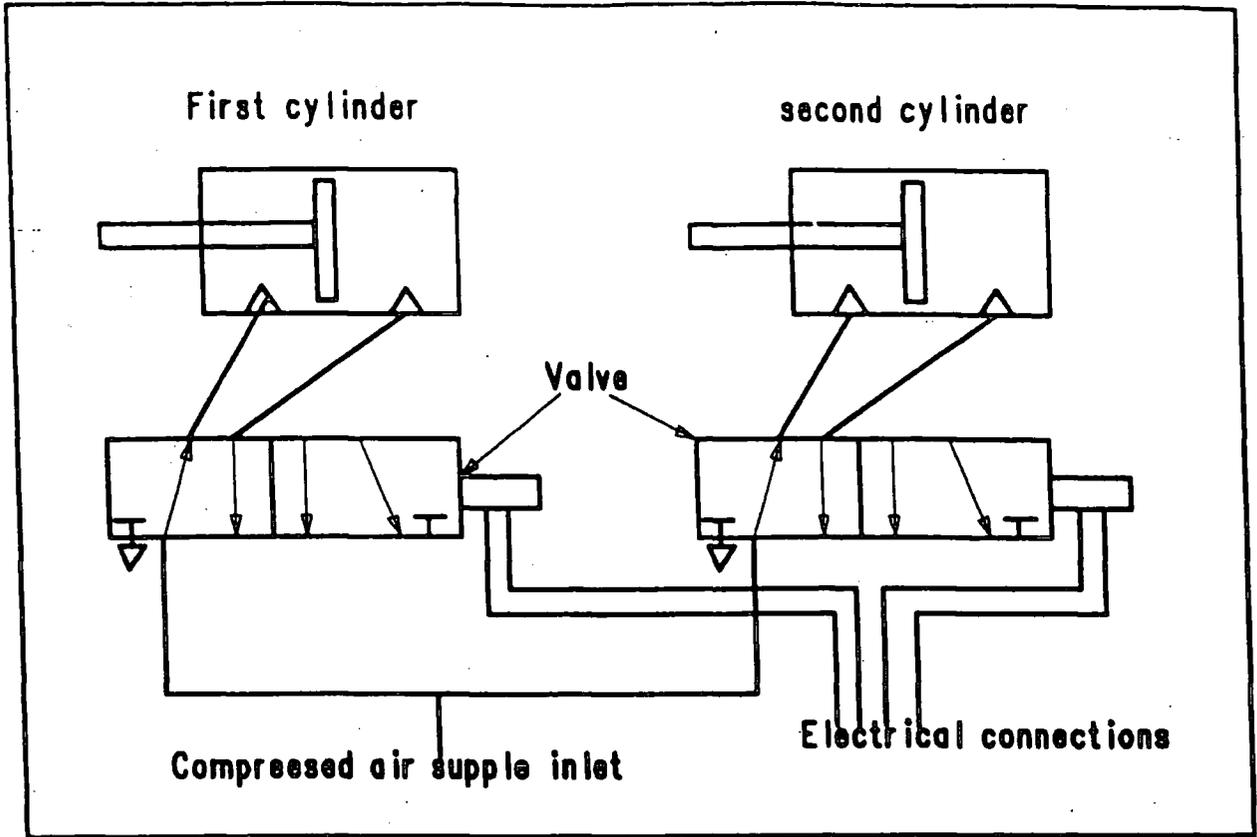
Figure 5.1 Previour control system
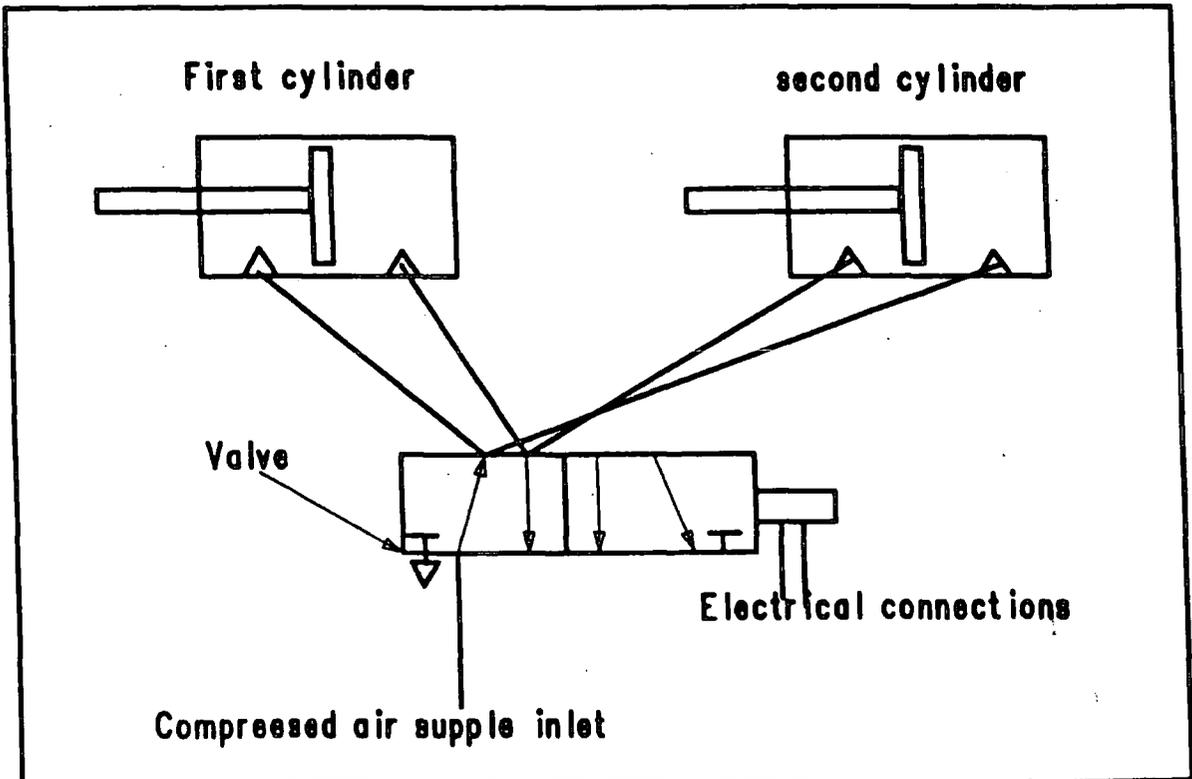
Figure 5.2 Modified control system

5.2   Improving The Structure Alignment System

The purpose of using wheels at all on the robot was to prevent diving or twisting of the brush during the time that the robot is moving. However, problems could arise if the robot encounters obstacles in the pipe, especially if it is a bent pipe.

If the through path's measurement is less than diameter (edge-to-edge) of the wheels, the robot will not be able to pass through without damaging the wheels, which was what happened when tests were carried out on the steel bristled robot.

As Figure 4.1.9 shows, at the peak force point, the robot stuck, and the wheels were damaged when there was a spacer in the brush. Spring wheels, however would allow the robot to overcome most obstacles and to negotiate sharper bends. When the through path narrows for whatever reason, the spring wheels would be forced to retract (temporarily) so as not to inhibit the robot's movement. Once past the obstacle, the wheels would return to their original position.

5.3 Artificially Intelligent Robot

The robot that was actually designed and tested was proven to be adept at moving progressively and effectively through pipes. The robot's overall performance, though, was dependent on the bristle. Table 1, which was included in part two of this thesis, set out the relationships between different factors pertaining to the bristle.

A version of pipe robot has now been developed at the School of Engineering, University of Durham, which utilises retractable brush, making possible the adjustment between the length of the bristle and the path gap *(h/l)*. In this way, the actual robot may be used, in accordance with the data given in Table 1, to negotiate through a large range of pipes, the brush being easily adjusted, to suit. Sensors or scanners would be used to provide detailed numerical information, and then according to the conditions detected, the bristles could be either retracted or extended to the required length. The addition of sensors and other control components would render the robot more effective and useful in a variety of working environments.

6 Conclusions

All the research objectives outlined at the start were reached during the course of this study.

- *A theory module for bristle was found*
- *A steel bristled propelled robot was designed, built and tested*
- *An experimental study of the mechanical behaviour of the robot, and some static tests were carried out*

During the study, a load cell was used to record the effect to the force value that the robot being utilised under different conditions experienced, with the result being the discovery that the operation to move the robot could be optimised from a three-stage to a two-stage cycle.

It was also found that the forward force of the steel brush was 82KN when the robot was travelling through a straight pipe, in comparison with the maximum force of 197KN when travelling through a 1½ D bent pipe, leading to conclude that the axial length of the brush unit is the design limit length.

The experiments carried out on the plastic bristled robot focused on the behaviour of the brushes when the robot was sent through a pipe, firstly with, and then without wheels. In both straight and bent pipes, a robot with wheels was capable of slightly less forward movement with one push of the cylinder, than its wheel-less counterpart.

The static test showed that the payload-carrying capacity of steel brush was three times greater than that of plastic brush, whereas the head payload carrying capacity of the steel brush was five times that of the plastic brush.

The fundamental principles governing the actual bristle, show that the maximum load is 39.2% greater than buckling force, and that the maximum length of bristles is 41.89% longer than the path gap between the pipe wall and the core of the bristle.

Many other ideas were generated during the course of the study, providing substantial scope for further development of these ideas. These included:

- *Improving the robot control system.* This could include the idea of using one instead of two valves, thus reducing the motion cycle from a three to two-stage cycle.

- *Improve the robot structure alignment system.* The development of wheels for the robot, and in particular, spring wheels, would allow easier negotiation of obstacles and bends, without causing hindrance by their presence.

- *Payload carrying Capability.* The steel bristled robot that was designed was capable of towing up to 320kg of extra load, and had a camera housing at the front to accommodate inspection cameras and suitable lighting. This could be improved upon.

7 References

1. NEIL STUTCHBURY,   'BRISTLED PROPULSION'

    PATENT, GB2305407A. 1997.

2. Dr.Joachim Schnell,   'PROPULSION FOR SLIDING VEHICLES'

    GERMANY PATENT, 1974.

3. C.Y.WANG,   'BUCKLING AND POST BUCKLING OF

    HEAVING COLUMN', Int.J.Mech.Sci.Vol.22, pp. 395-400, 1987.

4. JOHN M. HOLLAND,   'BASIC ROBOTICS CONCEPTS',

    HOWARD W. SAMS & Co. INC, 1983.

5. THRING M. W,   'AUTOMATION ON THE HOME',

    ELECTRON & POWER, 14 Nov. 1968.

6. JOHN F. YOUNG,   'ROBOTICS',

    LONDON, BUTTERWORTHS, 1973.

7. B'O.PEIRCE,   'A SHORT TABLE OF INTEGRALS',

    Ginn and Company, p72, 1957.

8. S.F.BORG,   'FUNDAMENTALS OF ENGINEERING

    ELASTICITY', D.VAN NUSTRAND CO. p240, 1952.

9. JOHN LUXMOORE, 'PIPE CRAWLER',

    UK Patent Application GB2167829A,1986.

10. BS308,   'British Standard Engineering Drawing practice'.

11.BS 4500,   'British Standard ISO Limits and Fits'

12 Peter Mucci   'Hand Book For Engineering Design'

                               P.E.R.MUCCI Ltd, 1991.

13. J.P.HOLMAN, 'EXPERIMENTAL METHODS FOR ENGINEERS'

                     Mc GRAW-HILL BOOK COMPANY, 1962.

14. RAY C. JOHNSON, 'MECHANICAL DESIGN SYNTHESIS:

                     With Optimisation Applications'

                     Van Nostrand Reinhold Company,1971.

15. Dr T. IWINSI,   'Theory of Beams'

                     PERGAMON PRESS, 1967.

16. K. ZBIROHOWSKI-KOSCIA,   'THIN WALLED BEAMS'

                CROSBY LOCKWOOD &SON LTD, 1967.

17. J.H.Abramson,M.D.   'Making Sense of Data'

             Milton Keynes: Open University Press, 1979.

Appendix A

Design drawings of the steel bristled robot

ORD. NO	DRG.NO.	TITLE	SPECIFICATION	AMOUNT	MATERIAL
1		WHEEL ASSEMBLY	D=32	48	
2	F00-01	CAMRER HOUSING		1	STEEL
3	F00-02/L	JOINT-1 /1-L		3 / 3	STEEL
4		BRISTLES	D=240,d=100,L=70	6	
5		CONNECTING BOLT	M10	6	
6	F00-03	WHEEL SUPPORT BODY (1)		2	STEEL
7	F00-04	INTERFACE		2	STEEL
8		PNEUMATIC CYLINDER	CQ2B80-50D	2	
9	F00-05	WHEEL SUPPORT BODY (2)		2	STEEL
10	F00-06	WHEEL SUPPORT BODY (3)		1	STEEL
11		VALVE	24V=11W	2	
12		CONNECTING BOLT (2)	M12 , L=160	3	
13	F00-07	WHEEL SUPPORT BODY (4)		1	STEEL
14		HEXAGON BOLT	M10,L=28	12	
15		WASHER	M10,T=7	12	
16		BEARING	MAC 16	12	
17		BOLT	M8,L=20	36	
18	F00-08	JOINT-3		6	STEEL
19	F00-09/L	JOINT-2 /2-L		6/ 6	STEEL
20	F00-10	RUBBER JOINT		18	
21		HEXAGON NUT	M5	18	
22		WASHER	M10	1	
23		SPRING WASHER	M10	1	
24		HEXAGON NUT	M10	1	
25		BOLT	M10	1	
26	F00-11	TOW		1	STEEL
27	F00-12	TOW SHAFT		1	STEEL
28		WASHER	D=20,d=4.5	1	
29		HEXAGON NUT	M4	1	
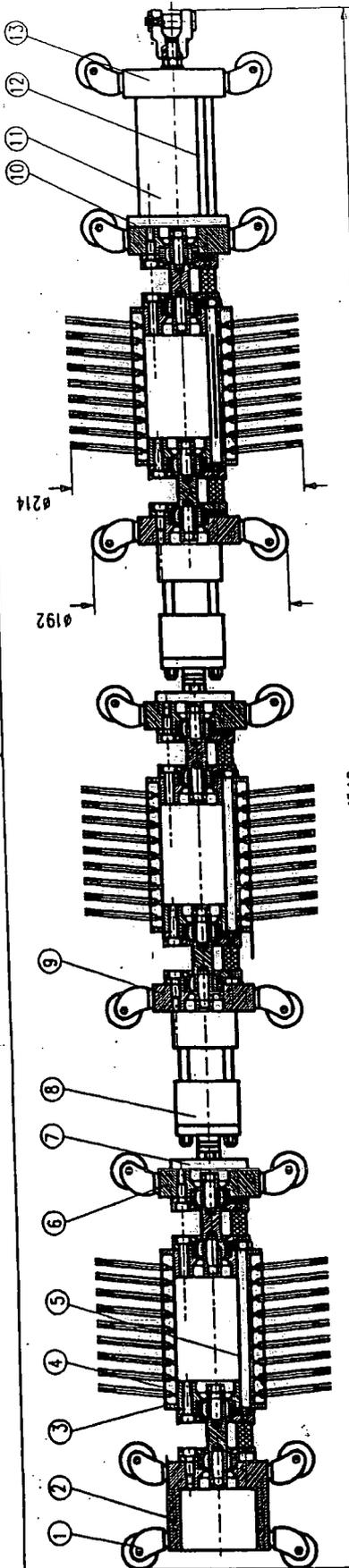
DETAIL OF TOW (1:1)

DETAIL OF JOINT (1:1)
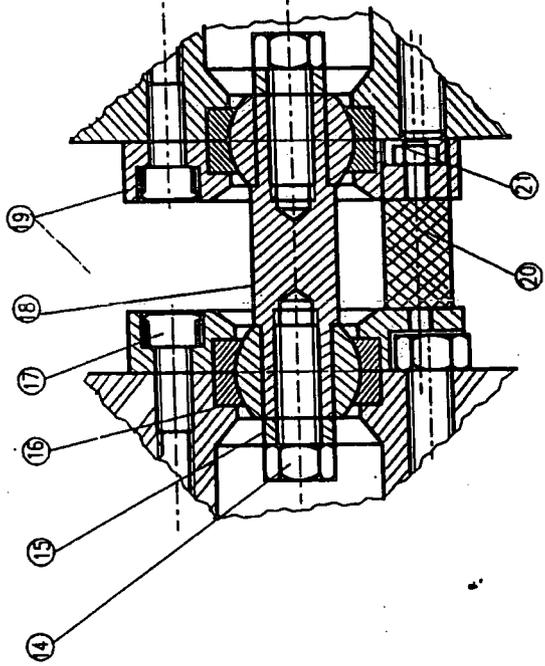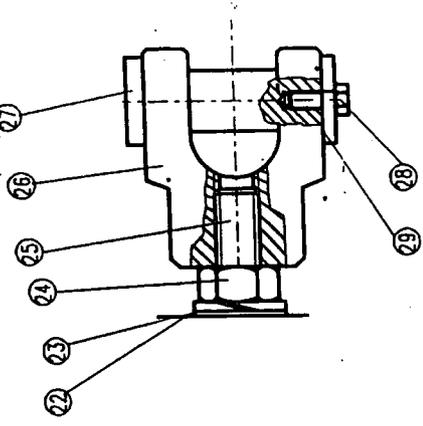
Ø214

Ø192

1542

MATERIAL:		
DRG. No.		F00-00
TITLE:		EXPERIMENTAL PIPE ROBOT

DRAWN BY	C.L. HAN	TOLERANCES UNLESS OTHERWISE STATED	
DATE	22/6/97	WHOLE No. ±1.0	
SCALE	1:4	DECIMAL (.00) ±0.2	
DIMENSIONS	MM	ANGLES ±0 30'	

3.2 ALL

3*M8

ø56

ø60

ø90

12*M4

ø100

12*ø8.5

11.5

10.5

7.5

ø38

ø28±0.1

ø38.5 +0.1 +0.0

14

90

28

14

NOTES:
* For explanation of dimensions,tolerances,notes ets,see BS 308;
* Limits on untoleranced machined dimensions to BS 4500;
* All sharp edges must be rounded.

DRAWN BY	C.L HAN		MATERIAL:	STEEL
DATE	21/6/97		DRG . No.	F00-01
SCALE	1:1		TITLE:	CAMERA HOUSING
DIMENSIONS	MM			

TOLERANCES UNLESS OTHERWISE STATED	
WHOLE No. +1.0	
DECIMAL(.00) +0.2	
ANGLES +0 30'	

64

ALL 3.2

3*M10

3*M8

Ø56

Ø60

Ø100

Ø76

Ø38

Ø28±0.1

Ø38.5 +0.1 +0.0

10.5

7.5

11.5

5

28

NOTES:
* For explanation of dimensions, tolerances, notes ets, see BS 308;
* Limits on untoleranced machined dimensions to BS 4500;
* All sharp edges must be rounded.

DRAWN BY	C.L HAN		MATERIAL :	STEEL
DATE	21/6/97	TOLERANCES UNLESS OTHERWISE STATED	DRG . No.	F00-02
SCALE	1:1	WHOLE No. +1.0 DECIMAL (.00) +0.2 ANGLES +0 30'	TITLE:	JOINT-1
DIMENSIONS	MM			

65

3.2 ALL

3*Ø10.5

3*M8

Ø56

Ø60

Ø100

Ø76-0.4 +0.0

Ø38

10.5

7.5

11.5

5

28

Ø28±0.1

Ø38.5+0.1 +0.0

NOTES:
* For explanation of dimensions, tolerances, notes ets, see BS 308;
* Limits on untoleranced machined dimensions to BS 4500;
* All sharp edges must be rounded.

MATERIAL:	STEEL
DRG. No.	F00-02L
TITLE:	JOINT-1-L

TOLERANCES UNLESS OTHERWISE STATED	
WHOLE No. +1.0 DECIMAL(.00) +0.2 ANGLES +0 30'	

DRAWN BY	C.L HAN
DATE	21/6/97
SCALE	1:1
DIMENSIONS	MM

66

3.2 ▽
ALL

6*M4

3*M8

ø56

ø60

ø90

ø100

ø38

10

6*ø8.5

28

11.5

10.5

7.5

ø28±0.1

ø38.5 +0.0
      +0.1

NOTES:
* For explanation of dimensions, tolerances, notes ets, see BS 308;
* Limits on untoleranced machined dimensions to BS 4500;
* All sharp edges must be rounded.

MATERIAL:	STEEL
DRG . No.	F00-03
TITLE: WHEEL SUPPORT-BODY(1)	

TOLERANCES UNLESS OTHERWISE STATED	
WHOLE No. +1.0	
DECIMAL (.00) +0.2	
ANGLES +0 30'	

DRAWN BY	C.L HAN
DATE	21/6/97
SCALE	1:1
DIMENSIONS	MM

3.2
ALL

M16

3*⌀8.5

⌀56

⌀76

10

NOTES:
* For explanation of dimensions,tolerances,notes ets,see BS 308;
* Limits on untoleranced machined dimensions to BS 4500;
* All sharp edges must be rounded.

DRAWN BY	C.L HAN		MATERIAL:	STEEL
DATE			DRG . No.	F00−04
SCALE	1:1		TITLE:	INTERFACE
DIMENSIONS	MM			

TOLERANCES UNLESS OTHERWISE STATED		
WHOLE No. +1.0 DECIMAL(.00) +0.2 ANGLES +0 30'		

68

3.2 ∇
ALL

4*M8

6*M4

3*M8

Ø56

Ø60

Ø90

Ø100

30.00

Ø38

10

6*Ø8.5

28

Ø28±0.1

Ø38.5 +0.0 / -0.1

11.5

10.5

7.5

NOTES:
* For explanation of dimensions, tolerances, notes ets, see BS 308;
* Limits on untoleranced machined dimensions to BS 4500;
* All sharp edges must be rounded.

DRAWN BY	C.L. HAN		TOLERANCES UNLESS OTHERWISE STATED		MATERIAL:	STEEL
DATE	21/6/97		WHOLE No. +1.0 DECIMAL (.00) +0.2 ANGLES +0 30'		DRG. No.	F00-05
SCALE	1:1				TITLE: WHEEL SUPPORT-BODY (2)	
DIMENSIONS	MM					

69

3.2 ALL

3*M12

6*M4

3*M8

Ø56

Ø75

Ø90

Ø100

Ø38
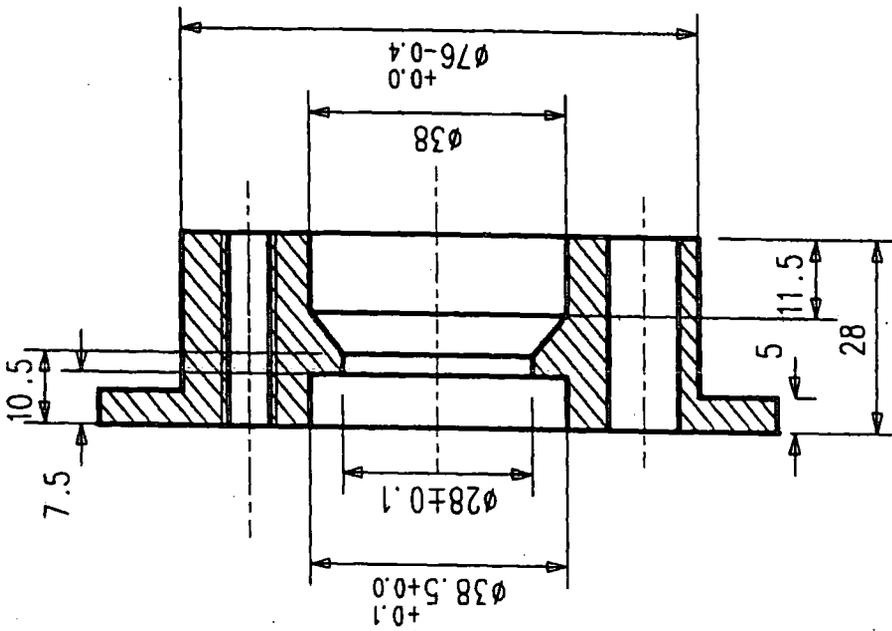
10

6*Ø8.5

11.5

10.5

7.5

28

Ø28±0.1

Ø38.5 +0.1 / +0.0

NOTES:
* For explanation of dimensions,tolerances,notes ets,see BS 308;
* Limits on untoleranced machined dimensions to BS 4500;
* All sharp edges must be rounded.

MATERIAL :	STEEL	
DRG . No.	F00-06	
TITLE: WHEEL SUPPORT-BODY (3)		

TOLERANCES UNLESS OTHERWISE STATED		
WHOLE No. +1.0 DECIMAL(.00) +0.2 ANGLES +0 30'		

DRAWN BY	C.L. HAN	
DATE	21/6/97	
SCALE	1:1	
DIMENSIONS	MM	

70

ALL $\sqrt{}$ 3.2

∅75

3*M12

6*M4

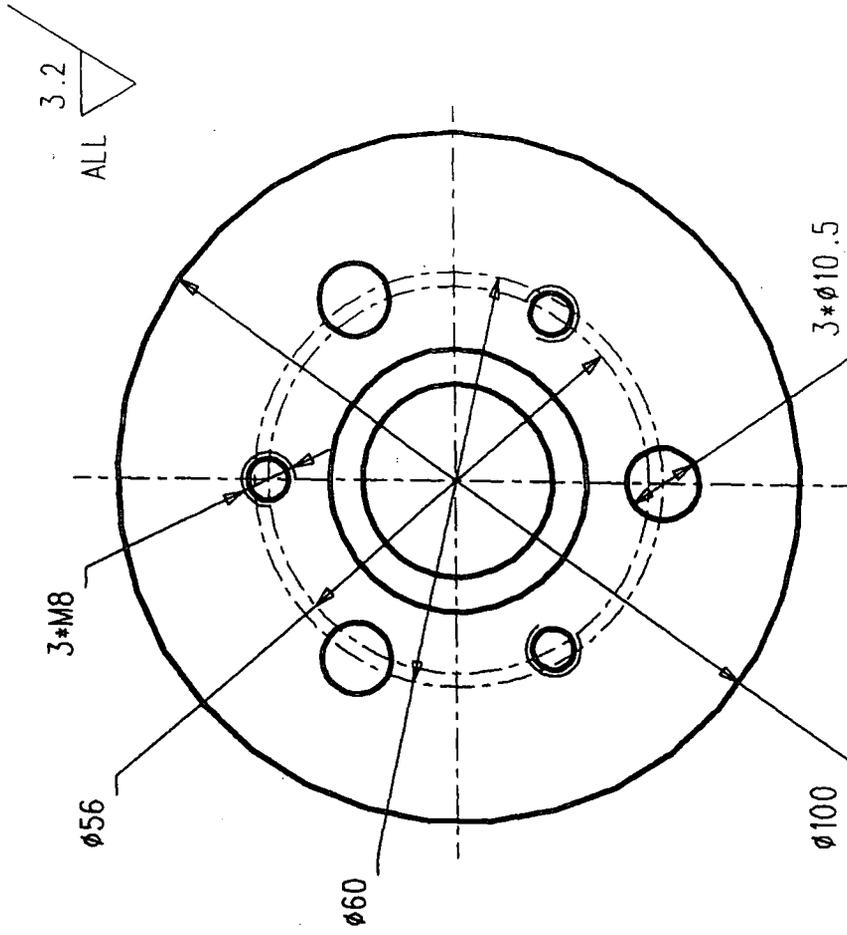∅100

∅90

M12

10

6*∅8.5

28

NOTES:
* For explanation of dimensions, tolerances, notes ets, see BS 308;
* Limits on untoleranced machined dimensions to BS 4500;
* All sharp edges must be rounded.

MATERIAL:	STEEL	
DRG . No.	F00-07	
TITLE: WHEEL SUPPORT-BODY (4)		

TOLERANCES UNLESS OTHERWISE STATED		
WHOLE No. +1.0 DECIMAL (.00) +0.2 ANGLES +0 30'		

DRAWN BY	C.L. HAN	
DATE	21/6/97	
SCALE	1:1	
DIMENSIONS	MM	

71

3.2
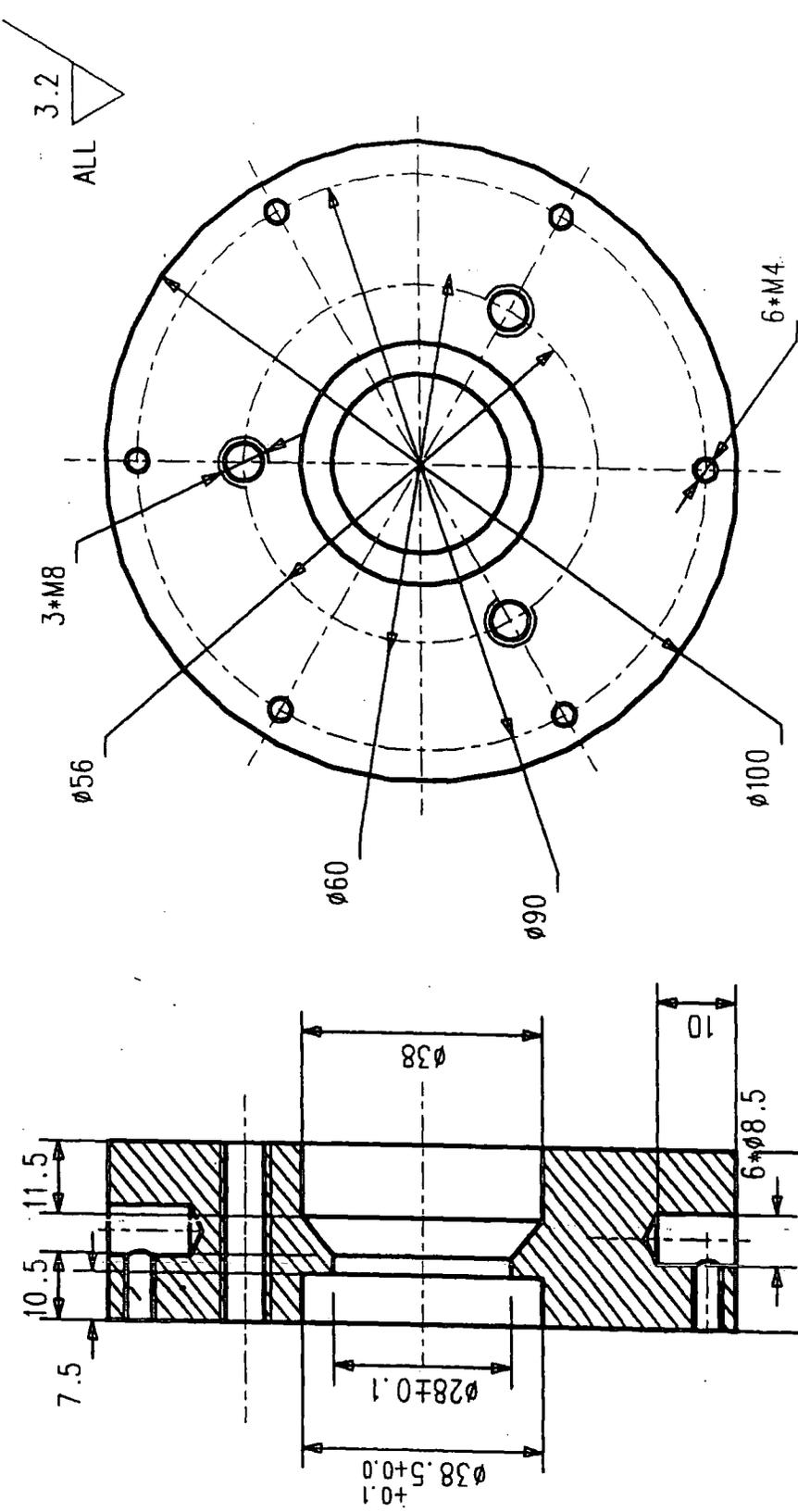ALL

ø19.3

ø16 -0.2 / -0.4

2*M10

26.5MAX

24.5MIN

32

74

21

NOTES:
* For explanation of dimensions, tolerances, notes ets, see BS 308;
* Limits on untoleranced machined dimensions to BS 4500;
* All sharp edges must be rounded.

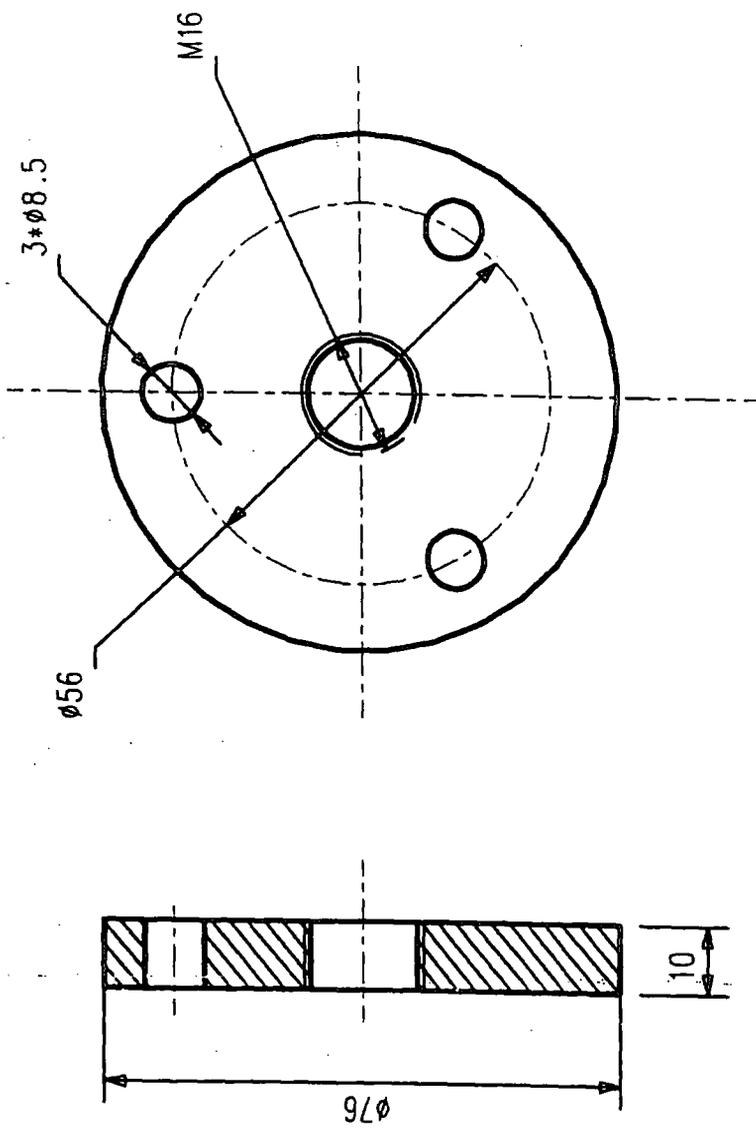| DRAWN BY	C.L. HAN	TOLERANCES UNLESS OTHERWISE STATED	MATERIAL:	STEEL
DATE	21/6/97	WHOLE No. +1.0 DECIMAL (.00) +0.2 ANGLES +0 30'	DRG. No.	F00-08
SCALE	1:1		TITLE:	JOINT-3
DIMENSIONS	MM			

3*∅8.5CBORE ∅14*8

∅56

3.2

ALL

3*∅5.5CBORE∅14*6

∅38

∅76

∅38.5 +0.0 -0.0

∅28±0.1 +0.1

7.5

10.5

14

NOTES:
* For explanation of dimensions,tolerances,notes ets,see BS 308;
* Limits on untoleranced machined dimensions to BS 4500;
* All sharp edges must be rounded.

MATERIAL:	STEEL
DRG .No.	F00-09
TITLE:	JOINT-2

TOLERANCES UNLESS OTHERWISE STATED		
WHOLE No.	+1.0	
DECIMAL(.00)	+0.2	
ANGLES	+0 30'	

DRAWN BY	C.L HAN
DATE	21/6/97
SCALE	1:1
DIMENSIONS	MM

3.2 ALL

3*ø8.5CBORE Ø14*8

ø56

ø76

3*Mø5

ø60

ø38.5+0.0 +0.0

ø28±0.1

3*ø18

7.5

10.5

9

14

ø38
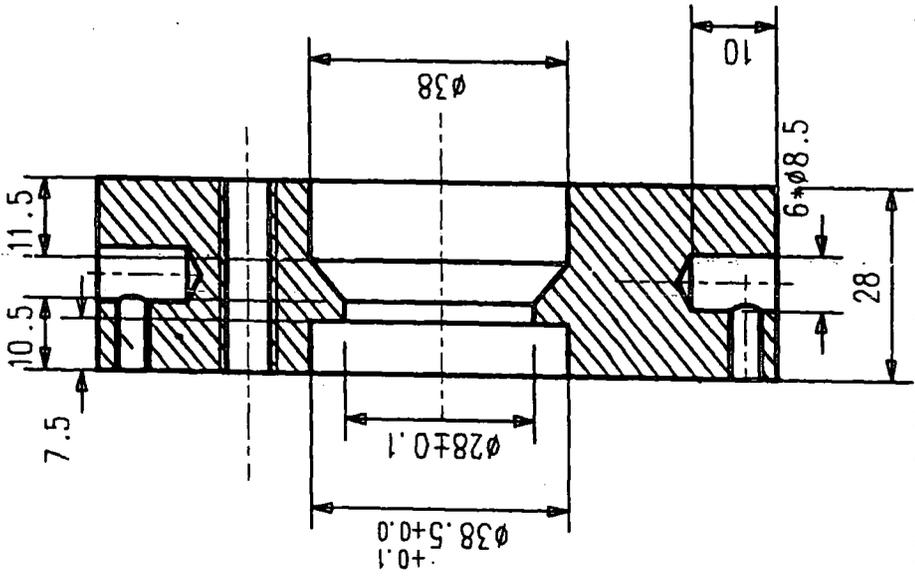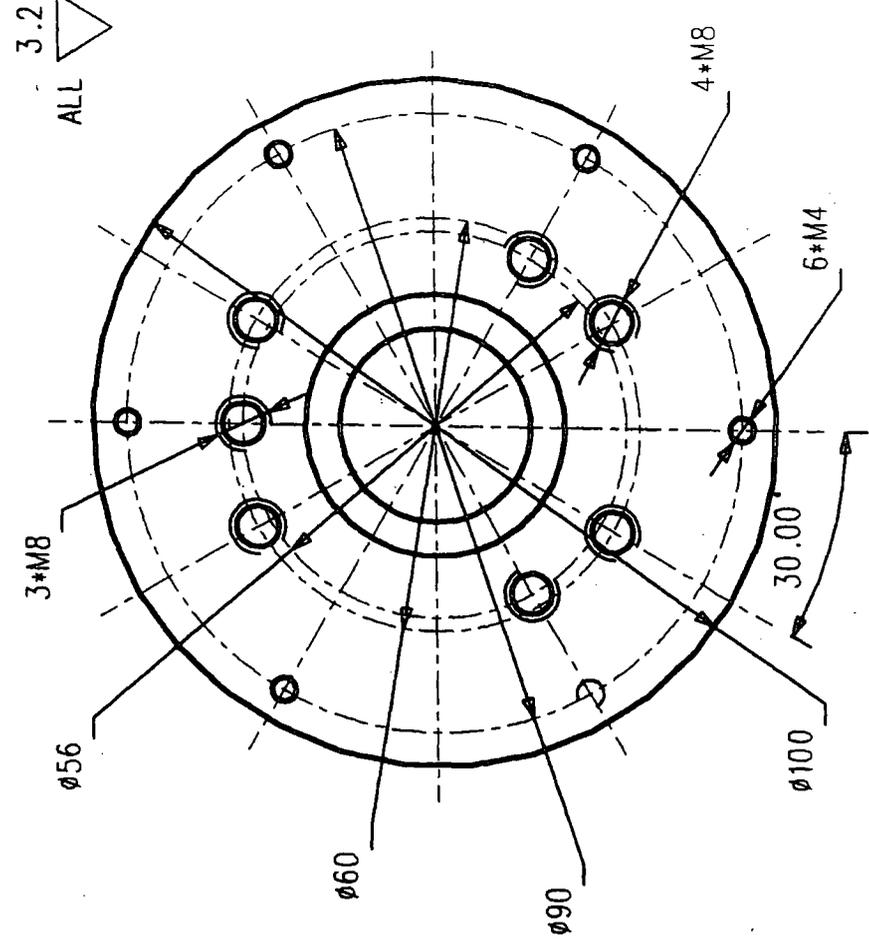
NOTES:
* For explanation of dimensions,tolerances,notes ets,see BS 308;
* Limits on untoleranced machined dimensions to BS 4500;
* All sharp edges must be rounded.

DRAWN BY	C.L HAN	MATERIAL:	STEEL
DATE	21/6/97	DRG.No.	F00-9L
SCALE	1:1	TITLE:	JOINT-2-L
DIMENSIONS	MM		

TOLERANCES UNLESS OTHERWISE STATED	
WHOLE No. +1.0	
DECIMAL(.00) +0.2	
ANGLES +0 30'	

74

ALL $\sqrt{\frac{3.2}{}}$

rubber joint

2-M5

ϕ24

bolt

25

16

57

21
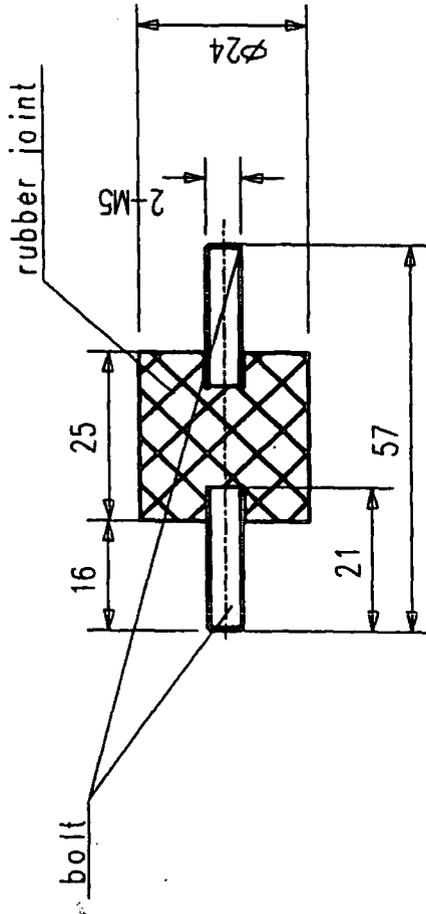
NOTES:

* Thread in accordance with table 3 of BS 4368:part:1974
* Thread runout as per BS 1936
* Dimension tolerances of unindicating in accordance with IT13 of ISO 286-2:1988(E)

DRAWN BY	C.L. HAN		MATERIAL :	
DATE	22/6/97	TOLERANCES UNLESS OTHERWISE STATED	DRG . No.	FOO-10
SCALE	1:1	WHOLE No. +1.0 DECIMAL(.00) +0.2 ANGLES +0 30'	TITLE:	
DIMENSIONS	MM			RUBBER JOINT
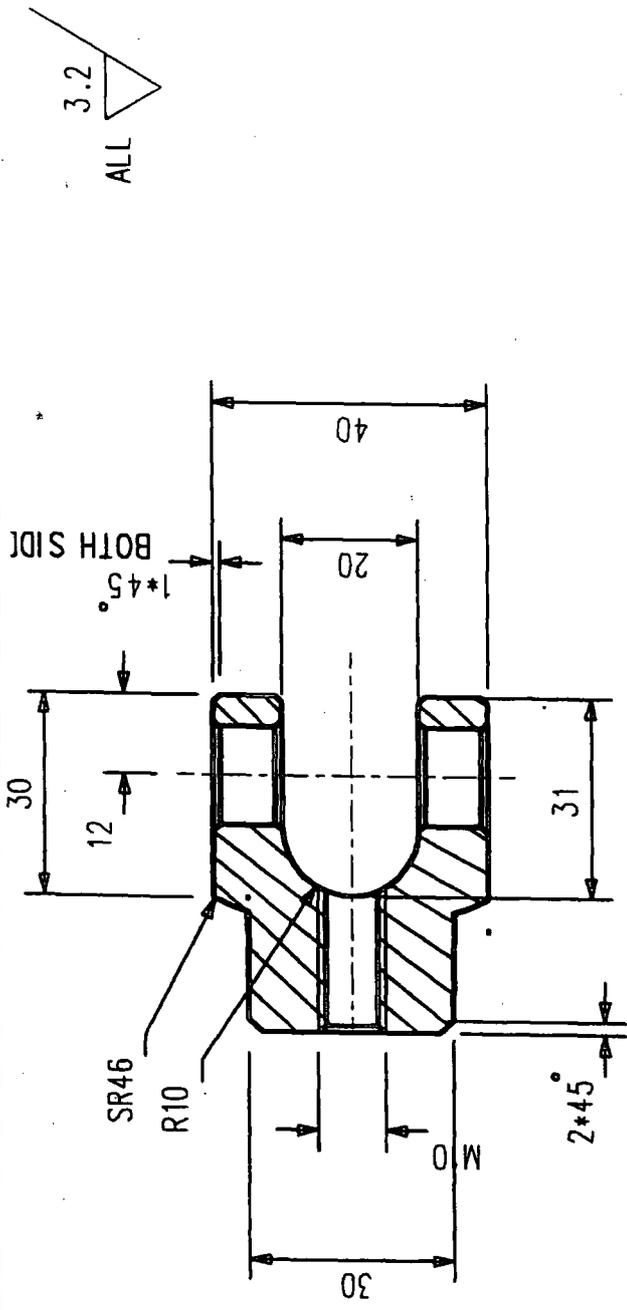
3.2 ▽
ALL

40

20

1*45° BOTH SIDE

30

12

31

30

SR46

R10

M10

30

2*45°

30

Ø14.50

50
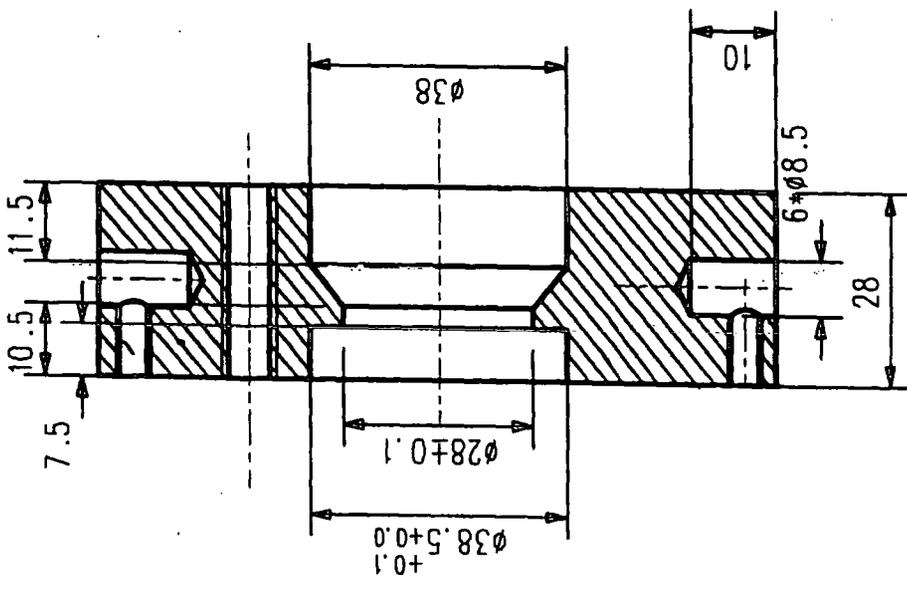
NOTES:
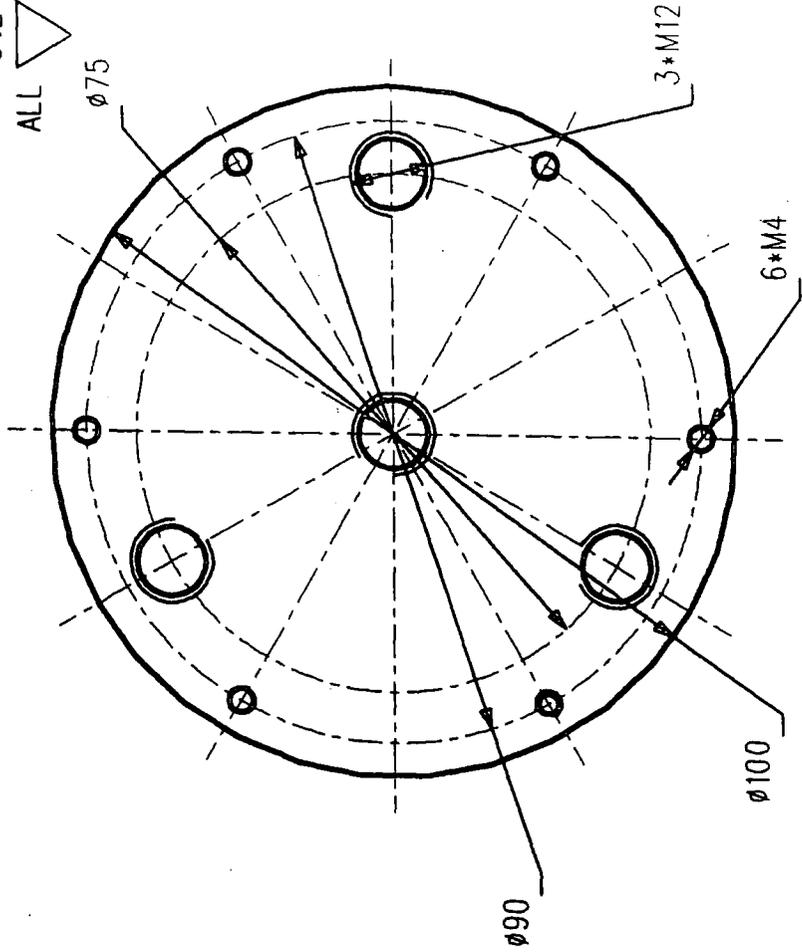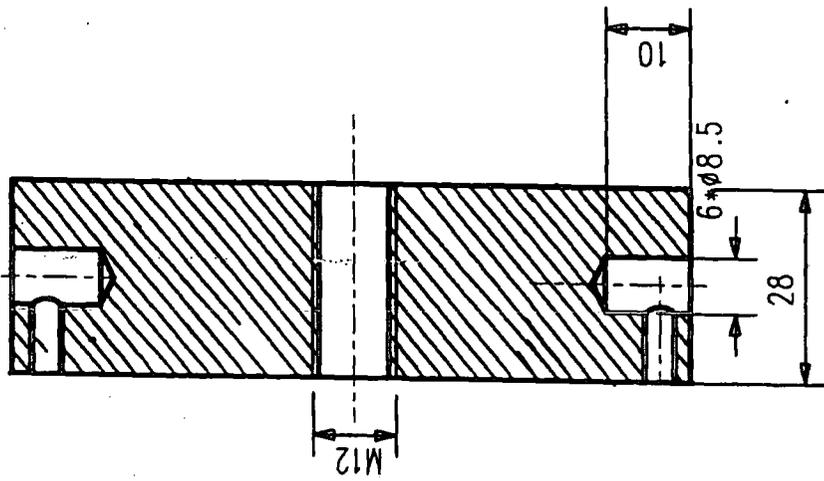* For explanation of dimensions,tolerances,notes ets,see BS 308;
* Limits on untoleranced machined dimensions to BS 4500;
* All sharp edges must be rounded.

MATERIAL :	STEEL
DRG . No.	F00-111
TITLE:	TOW

| TOLERANCES UNLESS OTHERWISE STATED | |
| WHOLE No. +1.0 DECIMAL (.00) +0.2 ANGLES +0 30' | |

DRAWN BY.	C.L HAN
DATE	22/6/97
SCALE	1:1
DIMENSIONS	MM

76

3.2
ALL

44

3

20

4

40

M4
14 MIN FULL THREAD

14

NOTES:
* For explanation of dimensions, tolerances, notes ets, see BS 308;
* Limits on untoleranced machined dimensions to BS 4500;
* All sharp edges must be rounded.

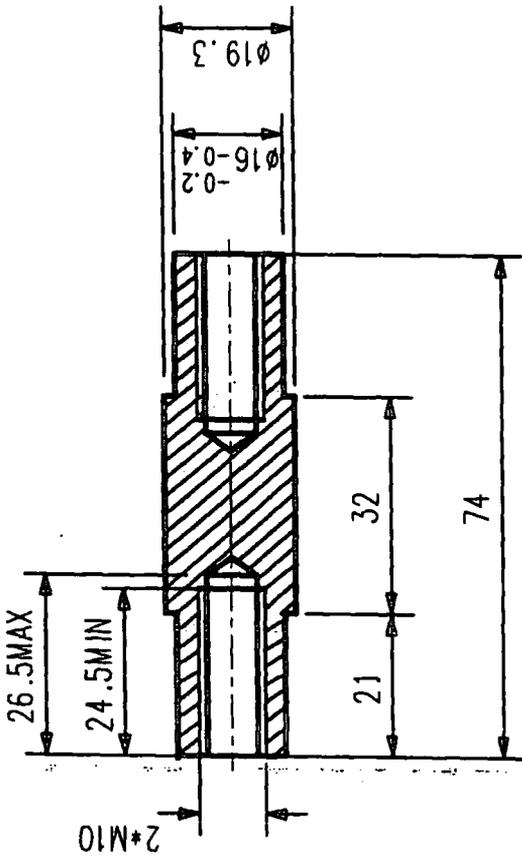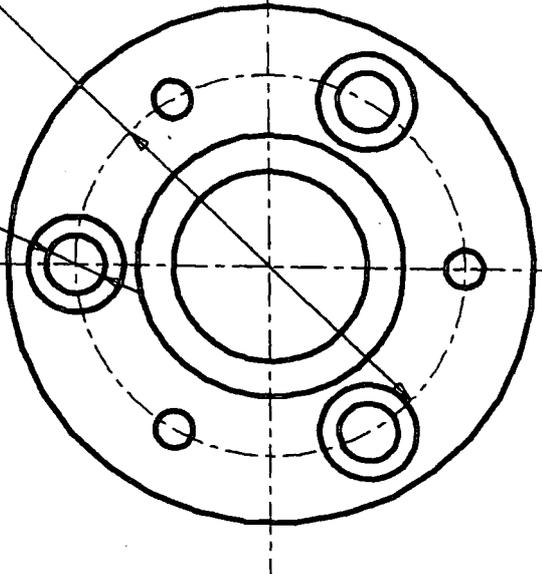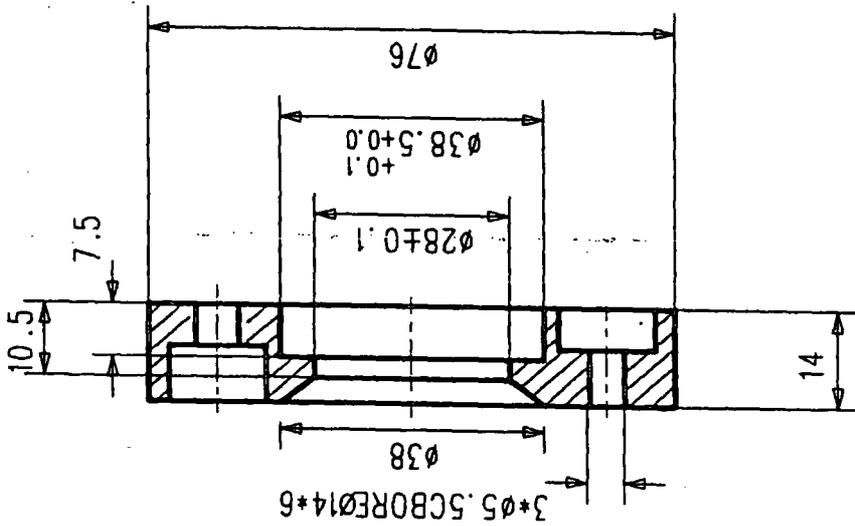| DRAWN BY	C.L HAN		TOLERANCES UNLESS OTHERWISE STATED		MATERIAL:	STEEL
DATE	22/6/97		WHOLE No. +1.0 DECIMAL (.00) +0.2 ANGLES +0 30'		DRG. No.	F00-12
SCALE	1:1				TITLE:	TOW SHAFT
DIMENSIONS	MM					

Specification

Housing   Carbon steel.
Phosphated.

Ball   1% carbon chromium steel.
Heat treated.
Chromium plated on the spherical surface.

Liner   Reinforced PTFE.

Temperature and fits

The normal maximum operating temperature for these bearings
is 120°C, although Rose Bearings technical department should
be consulted where the normal operating temperature exceeds
80°C.

There is no measurable clearance in these bearings in the no
load condition, and the tightness of the bearing is measured by
the breakaway torque as indicated below.

Bearing size mAC	No load breakaway torque (Nm)
05 – 20	0 – 0,56
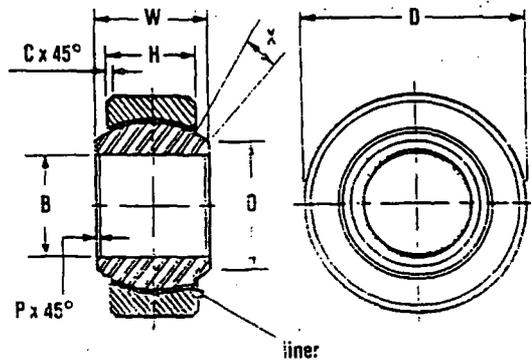
Metric dimensions

Bearing number	B Bore H7	D Outside dia h6	W Ball width + 0 -0,1	H Housing width +0,1 -0,1	O Ball flat dia	C Chamfer +0,4 - 0	P Chamfer +0,4 - 0	X Angle deg	Ball dia nom	Maximum static radial load in Newtons approx	Weight in kg each approx
MAC 05	5	16	8	6,0	7,7	0,5	0,2	12,5	11,11	26 480	0,009
.C 06	6	18	9	6,75	8,9	0,5	0,3	12,5	12,70	33 340	0,013
MAC 08	8	22	12	9,0	10,4	0,8	0,3	14,0	15,87	56 880	0,024
MAC 10	10	26	14	10,5	12,9	0,8	0,4	13,5	19,05	80 410	0,040
MAC 12	12	30	16	12,0	15,4	0,8	0,4	13,0	22,22	108 850	0,080
MAC 16	16	38	21	15,0	19,3	1,0	0,5	15,0	28,57	176 520	0,130
MAC 20	20	46	25	18,0	24,3	1,0	0,8	14,5	34,92	256 930	0,230

Appendix C

Specification of the cylinder

Rod End Styles 4 & 7
– All Except JJ Mount
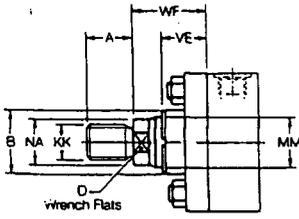
Rod End Styles 4 & 7
– JJ Mount

Rod End Styles 4 & 7
The smallest diameter rod end thread for each bore size is designated Style 4 when supplied with a No.1 rod. When the same rod end thread is supplied with a No.2 or No.3 rod, it is designated Style 7.

25 & 32mm Bore Cylinders

5mm extra height applies to port face at head end only.

Rod End Style 9
– All Except JJ Mount

Rod End Style 9
– JJ Mount

Rod End Style 9
– Short Stroke Cylinders
Style 9 (female) rod ends should not be used on 160mm or 200mm bore cylinders with a stroke of 50mm or less. Please consult the factory, with details of the application.

Rod End Style 3
Non-standard piston rod ends are designated 'Style 3'. A dimensional sketch or description should accompany the order. Please specify dimensions KK or KF, A, rod stand out (WF – VE) and thread form.

Gland Retainer
– 160 and 200mm Bore
On all 160mm and 200mm bore ISO mounting styles except TB and TD, the gland retainer is separately bolted to the head, as shown.
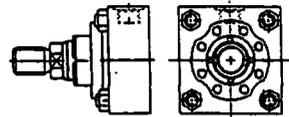
Piston Rod End Dimensions – Check pressure limitations of piston rods on page 31

Bore φ	Rod No.	MM Rod φ	Style 4		Style 7		Style 9		B f9	D	NA	VE	WF	JJ Mount Only			
			KK	A	KK	A	KF	A						VL min	RD f8	VJ	FJ
25	1	12	M10x1.25	14	-	-	M8x1	14	24	10	11	16	25	3	38	6	10
	2	18	M14x1.5	18	M10x1.25	14	M12x1.25	18	30	15	17	16					
32	1	14	M12x1.25	16	-	-	M10x1.25	16	26	12	13	22	35	3	42	12	10
	2	22	M16x1.5	22	M12x1.25	16	M16x1.5	22	34	18	21	22					
40	1	18	M14x1.5	18	-	-	M12x1.25	18	30	15	17	16	35	3	62	6 / 12	10
	2	28	M20x1.5	28	M14x1.5	18	M20x1.5	28	42	22	26	22					
50	1	22	M16x1.5	22	-	-	M16x1.5	22	34	18	21	22	41	4	74	6 / 9 / 6	16
	2	36	M27x2	36	M16x1.5	22	M27x2	36	50	30	34	25					
	3	28	M20x1.5	28	M16x1.5	22	M20x1.5	28	42	22	26	22					
63	1	28	M20x1.5	28	-	-	M20x1.5	28	42	22	26	22	48	4	75 / 88	6 / 13 / 9	16
	2	45	M33x2	45	M20x1.5	28	M33x2	45	60	39	43	29					
	3	36	M27x2	36	M20x1.5	28	M27x2	36	50	30	34	25					
80	1	36	M27x2	36	-	-	M27x2	36	50	30	34	25	51	4	82 / 105	5 / 9	20
	2	56	M42x2	56	M27x2	36	M42x2	56	72	48	54	29					
	3	45	M33x2	45	M27x2	36	M33x2	45	60	39	43	29					
100	1	45	M33x2	45	-	-	M33x2	45	60	39	43	29	57	5	92 / 125	7 / 10 / 7	22
	2	70	M48x2	63	M33x2	45	M48x2	63	88	62	68	32					
	3	56	M42x2	56	M33x2	45	M42x2	56	72	48	54	29					
125	1	56	M42x2	56	-	-	M42x2	56	72	48	54	29	57	5	105 / 150	9 / 10	20 / 22
	2	90	M64x3	85	M42x2	56	M64x3	85	108	80	88	32					
	3	70	M48x2	63	M42x2	56	M48x2	63	88	62	68	32					
160	1	70	M48x2	63	-	-	M48x2	63	88	62	68	32	57	5	125 / 170	10 / 7	22 / 25
	2	110	M80x3	95	M48x2	63	M80x3	95	133	100	108	32					
	3	90	M64x3	85	M48x2	63	M64x3	85	108	80	88	32					
200	1	90	M64x3	85	-	-	M64x3	85	108	80	88	32	57	5	150 / 210	10 / 7	22 / 25
	2	140	M100x3	112	M64x3	85	M100x3	112	163	128	138	32					
	3	110	M80x3	95	M64x3	85	M80x3	95	133	100	108	32					

All dimensions are in millimetres unless otherwise stated.

Appendix D

Experimental results of the steel bristled robot

THE LARGE LOAD CELL CALIBRITION

Series1
Series2

Tension

Compression

LOAD KN

CHART RECORDER MM
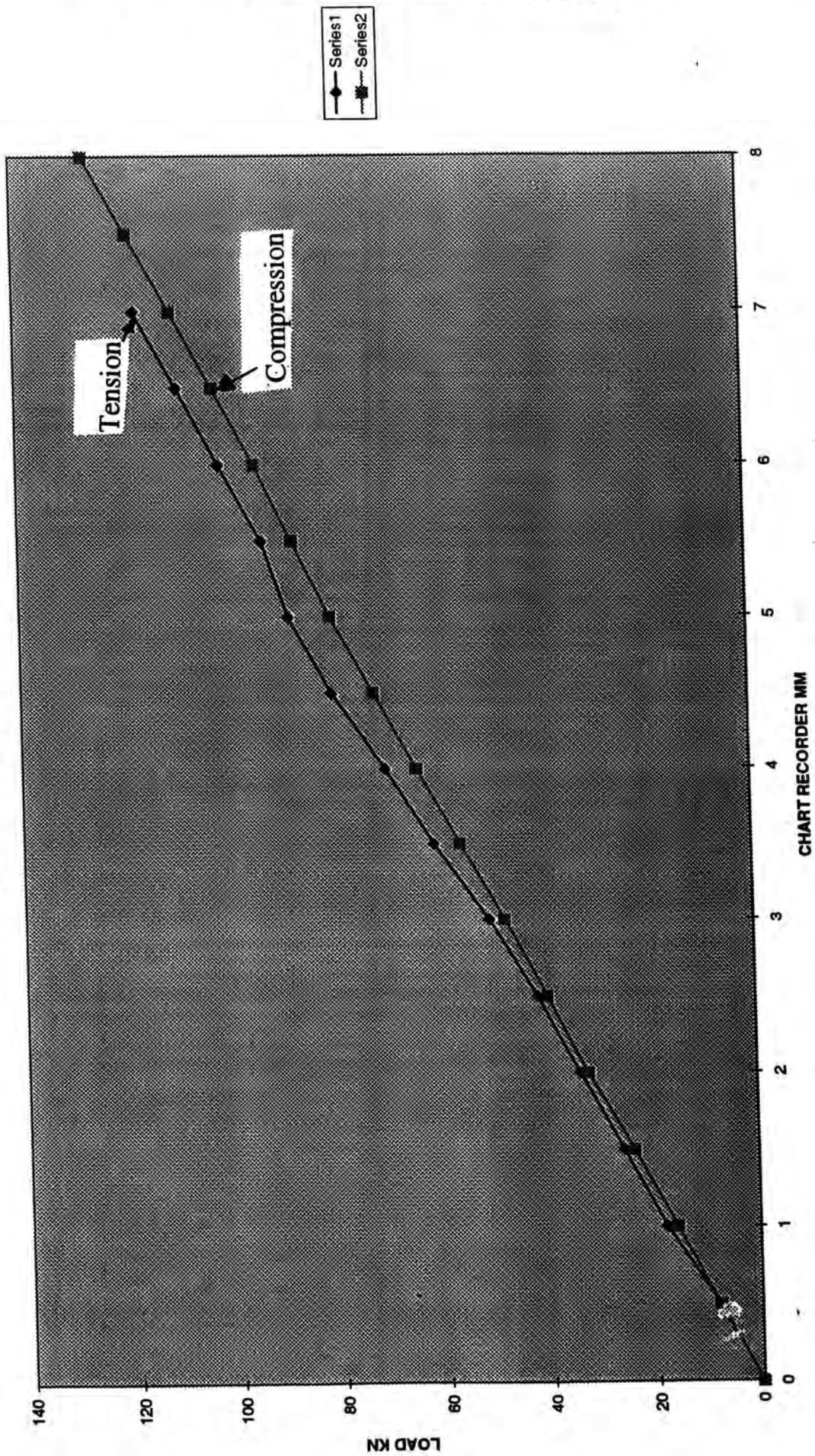
METHANIC BEHAVIOR OF THE STEEL ROBOT THROUGH A BEND PIPE WHICH THE LOAD CELL WAS FITTED BEFORE THE FIRST CYLINDER
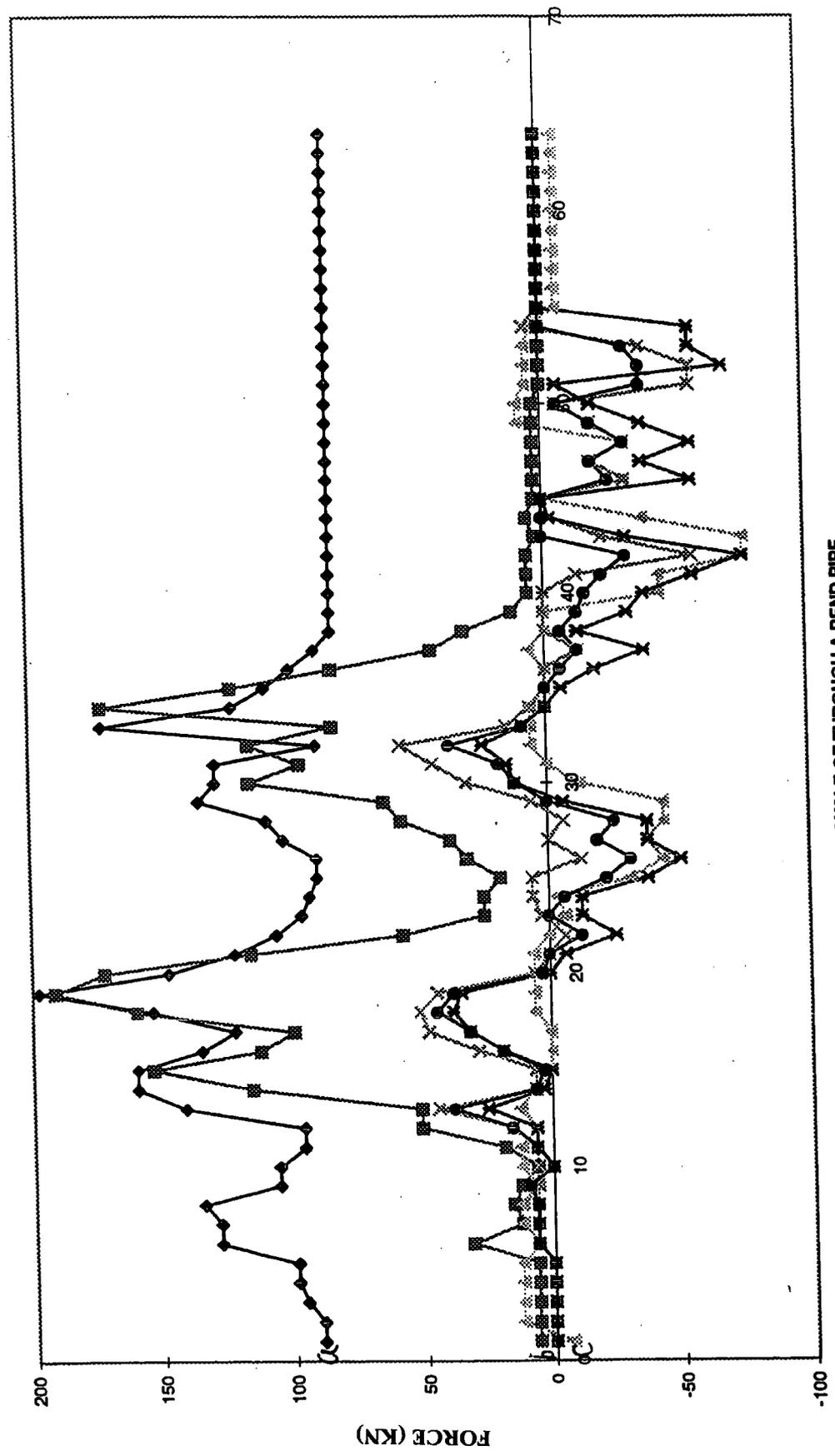
CYCLE OF THROUGH A BEND PIPE

FORCE (KN)

a
b
c
d
e
f

Series1
Series2
Series3
Series4
Series5
Series6

MECHANIC BEHAVIOR OF THE STEEL ROBOT THROUGH A BEND PIPE THAT THE LOAD CELL WAS FITTED BEFORE THE SECONDE CYLINDER
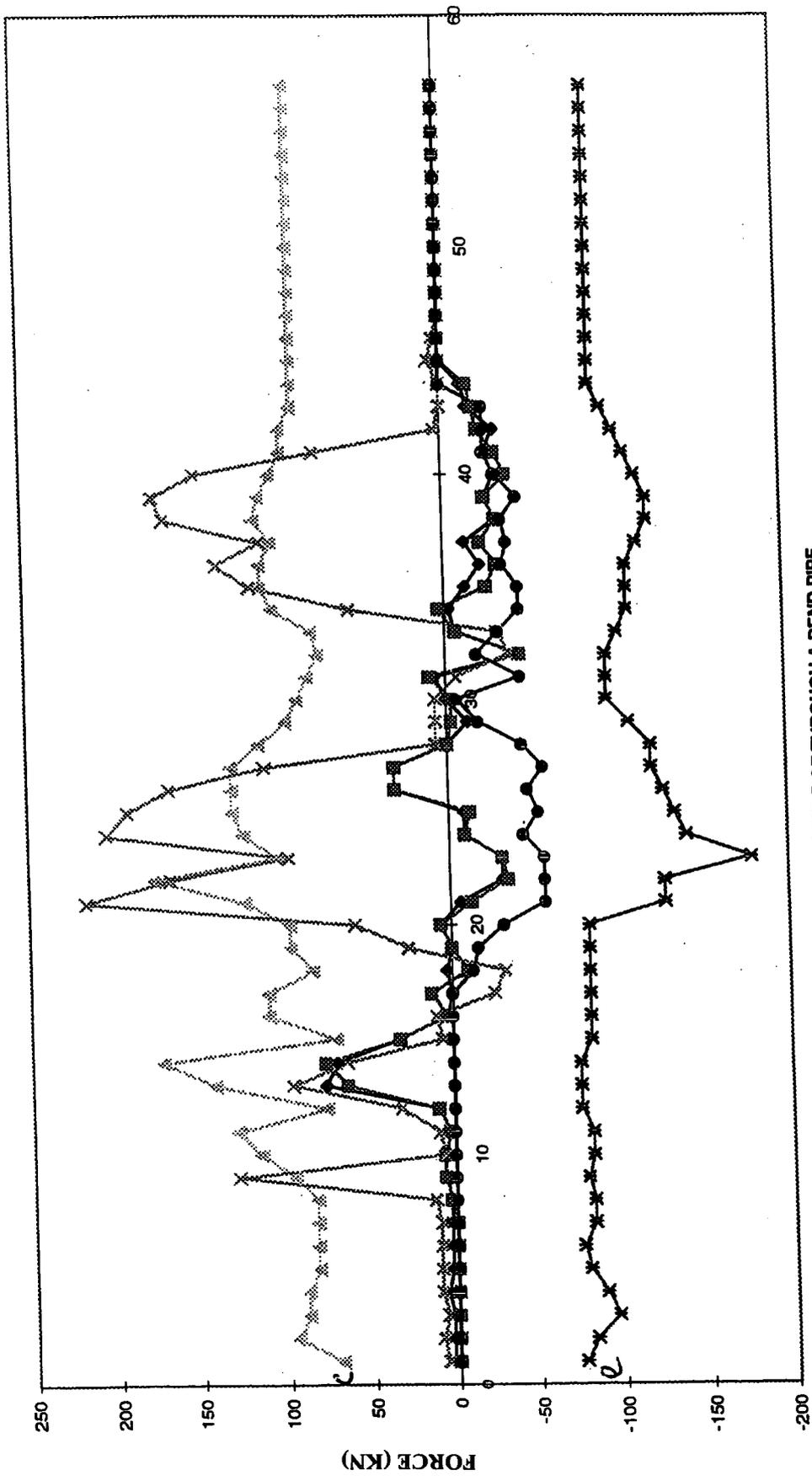
Legend:
- Series1
- Series2
- Series3
- Series4
- Series5
- Series6

Y-axis: FORCE (KN) ranging from -200 to 250

X-axis: CYCLE OF THROUGH A BEND PIPE

MECHENICAL BEHAVIOUR OF THE STEEL BRISTLES'S ROBOT WITH A WOODSPACE IN THE MIDDLE BRISTLES
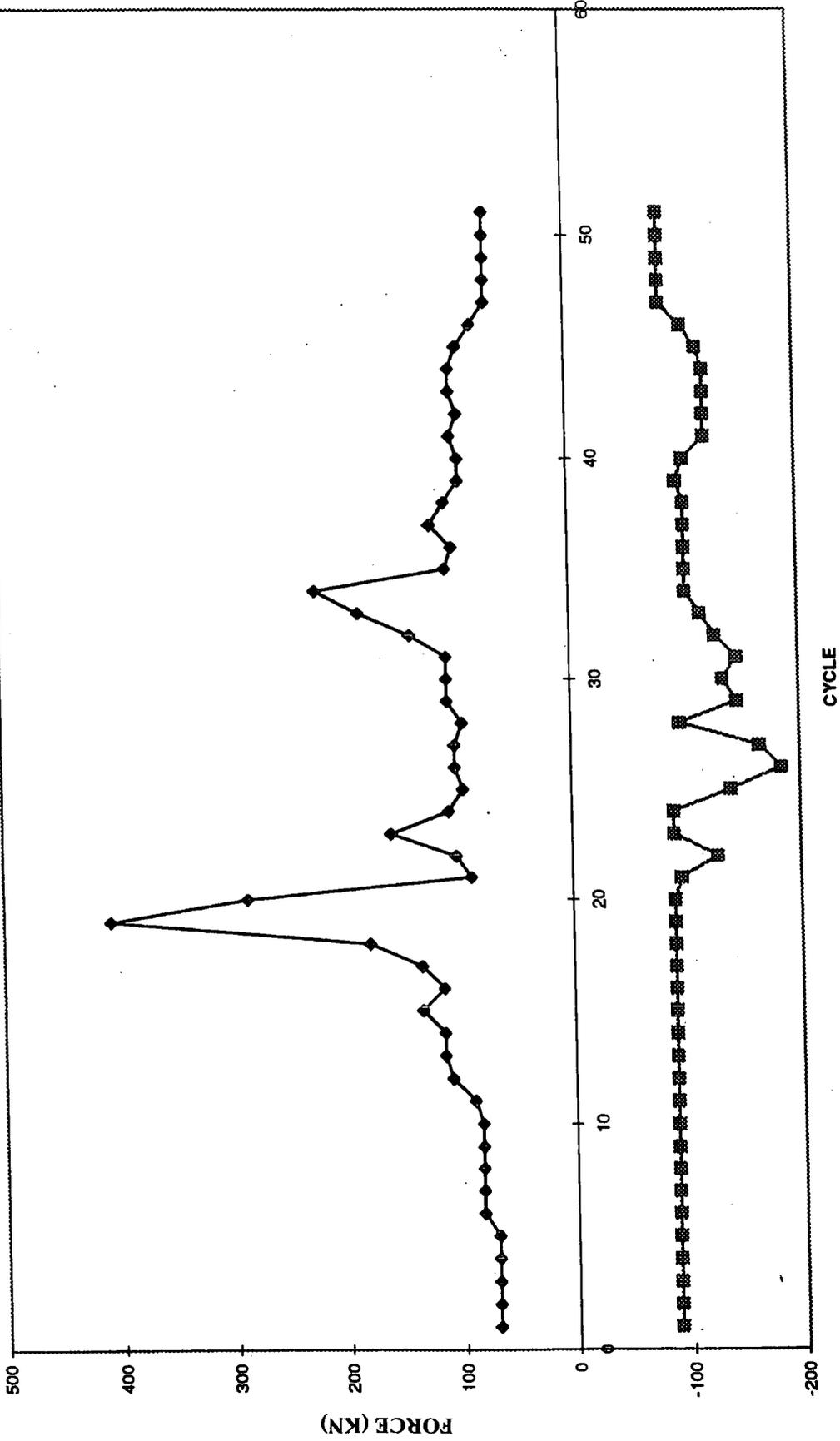
83

Load cell on the first position

cycle	Fa (KN)	Fb(KN)	Fc (KN)	Fd (KN)	Fe(KN)	Ff (KN)
1	89.28571	6.377551	-6.37755	0	0	0
2	89.28571	6.377551	12.7551	0	0	0
3	95.66327	6.377551	12.7551	0	0	0
4	98.85204	6.377551	12.7551	0	0	0
5	98.85204	6.377551	12.7551	0	0	0
6	127.551	31.88776	6.377551	6.377551	6.377551	6.377551
7	127.551	12.7551	12.7551	6.377551	6.377551	6.377551
8	133.9286	15.94388	12.7551	6.377551	6.377551	6.377551
9	105.2296	12.7551	6.377551	6.377551	9.566327	9.566327
10	105.2296	6.377551	12.7551	6.377551	0	0
11	95.66327	19.13265	12.7551	6.377551	6.377551	6.377551
12	95.66327	51.02041	6.377551	15.94388	6.377551	15.94388
13	140.3061	51.02041	12.7551	44.64286	25.5102	38.26531
14	159.4388	114.7959	6.377551	6.377551	3.188776	6.377551
15	159.4388	153.0612	0	6.377551	0	3.188776
16	133.9286	111.6071	0	28.69898	19.13265	19.13265
17	121.1735	98.85204	0	47.83163	31.88776	31.88776
18	153.0612	159.4388	6.377551	51.02041	38.26531	44.64286
19	197.7041	191.3265	6.377551	44.64286	35.07653	38.26531
20	146.6837	172.1939	6.377551	6.377551	0	3.188776
21	121.1735	114.7959	6.377551	0	-6.37755	0
22	105.2296	57.39796	0	-6.37755	-25.5102	-12.7551
23	95.66327	25.5102	-6.37755	3.188776	-12.7551	0
24	92.47449	25.5102	-3.18878	6.377551	-12.7551	-6.37755
25	89.28571	19.13265	-31.8878	6.377551	-38.2653	-22.3214
26	89.28571	31.88776	-44.6429	-12.7551	-51.0204	-31.8878
27	102.0408	38.26531	-38.2653	0	-38.2653	-19.1327
28	108.4184	57.39796	-44.6429	-6.37755	-38.2653	-25.5102
29	133.9286	63.77551	-44.6429	6.377551	-6.37755	0
30	127.551	114.7959	-12.7551	31.88776	12.7551	12.7551
31	127.551	95.66327	0	44.64286	15.94388	19.13265
32	89.28571	114.7959	6.377551	57.39796	25.5102	38.26531
33	172.1939	82.90816	6.377551	15.94388	9.566327	9.566327
34	121.1735	172.1939	6.377551	6.377551	0	0
35	108.4184	121.1735	0	0	-6.37755	0
36	98.85204	82.90816	0	0	-19.1327	-6.37755
37	89.28571	44.64286	6.377551	-12.7551	-38.2653	-12.7551
38	82.90816	31.88776	0	0	-12.7551	-6.37755
39	82.90816	12.7551	0	0	-31.8878	-12.7551
40	82.90816	6.377551	-44.6429	0	-38.2653	-15.9439
41	82.90816	6.377551	-44.6429	-12.7551	-57.398	-22.3214
42	82.90816	6.377551	-76.5306	-57.398	-76.5306	-31.8878
43	82.90816	3.188776	-76.5306	-22.3214	-31.8878	0
44	82.90816	6.377551	-38.2653	-3.18878	-3.18878	0
45	82.90816	3.188776	0	0	0	0
46	82.90816	3.188776	-31.8878	-31.8878	-57.398	-25.5102
47	82.90816	3.188776	-19.1327	-19.1327	-38.2653	-19.1327
48	82.90816	3.188776	-31.8878	-31.8878	-57.398	-31.8878
49	82.90816	3.188776	9.566327	-19.1327	-38.2653	-19.1327
50	82.90816	3.188776	9.566327	-6.37755	-19.1327	-6.37755
51	82.90816	0	6.377551	-57.398	-6.37755	-38.2653
52	82.90816	0	6.377551	-57.398	-70.1531	-38.2653
53	82.90816	0	6.377551	-38.2653	-57.398	-31.8878
54	82.90816	0	3.188776	6.377551	-57.398	0

Load cell on the second position

cycle	Fa (KN)	Fb (KN)	Fc (KN)	Fd (KN)	Fe (KN)	Ff (KN)
1	3.188776	0	70.15306	6.377551	-76.5306	0
2	3.188776	0	95.66327	9.566327	-82.9082	0
3	3.188776	0	89.28571	6.377551	-95.6633	0
4	6.377551	0	89.28571	9.566327	-89.2857	0
5	3.188776	0	82.90816	9.566327	-79.7194	0
6	3.188776	0	82.90816	9.566327	-76.5306	0
7	3.188776	0	82.90816	9.566327	-82.9082	0
8	3.188776	3.188776	82.90816	12.7551	-82.9082	0
9	6.377551	6.377551	95.66327	127.551	-79.7194	0
10	6.377551	6.377551	114.7959	6.377551	-82.9082	0
11	3.188776	3.188776	127.551	9.566327	-82.9082	0
12	9.566327	9.566327	76.53061	31.88776	-76.5306	0
13	76.53061	63.77551	140.3061	95.66327	-76.5306	0
14	70.15306	76.53061	172.1939	63.77551	-76.5306	0
15	31.88776	31.88776	70.15306	6.377551	-82.9082	0
16	3.188776	3.188776	108.4184	9.566327	-82.9082	0
17	0	12.7551	108.4184	-25.5102	-82.9082	0
18	3.188776	-9.56633	82.90816	-31.8878	-82.9082	-12.7551
19	0	0	95.66327	25.5102	-82.9082	-15.9439
20	6.377551	6.377551	95.66327	57.39796	-82.9082	-31.8878
21	-6.37755	-12.7551	121.1735	216.8367	-127.551	-57.398
22	-31.8878	-35.0765	175.3827	165.8163	-127.551	-57.398
23	-31.8878	-31.8878	102.0408	95.66327	-178.571	-57.398
24	-9.56633	-9.56633	121.1735	204.0816	-140.306	-44.6429
25	-9.56633	-12.7551	127.551	191.3265	-133.929	-54.2092
26	31.88776	31.88776	127.551	165.8163	-127.551	-47.8316
27	31.88776	31.88776	127.551	108.4184	-121.173	-57.398
28	0	0	111.6071	6.377551	-121.173	-44.6429
29	-12.7551	-3.18878	95.66327	6.377551	-108.418	-19.1327
30	0	-3.18878	89.28571	6.377551	-95.6633	-6.37755
31	6.377551	9.566327	82.90816	-6.37755	-95.6633	-44.6429
32	-44.6429	-44.6429	76.53061	-38.2653	-95.6633	-19.1327
33	-6.37755	-6.37755	79.71939	-31.8878	-102.041	-31.8878
34	-3.18878	3.188776	102.0408	57.39796	-108.418	-44.6429
35	-12.7551	-25.5102	108.4184	114.7959	-108.418	-44.6429
36	-22.3214	-31.8878	108.4184	133.9286	-108.418	-35.0765
37	-12.7551	-22.3214	102.0408	108.4184	-114.796	-38.2653
38	-31.8878	-31.8878	111.6071	165.8163	-121.173	-35.0765
39	-25.5102	-25.5102	108.4184	172.1939	-121.173	-44.6429
40	-31.8878	-38.2653	102.0408	146.6837	-114.796	-31.8878
41	-25.5102	-31.8878	95.66327	76.53061	-108.418	-25.5102
42	-31.8878	-22.3214	95.66327	3.188776	-102.041	-25.5102
43	-15.9439	-19.1327	89.28571	0	-95.6633	-25.5102
44	-12.7551	-15.9439	89.28571	0	-89.2857	0
45	0	0	89.28571	6.377551	-89.2857	0
46	0	0	89.28571	3.188776	-89.2857	0
			0	0	0	0

Load cell on the second position with a wood spacer in the bristles

				wood space in the middle bristles of the steel robot				
				cycle	Fc (KN)	Fd (KN)		
11	-14			1	70.15306	-89.2857		
11	-14			2	70.15306	-89.2857		
11	-14			3	70.15306	-89.2857		
11	-14			4	70.15306	-89.2857		
11	-14			5	70.15306	-89.2857		
13	-14			6	82.90816	-89.2857		
13	-14			7	82.90816	-89.2857		
13	-14			8	82.90816	-89.2857		
13	-14			9	82.90816	-89.2857		
13	-14			10	82.90816	-89.2857		
14	-14			11	89.28571	-89.2857		
17	-14			12	108.4184	-89.2857		
18	-14			13	114.7959	-89.2857		
18	-14			14	114.7959	-89.2857		
21	-14			15	133.9286	-89.2857		
18	-14			16	114.7959	-89.2857		
21	-14			17	133.9286	-89.2857		
28	-14			18	178.5714	-89.2857		
64	-14			19	408.1633	-89.2857		
45	-14			20	286.9898	-89.2857		
14	-15			21	89.28571	-95.6633		
16	-20			22	102.0408	-127.551		
25	-14			23	159.4388	-89.2857		
17	-14			24	108.4184	-89.2857		
15	-22			25	95.66327	-140.306		
16	-29			26	102.0408	-184.949		
16	-26			27	102.0408	-165.816		
15	-15			28	95.66327	-95.6633		
17	-23			29	108.4184	-146.684		
17	-21			30	108.4184	-133.929		
17	-23			31	108.4184	-146.684		
22	-20			32	140.3061	-127.551		
29	-18			33	184.949	-114.796		
35	-16			34	223.2143	-102.041		
17	-16			35	108.4184	-102.041		
16	-16			36	102.0408	-102.041		
19	-16			37	121.1735	-102.041		
17	-16			38	108.4184	-102.041		
15	-15			39	95.66327	-95.6633		
15	-16			40	95.66327	-102.041		
16	-19			41	102.0408	-121.173		
15	-19			42	95.66327	-121.173		
16	-19			43	102.0408	-121.173		
16	-19			44	102.0408	-121.173		
15	-18			45	95.66327	-114.796		
13	-16			46	82.90816	-102.041		
11	-13			47	70.15306	-82.9082		
11	-13			48	70.15306	-82.9082		
11	-13			49	70.15306	-82.9082		
11	-13			50	70.15306	-82.9082		
11	-13			51	70.15306	-82.9082		

Load cell on the second position with a steel spacer in the bristles

|			steel space in the middle bristles ;weight of steel space=6.1kg					
			cycle	Fc (KN)	Fd (KN)			
11	-14		1	70.15306	-89.2857			
11	-14		2	70.15306	-89.2857			
11	-14		3	70.15306	-89.2857			
11	-14		4	70.15306	-89.2857			
11	-14		5	70.15306	-89.2857			
12	-15		6	76.53061	-95.6633			
13	-15		7	82.90816	-95.6633			
13	-15		8	82.90816	-95.6633			
13	-15		9	82.90816	-95.6633			
14	-15		10	89.28571	-95.6633			
14	-15		11	89.28571	-95.6633			
14	-15		12	89.28571	-95.6633			
17	-15		13	108.4184	-95.6633			
18	-15		14	114.7959	-95.6633			
19	-15		15	121.1735	-95.6633			
34	-15		16	216.8367	-95.6633			
32	-15		17	204.0816	-95.6633			
22	-15		18	140.3061	-95.6633			
27	-15		19	172.1939	-95.6633			
64	-14		20	408.1633	-89.2857			
52	-14		21	331.6327	-89.2857			
16	-15		22	102.0408	-95.6633			
18	-17		23	114.7959	-108.418			
23	-16		24	146.6837	-102.041			
16	-15		25	102.0408	-95.6633			
13	-30		26	82.90816	-191.327			
13	-28		27	82.90816	-178.571			
14	-26		28	89.28571	-165.816			
14	-19		29	89.28571	-121.173			
16	-10		30	102.0408	-63.7755			
17	-20		31	108.4184	-127.551			
20	-22		32	127.551	-140.306			
28	-22		33	178.5714	-140.306			
42	-20		34	267.8571	-127.551			
15	-18		35	95.66327	-114.796			
17	-18		36	108.4184	-114.796			
19	-17		37	121.1735	-108.418			
16	-17		38	102.0408	-108.418			
13	-17		39	82.90816	-108.418			
13	-23		40	82.90816	-146.684			
13	-21		41	82.90816	-133.929			
13	-18		42	82.90816	-114.796			
14	-18		43	89.28571	-114.796			
14	-18		44	89.28571	-114.796			
14	-18		45	89.28571	-114.796			
13	-20		46	82.90816	-127.551			
12	-20		47	76.53061	-127.551			
13	-20		48	82.90816	-127.551			
11	-18		49	70.15306	-114.796			
11	-17		50	70.15306	-108.418			
11	-16		51	70.15306	-102.041			
11	-15		52	70.15306	-95.6633			
11	-14		53	70.15306	-89.2857			

Appendix E

Experimental results of the plastic bristled robot

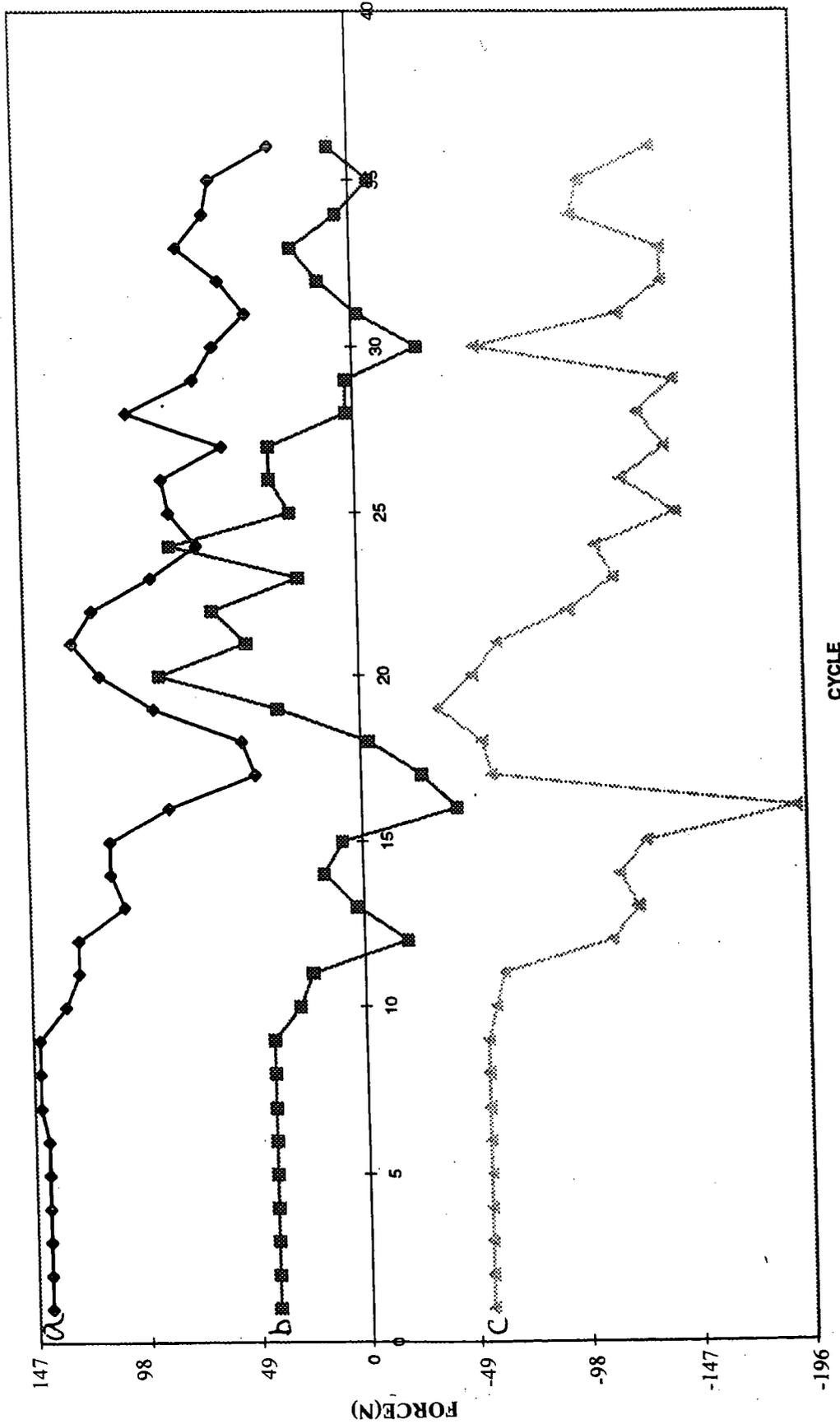| compress				tension		
mm	load (kg)	load (N)		mm	load (kg)	load(N)
0	0	0		0	0	0
13.5	3.874	37.9652		27	10.569	103.5762
16.5	4.874	47.7652		30	11.569	113.3762
21	5.874	57.5652		32	12.569	123.1762
22	6.874	67.3652		34	13.569	132.9762
25	7.874	77.1652		36	14.569	142.7762
40	12.874	126.1652		46	10.569	103.5762
53	17.874	175.1652		58.5	24.569	240.7762
70	22.874	224.1652		74	29.569	289.7762
97	26.874	263.3652				

SMALL LOAD CELL CALIBRIT COMPRESSION
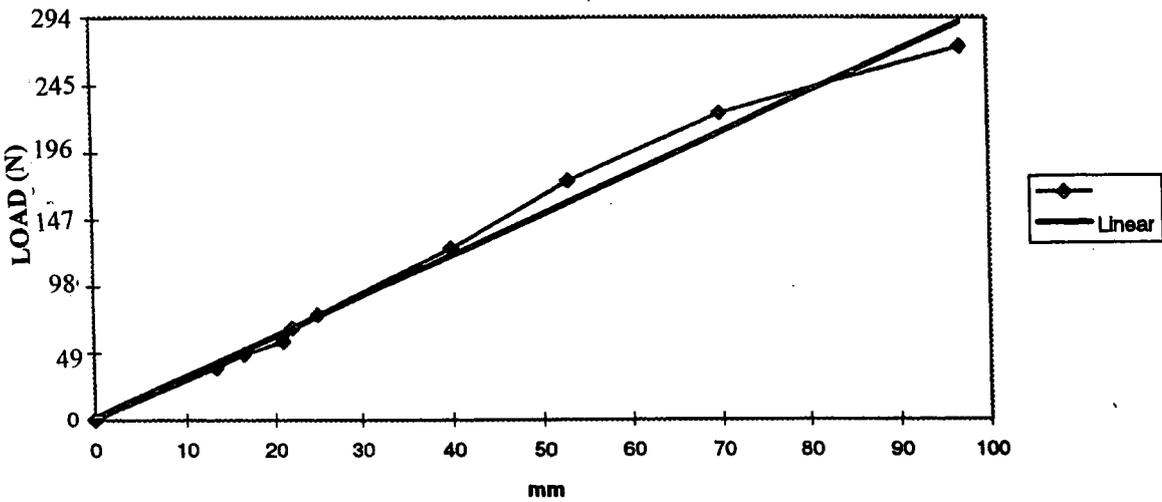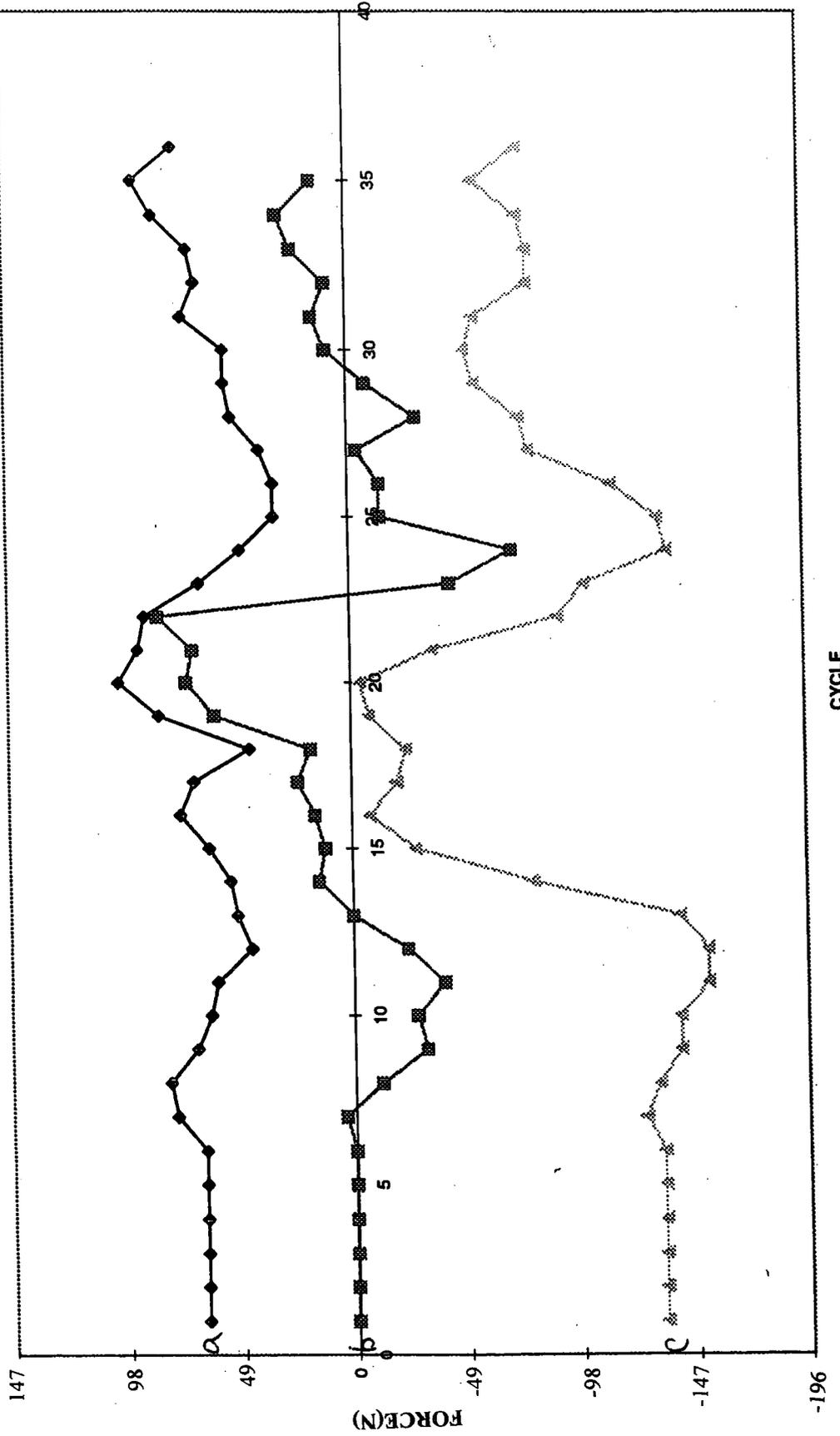

SMALL LOAD CELL CALIBRITE FOR TENSION
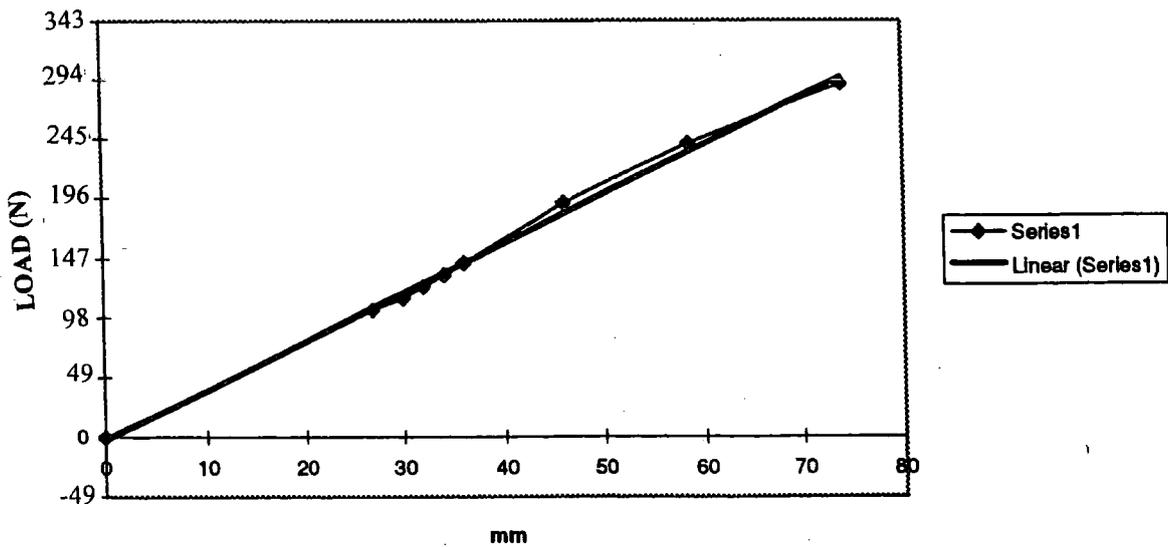
MECHANICAL BEHAVIOUR OF THE PLASTIC ROBOT THROUGH A BEND PIPE WHEN TEH LOAD CELL FITTED BEFORE THE FIRST CYLINDER
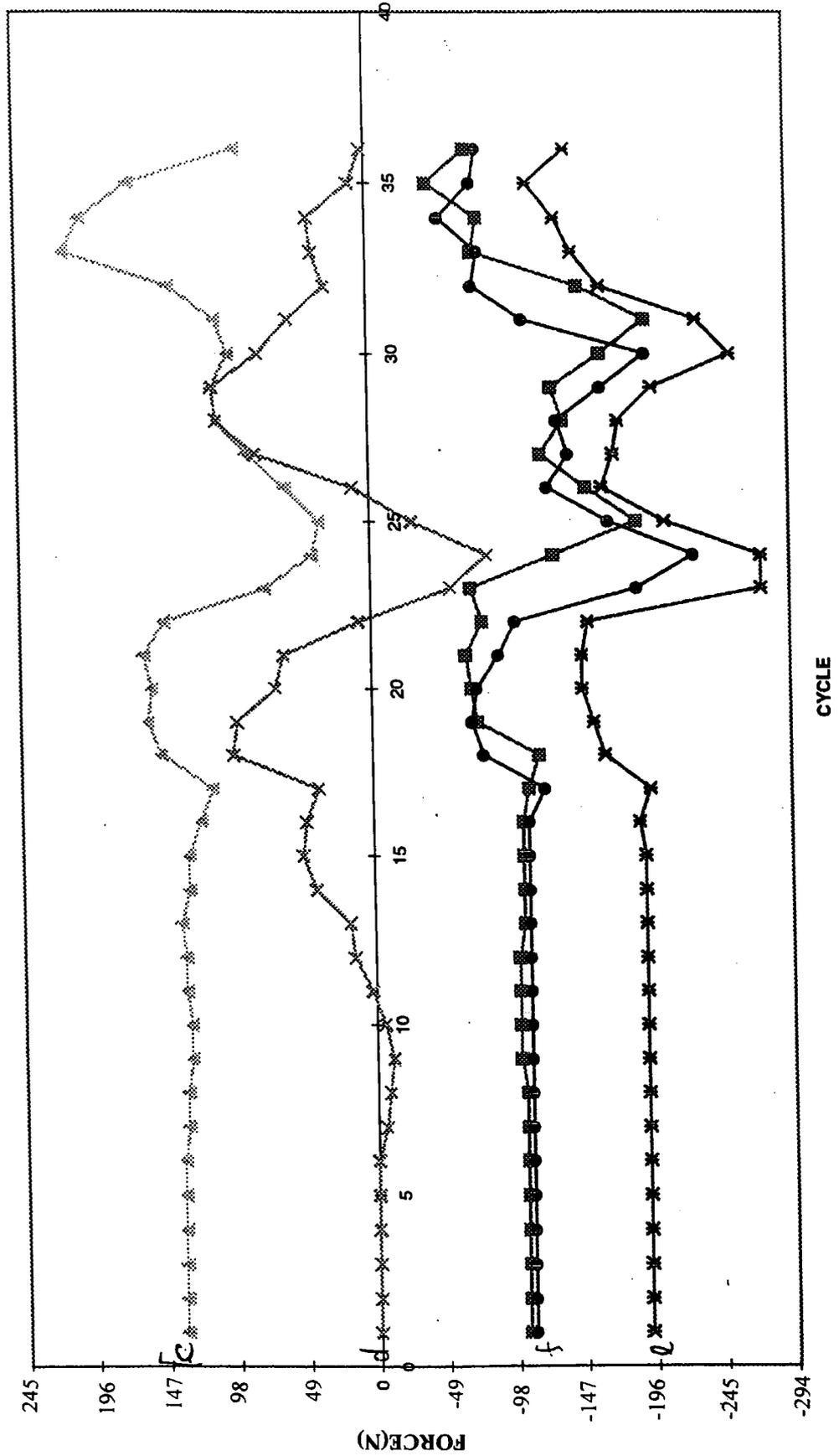
MECHANIC BEHAVIOUR OF THE PLASTIC ROBOT THROUGH A BEND PIPE WITHOUT WHEEL WHEN THE LOAD CELL FITTED BEFORE THE FIRST CYLINDER

FORCE(N)

CYCLE

Series1 a
Series2 b
Series3 c

90

MECHANIC BEHAVIOUR OF THE PLASTIC ROBOT THROUGH A BEND PIPE WHEN THE LOAD CELL FITTED BEFORE THE SECOND CYLINDER

FORCE(N)

CYCLE

Series1
Series2
Series3
Series4
Series5
Series6

MECHNIC BEHAVIOUR OF THE PLASTIC ROBOT WITHOUT WHEELS WHEN THE LOAD CELL FITTED BEFORE THE SECOND CYLINDER

Legend:
- Series1
- Series2
- Series3
- Series4
- Series5
- Series6

Y-axis: FORCE(N) — 245, 196, 147, 98, 49, 0, -49, -98, -147

X-axis: CYCLE — 5, 10, 15, 20, 25, 30

92

26